CANONICAL CORRELATION OF SHIPPING FORWARD CURVES

By

Nicholas A. Hadjiyiannis

MEng., Mechanical Engineering with Transport Engineering, Imperial College London (2006)

S.M., Transportation, Massachusetts Institute of Technology (2007)

S.M., Naval Architecture and Marine Engineering, Massachusetts Institute of Technology (2009)

MBA, Business Administration, Harvard Business School (2010)

PhD, Mechanical Engineering, Massachusetts Institute of Technology (2010)

Submitted to the Department of Mechanical Engineering

In Partial Fulfillment of the Requirements for the Degree of

Master of Science in Ocean Engineering

At the

Massachusetts Institute of Technology

September 2010

Signature of Author.....

Department of Mechanical Engineering

July 29, 2010

Certified by.....

Paul D. Sclavounos

Professor, Department of Mechanical Engineering

Thesis Supervisor

Accepted by .....

David Hardt

Professor of Mechanical Engineering

Chairman, Department Committee for Graduate Students

CANONICAL CORRELATION OF SHIPPING FORWARD CURVES

By

NICHOLAS A. HADJIYIANNIS

Submitted to the Department of Mechanical Engineering
on 29th July 2010 in partial fulfillment of the requirements for the Degree of
Master of Science in Ocean Engineering

ABSTRACT

The behavior and interrelations between the main shipping forward curves are analyzed using multivariate statistics after removing the volatility distortions dictated by the Samuelson hypothesis. Principal Components Analysis and Canonical Correlation analysis were used to demonstrate how the task of explaining the various shipping forward curves can be simplified substantially and how very high correlations can be achieved between shipping forward curves. The conditions under which correlations are higher are discussed as well as the various applications of these results using case studies. Applications include trading from a hedge fund perspective, cross hedging any physical exposure in illiquid markets and portfolio optimization. Conditioning as a tool is also examined to demonstrate how more reliable correlation results can be obtained for cross-hedging or other purposes, and how the best trading opportunities can be unveiled conditional on recently observed data. Tanker valuations are carried out using the adjusted forward curves with the RAFL ship valuation model. The results are very close to transaction prices for relatively modern vessels while deviations in older ships are explained with regards to phase out regulations and other factors. The ship value volatility and consequently the valuations of typical options are substantial and increase as a percentage of the ship value with age. These results have to be considered seriously in shipping transactions that include optionalities which are very common.

Thesis Supervisor: Paul D. Sclavounos
Title: Professor, Department of Mechanical Engineering

Acknowledgments

First and foremost I would like to thank my supervisor Professor Paul D. Sclavounos for his valuable guidance in my research. I would also like to thank Vassilis Karakoulakis of Clarksons and Per Einar Ellefsen of Arrowhawk Capital Partners for the data that was used in the preparation of this thesis.

Table of Contents

Abbreviations

BCI: Baltic Capesize Index

BOD: Board of Directors

BPI: Baltic Panamax Index

CAPE: Capesize Bulk Carrier (~175,000dwt)

CCA: Canonical Correlation Analysis

FFA: Forward Freight Agreements

MR: Medium Range Tanker

PCA: Principal Components Analysis

PMX: Panamax Bulk Carrier (~75,000dwt)

RAFL: Risk Adjusted Forward Looking Ship Valuation Model

S&P: Sale and Purchase

SVD: Singular Value Decomposition

TC: Tanker – Clean (Products)

4TCA: 4-Route Time Charter Average

TCE: Time Charter Equivalent

TD: Tanker – Dirty (Crude Oil)

VLCC: Very Large Crude Oil Carrier (~200,000dwt - 300,000dwt)

WS: Worldscale

1. Introduction

The purpose of this thesis is to analyze the behavior and interrelations between the main shipping forward curves and then use them for tanker valuations. Five high liquidity dry bulk and tanker routes were chosen as summarized in Table 1.1.

ROUTE	DESCRIPTION
BCI TCA:	Average time charter earnings on the four main Cape routes
BPI TCA:	Average time charter earnings on the four main Panamax routes
TD5:	Suezmax - Crude Oil from West Africa to East US Coast
TD3:	VLCC - Crude Oil from Saudi Arabia to Japan
TC2:	MR Product Carrier - Clean Product from Rotterdam to New York

Table 1.1: Chosen Shipping Forward Curve Routes

The Baltic publishes indices for these routes on a daily basis and futures are traded on these indices either over the counter or through clearing houses. Contracts of various tenors are traded daily that span out to 2 – 5 years. Note that these are Asian futures that settle over a period as opposed to a particular date. Data was collected on contracts of the various tenors on the above routes. This data is in the form of time series of daily futures prices from February 10th 2005 to July 29th 2010.

The traded futures have fixed maturity dates, so the time to maturity decreases with time. It is well known that the volatility of futures prices increases as we approach maturity by virtue of the Samuelson hypothesis i.e. due to reasons including the increased information for the immediate future [Samuelson 1965]. We want to exclude this effect so we can analyze the data and its volatility more effectively. The first step of the analysis, therefore, is to create new time series of prices for contracts with a continuously rolling tenor, meaning that the time to maturity is kept constant.

Using the continuously rolling contracts, Principal Components Analysis (PCA) will be carried out to identify the number of factors required to explain an adequate amount of the variance of these forward curves. Canonical Correlation Analysis (CCA)

will then be applied to determine the maximum possible correlation between those forward curves and how that can be achieved. Finally, tanker valuations will be carried out using the rolling contracts with the Risk Adjusted Forward Looking (RAFL) ship valuation model which was originally developed by [Hadjiyiannis 2010] for the valuation of Capesize bulk carriers.

2. Canonical Correlation Analysis (CCA)

Using CCA, we can determine the maximum possible correlation between two sets of variables and the way that can be achieved. In our case, we will be maximizing the possible correlation between various shipping forward curves. The two sets of variables in this case are two portfolios of futures contracts with various tenors. The applications of this analysis are discussed in Section 6. They include cross hedging in markets where a illiquidity prevents a "perfect" hedge, trading from a hedge fund perspective etc. What follows is a brief mathematical explanation of canonical correlation analysis and the way it can be applied to our particular problem.

Consider 2 sets of variables e.g. one set of futures for Capesize bulk carriers, $(C_1, C_2, ..., C_{p_1})$ and one set of futures for Suezmax Tankers $(S_1, S_2, ..., S_{p_2})$. Denote the number of variables in the two datasets as p_1 and p_2 respectively, where $p_1 \leq p_2$ and assume these variables are measured about their means. The data for each variable is recorded as a time series over a period of "n" days. The data matrix can be written in a vertically partitioned form where [C] is $(n \times p_1)$ and [S] is $(n \times p_2)$:

$$[X] = \begin{pmatrix} [C] \\ [S] \end{pmatrix} \tag{2.1}$$

The Covariance matrix is also partitioned as follows:

$$[\Sigma] = \begin{pmatrix} [\Sigma_{11}] & [\Sigma_{12}] \\ [\Sigma_{12}] & [\Sigma_{22}] \end{pmatrix} \tag{2.2}$$

We want to find the maximum possible correlation between a portfolio of Cape futures $\vec{u}$ with weights $\vec{a}$ and a portfolio of Suezmax futures $\vec{v}$ with weights $\vec{\beta}$.

$$\vec{u} = a_1 C_1 + a_2 C_2 + ... + a_n C_n = \vec{a}^T [C] \tag{2.3}$$

$$\vec{v} = \beta_1 S_1 + \beta_2 S_2 + ... + \beta_n S_n = \vec{\beta}^T [S] \tag{2.4}$$

For simplicity, we standardize both linear combinations to unit variance:

$$\mathrm{var}(\vec{u}) = E(\vec{u}^2) = E\left(\vec{a}^T [C][C]^T \vec{a}\right) = \vec{a}^T [\Sigma_{11}]\vec{a} = 1 \tag{2.5}$$

$$\mathrm{var}(\vec{v}) = E(\vec{v}^2) = E\left(\vec{\beta}^T [S][S]^T \vec{\beta}\right) = \vec{\beta}^T [\Sigma_{22}]\vec{\beta} = 1 \tag{2.6}$$

Since the variables are zero centered, we have: $E(\vec{u}) = E(\vec{v}) = 0$ (2.7)

Therefore, the Correlation between u and v is given by:

$$E(\vec{u}\vec{v}) = E\left(\vec{a}^T [C][S]^T \vec{\beta}\right) = \vec{a}^T [\Sigma_{12}]\vec{\beta} \tag{2.8}$$

Equation 2.8 is to be maximized subject to the constraint that $\vec{u}$ and $\vec{v}$ are unit vectors (Equations 2.5 and 2.6). We use the Lagrangian expression,

$$\psi = \vec{a}^T [\Sigma_{12}]\vec{\beta} - \frac{1}{2}\lambda\left(\vec{a}^T [\Sigma_{11}]\vec{a} - 1\right) - \frac{1}{2}\mu\left(\vec{\beta}^T [\Sigma_{22}]\vec{\beta} - 1\right) \tag{2.9}$$

where λ and μ are Lagrangian multipliers. Note that subject to constraints (2.5) and (2.6), ψ is equal to the correlation (Equation 2.8). We maximize ψ by differentiating with respect to vectors $\vec{a}$ and $\vec{\beta}$, and setting the derivatives simultaneously equal to zero:

$$\frac{\partial \psi}{\partial \vec{a}} = [\Sigma_{12}]\vec{\beta} - \lambda[\Sigma_{11}]\vec{a}^T = 0 \tag{2.10}$$

$$\frac{\partial \psi}{\partial \vec{\beta}} = [\Sigma_{12}]^T \vec{a} - \mu[\Sigma_{22}]\vec{\beta} = 0 \tag{2.11}$$

Combining with constraints 2.5 and 2.6 (unit variance), we get:

$$\vec{a}^T \frac{\partial \psi}{\partial \vec{a}} = \vec{a}^T [\Sigma_{12}] \vec{\beta} - \lambda(1) = 0 \tag{2.12}$$

$$\vec{\beta}^T \frac{\partial \psi}{\partial \vec{a}} = \vec{\beta}^T [\Sigma_{12}]^T \vec{a} - \mu(1) = 0 \tag{2.13}$$

Combining (2.12) and (2.13) yields:

$$\lambda = \mu = \vec{a}^T [\Sigma_{12}] \vec{\beta} \tag{2.14}$$

From equation (2.8) and (2.14), we see that the Lagrangian multiplier λ is equal to the correlation between the two data sets. Since $[\Sigma_{12}]^T = [\Sigma_{21}]$, we can rewrite (2.10) and (2.11) directly in matrix form as follows:

$$\begin{pmatrix} -\lambda[\Sigma_{11}] & [\Sigma_{12}] \\ [\Sigma_{21}] & -\lambda[\Sigma_{22}] \end{pmatrix} \begin{pmatrix} \vec{a} \\ \vec{\beta} \end{pmatrix} = 0 \tag{2.16}$$

The combined vector in Equation 2.16 contains the portfolio weights of the two data sets (e.g. Capes and Suezmax Tankers) and is of length $p_1 + p_2$. Denote this as vector $\vec{w}$ and the partitioned matrix preceding it, matrix $[A]$. Rewriting Equation 2.16, we have:

$$[A]\vec{w} = 0 \tag{2.17}$$

Note that this is not a classical Eigenvalue problem because $[A]$ is a block matrix in which the λ values also lie off the diagonal. Equation 2.17 has to be solved for the $p_1 + p_2$ possible non-trivial pairs of λ and $\vec{w}$. The largest real value of λ is the maximum attainable correlation between the two data sets and the corresponding portfolio weights are defined by Equation 2.17 for a given λ. There are two ways to proceed from this point to solve Equation 2.17.

Method 1.

By further manipulation, we can reduce Equation 2.16 into a classical Eigenvalue problem and then solve for the Eigenvalues and Eigenvectors. We start by breaking Equation 2.16 back into equation form:

$$-\lambda[\Sigma_{11}]\vec{a}+[\Sigma_{12}]\vec{\beta}=0 \tag{2.18}$$

$$[\Sigma_{21}]\vec{a}-\lambda[\Sigma_{22}]\vec{\beta}=0 \tag{2.19}$$

We then Multiply Equation 2.18 by the inverse of matrix $[\Sigma_{11}]$ and Equation 2.19 by the inverse of matrix $[\Sigma_{22}]$ to get:

$$-\lambda[I]\vec{a}+\left[\Sigma_{11}^{-1}\Sigma_{12}\right]\vec{\beta}=0 \tag{2.20}$$

$$\left[\Sigma_{22}^{-1}\Sigma_{21}\right]\vec{a}-\lambda[I]\vec{\beta}=0 \tag{2.21}$$

Equations 2.20 and 2.21 can now again be written in partitioned block matrix form as follows:

$$\begin{pmatrix} 0 & \left[\Sigma_{11}^{-1}\Sigma_{12}\right] \\ \left[\Sigma_{22}^{-1}\Sigma_{21}\right] & 0 \end{pmatrix}\begin{pmatrix}\vec{a}\\ \vec{\beta}\end{pmatrix}-\lambda\begin{pmatrix}[I] & 0\\ 0 & [I]\end{pmatrix}\begin{pmatrix}\vec{a}\\ \vec{\beta}\end{pmatrix}=0 \tag{2.22}$$

Note that the block matrix multiplied by λ is simply the identity matrix, while the joint vector following it is vector $\vec{w}$. Naming the new block matrix on the left $[B]$, we are left with:

$$[B]\vec{w}-\lambda[I]\vec{w}=0 \quad \Rightarrow \quad [B-\lambda I]\vec{w}=0 \tag{2.23}$$

This is a simple Eigenvalue problem with the Eigenvalues lying only on the diagonal. Therefore, it can simply be solved on MATLAB for the Eigenvalue / Eigenvector pairs. We are interested in maximizing the correlation between the two data sets so we chose the pair involving the highest real Eigenvalue.

Note that $[\Sigma_{21}] = [\Sigma_{12}]^T$, but $[\Sigma_{11}]$ is unrelated to $[\Sigma_{22}]$, since the two matrices are each wholly derived from two separate sets of variables. That means that matrix $[B]$ is not symmetric, even though its Eigenvalues are real.

Method 2.

For non-trivial solutions of Equation 2.17, we set the determinant of matrix $[A]$ equal to zero to get a polynomial of order $p_1 + p_2$ which is then solved for $p_1 + p_2$ values of λ. We select the highest value of λ which is the maximum correlation. Call this λ^* and the corresponding vector of portfolio weights $\vec{w}^*$. In equation terms:

Solve directly for λ:
$$\begin{vmatrix} -\lambda[\Sigma_{11}] & [\Sigma_{12}] \\ [\Sigma_{12}] & -\lambda[\Sigma_{22}] \end{vmatrix} = 0 \qquad (2.24)$$

Maximum correlation:
$$\lambda^* = MAX(\lambda_1, \lambda_2, ..., \lambda_n) \qquad (2.25)$$

Substitute λ^* into (Eq. 2.17):
$$\begin{pmatrix} -\lambda^*[\Sigma_{11}] & [\Sigma_{12}] \\ [\Sigma_{12}] & -\lambda^*[\Sigma_{22}] \end{pmatrix} \vec{w}^* = [C]\vec{w}^* 0 \qquad (2.26)$$

This is simply Equation 2.16, but now with a known value of λ. In other words, all the elements of matrix $[C]$ are known. The only unknown in Equation 2.26 is the vector $\vec{w}^*$. This cannot simply be solved as a system of simultaneous equations using singular value decomposition (SVD) because by definition, two of the equations are

interdependent (we don't know which). There are infinite solutions since vector $\vec{w}^*$ can take any magnitude. However, also by definition, matrix $[C]$ will have an Eigenvalue which is equal to zero and we can use that as follows:

Solve the Eigenvalue Problem for matrix $[C]$, to get Eigenvalues "k" and Eigenvectors $\vec{e}$:

Eigenvalues (k) from:
$$\left|[C]-k[I]\right| = \begin{vmatrix} -\lambda^*[\Sigma_{11}]-k & [\Sigma_{12}] \\ [\Sigma_{12}] & -\lambda^*[\Sigma_{22}]-k \end{vmatrix} = 0 \qquad (2.27)$$

Eigenvectors ($\vec{e}$) from:
$$\left([C]-k[I]\right)\vec{e} = \begin{pmatrix} -\lambda^*[\Sigma_{11}]-k & [\Sigma_{12}] \\ [\Sigma_{12}] & -\lambda^*[\Sigma_{22}]-k \end{pmatrix}\vec{e} = 0 \qquad (2.28)$$

By definition, the eigenvector corresponding to k=0 satisfies the equation:

$$[C]\vec{e} = \begin{pmatrix} -\lambda^*[\Sigma_{11}] & [\Sigma_{12}] \\ [\Sigma_{12}] & -\lambda^*[\Sigma_{22}] \end{pmatrix}\vec{e} = 0 \qquad (2.29)$$

Note that Equation 2.29 is the same as Equation 2.26. In other words:

$$\vec{w}^* = \vec{e} \qquad (2.25)$$

So, all we have to do to find the vector of portfolio weights $\vec{w}^*$ after finding λ^*, is solve the Eigenvalue problem for matrix $[C]$ and select the Eigenvector that corresponds to the zero Eigenvalue.

3. Principal Components Analysis (PCA)

PCA will be carried out in order to identify the number of principal components necessary to explain an adequate portion of the variance of the main shipping forward curves. PCA is analogous to a canonical correlation of the data set with itself. In simple terms, PCA maximizes the variance of the data set. The Eigenvalues of the covariance matrix correspond to the maximum variance while the eigenvectors correspond to the portfolio of variables that achieves that variance.

A brief mathematical explanation along the lines of the canonical correlation analysis goes as follows. We start with a set of p zero-centered variables e.g. a set of futures series for Capesize bulk carriers, $(C_1, C_2, ..., C_p)$. Now $[X]$ has p components and the covariance matrix $[\Sigma]$. We want to find a weight vector $\vec{\alpha}$ which maximizes the variance of the portfolio, subject to the constraint:

$$\vec{\alpha}^T \vec{\alpha} = 1 \tag{3.1}$$

The variance of the portfolio is given by:

$$E\left(\vec{\alpha}^T [X]\right)^2 = E\left(\vec{\alpha}^T [X][X]^T \vec{\alpha}\right) = \vec{\alpha}^T \Sigma \vec{\alpha} \tag{3.2}$$

Again, we introduce a Lagrangian multiplier λ:

$$\psi = \vec{a}^T [\Sigma] \vec{a} - \lambda\left(\vec{a}^T \vec{a} - 1\right) \tag{3.3}$$

Note that the Lagrangian expression reduces to Equation 3.2, subject to constraint 3.1. Next, we maximize the variance by differentiating the Lagrangian expression with respect to vector $\vec{\alpha}$ and setting the derivative equal to zero:

$$\frac{\partial \psi}{\partial \vec{a}} = 2[\Sigma]\vec{a} - 2\lambda\vec{a} = 0 \tag{3.4}$$

Multiplying Equation 3.4 by $\vec{\alpha}^T$, and combining with Equation (3.1) we get:

$$a^T[\Sigma]\vec{a} = \lambda a^T\vec{a} = \lambda \tag{3.5}$$

From 3.2 and 3.5, we see that the Lagrangian multiplier λ is equal to the variance of the portfolio, in much the same way as it was equal to the correlation between the datasets in the CCA. This time, however, the analysis is much simpler as Equation 3.4, directly reduces into an Eigenvalue problem described by Equation 3.6.

$$(\Sigma - \lambda I)\vec{a} = 0 \tag{3.6}$$

More can be read about PCA and Canonical Correlations in [Basilevsky 1994] and [Anderson 2003]. The Singular Value Decomposition (SVD) of the covariance matrix $[\Sigma]$ takes the form:

$$[\Sigma] = [U]^T[\Lambda][U] = [V][V]^T, \text{ where } [V] = [U][\Lambda]^{1/2} \tag{3.7}$$

$[U]$ is the matrix containing the Eigenvectors of $[\Sigma]$ and $[\Lambda]$ is the diagonal matrix containing its Eigenvalues. Equation 3.7 tells us that the volatility of an independent statistical factor, as it affects the i^{th} price series is equal to the square root of the Eigenvalue corresponding to that factor, multiplied by the i^{th} element of the corresponding Eigenvector.

Since the factors are independent Gaussian random variables, we know that that the total variance is equal to the sum of the variance by each factor. So the variance explained by each factor is simply the Eigenvalue corresponding to that factor, divided by the sum of the Eigenvalues. The shape of the corresponding Eigenvector then tells us how that factor affects the contracts of various tenors.

4. Data Analysis and Procedure

4.1 Procedure Overview

The first big part of the analysis is the calculation of the covariance matrices that will be used in both the canonical correlation and principal components analysis. This can be broken down into five steps.

The raw data is in the form of time series of futures prices with various tenors. The expiration period of these futures is defined by the trading date and a set of rules that vary between trading houses and over time. The first step of the analysis is to determine the precise expiration dates of all the fixed futures contracts for each day throughout the time series. The expiration periods are months, quarters or years, but they are always fixed meaning that they always start on the first trading day of the first month of the expiration period.

The next step is to create a new set of futures price series for fictitious contracts that have a continuously rolling tenor i.e. a constant time to maturity. This will remove the effect of volatility increasing as maturity is approached (Samuelson hypothesis).

For the dry bulk routes, futures prices are quoted $/day whereas for tanker routes, they are quoted in worldscale. Worldscale is a percentage of a flat rate which is quoted in $/ton and is updated every year for each route. In order to carry out the canonical correlation analysis between bulk carrier and tanker routes, we have to convert the tankers time series from worldscale to time charter equivalent (TCE). We do that using the specifics of each route (miles, port fees etc) and time varying quantities including each year's flat rate and bunker prices.

The next step is to zero-center the original data for the "trended" volatility, and to zero-center the log differences of the data for the "de-trended" volatility.

Finally, we combine the series to produce covariance matrices for each individual dataset and for each dataset pair. These will then be used directly in the PCA, or combined with others to form the block matrices that are used in the CCA.

4.2 Creation of Continuously Rolling Contracts

The objective of this section is to use the prices of fixed maturity contracts in order to determine the prices of contracts with continuously rolling maturity dates (rolling contracts). This has to be carried out for each day in the time series. Taking the CAPE 4TCA for example, on a given business day there are futures prices quoted for the next month (M+1), the month after that, the next quarter (Q+1) and the next 5 quarters after that (Q+2 to Q+5), the next year (Y+1) and the 4 years after that (Y+2 to Y+5). We want to use those prices to determine the prices for the first quarter starting today (R1), the quarter beginning exactly one quarter from today (R2) etc. Note that on any given day, the maturity periods of the rolling quarters will overlap with those of fixed periods. In other words, the rolling contracts are combinations of fixed contracts.

There are various methods that can be used to solve this. One of the most intuitive is to assign a price to each future day based on the fixed contracts and then take the average across the days that lie in the rolling quarter in order to get the price of the rolling quarter. That is essentially taking a weighted average. A more robust and efficient method involves linear interpolation between fixed contracts. This is summarized in the following three steps:

Step 1:

First we determine the precise maturity dates of the fixed contracts. The days on which the roll-over occurs (definition of M+1, Q+1, Y+1 etc. on any given date) differs between clearing houses and has also changed on several occasions in the past. The data on tanker futures is from IMAREX and the data on dry bulk futures is from the Baltic Exchange. Tables 4.1 to 4.5 summarize the roll over rules for both throughout the period over which the data was collected.

Note that fixed contracts always start on the 1st day of the month. M+2 is always the whole month after M+1, Q+2 is the whole quarter after Q+1, Y+2 is the whole year after Y+1, M+3 is the whole month after M+2 etc. This means that the roll over rules for all the contracts can be defined by those for M+1, Q+1 and Y+1.

IMAREX - MONTHLY CONTRACT ROLL OVER		
Dates	Day of Month	M+1 Definition
Since Jul-01-08	All	Next month
Feb-01-07 – Jun-30-08	Up until 20	Next month
Feb-01-07 – Jun-30-08	After 20	Month after next
Before Feb-01-07	Up until 15	Next month
Before Feb-01-07	After 15	Month after next

Table 4.1: Roll Over Rules for Monthly Contracts of IMAREX

IMAREX – QUARTERLY AND YEARLY CONTRACT ROLL OVER			
Dates	Month	Q+1 Definition	Y+1 Definition
All	1, 4, 7, 10	Next Quarter	Next Year
All	2,3,5,6,8,9,11,12	Quarter after next	Next Year

Table 4.2: Roll Over Rules for Quarterly and Yearly Contracts of IMAREX

BALTIC - MONTHLY CONTRACT ROLL OVER		
Dates	Day of Month	M+1 Definition
Since Jan-01-2007	Last business day of month	Month after the next
Since Jan-01-2007	Before last business day of month	Next month
Before Jan-01-2007	All	Next Month

Table 4.3: Roll Over Rules for Monthly Contracts of the Baltic Exchange

BALTIC - QUARTERLY CONTRACT ROLL OVER		
Dates	Day of Month	Q+1 Definition
Since Jan-01-2007	Last business day of Quarter	Quarter after the next
Since Jan-01-2007	Before last business day of Quarter	Next Quarter
Before Jan-01-2007	All	Next Quarter

Table 4.4: Roll Over Rules for Quarterly Contracts of the Baltic Exchange

BALTIC - YEARLY CONTRACT ROLL OVER		
Dates	Day of Month	Q+1 Definition
Since Jan-01-2007	Last business day of Year	Year after the next
Since Jan-01-2007	Before last business day of Year	Next Year
Before Jan-01-2007	All	Next Year

Table 4.5: Roll Over Rules for Yearly Contracts of the Baltic Exchange

Step 2:

In Step 1 we defined the precise expiration period for each futures contract on every day of the time series. Next, we define the mid-point of expiration for each contract on each day of the time series. That is simply taking the date that lies in the middle between the starting and ending dates of the expiration period. We assign the prices of the futures contracts to their mid-point of expiration date. On each given day we will have values for various future dates. These points will be from monthly, quarterly and yearly contracts. Then we join these points to create a futures curve using linear interpolation. Other functions could be used here but linear interpolation is simple and robust.

Step 3:

The next step is to determine the mid-point of expiration date for the rolling contracts that we want to price. For example, the mid-point of expiration date for the first rolling quarter (R1) will be exactly half a quarter from today. Then the mid-point of expiration for R2 will be one quarter after that and so on. Having defined the mid-point of expiration dates for the rolling quarters in each day of the time series, we go back to Step 2, and interpolate for the corresponding futures prices.

Note that it is important to only interpolate - not extrapolate, particularly when using linear interpolation, because the gradient of the forward curve can be quite steep at some points leading to extreme results by extrapolation. Following this procedure, we create time series for the rolling contract futures prices spanning over the same time frame as the initial data. That is from Feb-10-2005 to July 29 2010 for 10 rolling quarters in all datasets, and from March-10-2008 to July-29-2010 for 22 rolling quarters for the dry bulk futures.

4.3 From Worldscale to Time Charter Equivalent

As explained earlier, tanker futures are quoted in worldscale, which is a percentage of a flat rate. The flat rate is a nominal value of $/ton, updated every year to reflect changes in bunker costs and other expenses. The annual updating of the flat rate is not reflected in our time series of futures that are quoted in worldscale. Therefore, it would make no sense to carry out a CCA between tanker futures quoted in worldscale and dry bulk carrier futures which are quoted in $/day. We must first convert everything to time charter equivalent ($/day) for the comparison to make sense. To convert from worldscale (WS) to time charter equivalent (TCE) we use Equation 4.1.

$$TCE = \frac{1}{d}\left[\frac{FWT}{100}(1-C) - Bb - P - O\right] \qquad 4.1$$

TCE: Time Charter Equivalent ($/day)

d: Total Return Voyage Days

F: Flat Rate ($/ton)

W: World Scale

T: Cargo Transported (tons)

C: Commissions (%)

B: Total Bunker Consumption (tons)

b: Bunker Price ($/ton)

P: Port Costs in Load and Discharge Ports ($)

O: Other Costs ($)

All the parameters are defined for the return voyage. In other words, when calculating duration, consumption and other parameters for each route, we assume that the ship will load at the origin, sail to the destination, discharge, and then return in ballast to where it started.

The parameters in Equation 4.1 are different for each route and also vary over time. For each route, the prevailing worldscale rate (W) changes daily, the bunker price (b) and the flat rate (F) change annually, and the remaining parameters remain constant. Table 4.6 provides a summary of the constant parameters for the selected tanker routes.

	TD3	TD5	TC2
Loading Port	Ras Tanura	Bonny (O.S.)	Rotterdam
Discharge Port	Chiba	Philadelphia	New York
D (days)	45.14	36.47	25.2
T (tons)	260,000	130,000	37,000
C	2.5%	2.5%	2.5%
B (tons)	3832.8	1864.9	705.6
P ($)	167,900	85,100	87,195
O ($)	1,000	1,000	1,000

Table 4.6 Constant Parameters for Worldscale to Time Charter Equivalent Conversions [Data from Clarksons 2010]

Table 4.7 shows the bunker prices (b) at the assumed bunkering ports for the various routes every year. Note that bunker prices for future years are based on futures prices for bunkers at the relevant ports.

	TD3	TD5	TC2
Bunker Port	Fujairah	Rotterdam	Rotterdam
2005	256,590	233,979	233,979
2006	310,881	293,040	293,040
2007	373,746	345,065	345,065
2008	509,354	471,909	471,909
2009	372,777	353,810	353,810
2010	467,354	447,450	447,450
2011	452,340	432,310	432,310

Table 4.7 Bunker Costs for the Selected Tanker Routes Since 2005 [Data from Clarksons 2010]

The flat rate of each year is based on the relevant costs for that route during the previous year until October. For example, the flat rate for the year 2011 will be based on bunker prices and other costs until October 2010. Therefore, as we approach October, our prediction of the next year's flat rate becomes more accurate. The flat rate is predominantly determined by bunker prices while other factors have a much smaller impact. Bunker futures are therefore also used to aid the predictions carried out before October. Table 4.8 shows the flat rates (F) each year for the selected trade routes.

	TD3	TD5	TC2
2005	13,4	10,4	7,56
2006	15,16	11,79	8,52
2007	17,72	13,93	9,97
2008	18,08	14,19	10,2
2009	25	19,63	13,78
2010	18,72	14,68	10,53
2011	22,3	17,51	12,42

Table 4.8 Flat Rates for the Selected Tanker Routes Since 2005 [Data from Clarksons 2010]

The major uncertainty in WS-TCE conversions of futures prices stems from the fact that the applied flat rate is the one prevalent upon expiration, which is often unknown at the time of contract. Therefore, an assumption is required to carry out the conversion. One could use the prevailing flat rate at the time of contract but that essentially assumes a constant flat rate until expiration. That is very crude since, as shown in Table 4.8, the flat rate has varied since 2005 by almost a factor of 2.

A more relevant assumption is that the actual flat rate was known in advance at the time of the contract. That means we convert futures contract prices to TCE in retrospect with the flat rates prevalent upon expiration. For contracts that are yet to expire, we can use current flat rate forecasts. This assumption is based on the fact that brokers provide a good estimate of the flat rate when closing a futures contract. These estimates are based on bunker prices and bunker futures prices, and have historically been very accurate.

4.4 The Covariance Matrix

Using the analysis described thus far, futures price series were created for 10 rolling quarters from Feb-10-2005 to July 29 2010 (1,383 trading days) in $/day for all 5 routes and in world scale for the 3 tanker routes. Futures price series were also created for 22 rolling quarters from March-10-2008 to July-29-2010 (605 trading days) for Capes and Panamaxes (distinguished by "22R") in $/day. That is a total of 10 datasets, 8 of which are (10x1383), and two of which are (22x605).

Next, we have to determine the covariance matrix for each individual dataset, and also between dataset pairs in order to create the block matrices required for the CCA. Note that each block matrix is composed of four covariance matrices. These are the two covariance matrices of the two individual datasets, a covariance matrix between the two datasets, and its transpose.

The analysis will be carried out using two different measures of volatility, so we will start by creating two sets of covariance matrices. The first set of covariance matrices derives from the de-trended daily log-differences of the futures price series. We call this the "de-trended volatility". The second set of covariance matrices is based on the measure of volatility by the standard deviation which, for lack of a better name, we call the "trended volatility".

One analogy that can be used to visualize the difference of the two volatility measures is that of short waves riding a long wave. The trended volatility is related to the departures of the free surface from the mean value of the long wave, whereas the de-trended volatility is related to the departures of the free surface of the short waves from their own mean which defines the long wave.

Covariance Matrices with "De-Trended Volatility"

To calculate the covariance matrix using the de-trended volatility, we have to first calculate the Gramian matrix. Denote the price for the rolling contract "r" on day "t" as "$p_{r,t}$". For the 8 datasets with 10 rolling quarters, index "r" ranges from 1 to 10 (R=10), and index "t" ranges from 1 to 1,383 (T=1,383). For the datasets with 22 rolling contracts, index "r" ranges from 1 to 22 (R=22) and index "t" ranges from 1 to 605 (T=605). Equation 4.2 shows the definition of the natural logarithm which allows us to express deviations relative to the current price level, while Equations 4.3 and 4.4 are the relevant logarithm properties.

$$\ln(x) \equiv \frac{dx}{x} \tag{4.2}$$

$$\ln(p_2) - \ln(p_1) \equiv \ln\left(\frac{p_2}{p_1}\right) \tag{4.3}$$

$$\ln(p_2) + \ln(p_1) \equiv \ln(p_2 \times p_1) \tag{4.4}$$

Using the logarithm properties expressed in Equations 4.3 and 4.4, the elements of the Gramian matrix $[X]$ are simply defined as per Equation 4.5.

$$x_{i,t} = \ln\left(\frac{p_{r,t+1}}{p_{r,t}}\right) - \frac{1}{T-1}\ln\left(\frac{p_{r,T}}{p_{r,1}}\right) \tag{4.5}$$

Note that as we go from the futures price data matrix to the Gramian matrix, the range of index "t" decreases by 1, so there are T-1 elements in each column. There are a total of 10 Gramian matrices, 8 of which are (10x1382), and two of which are (22x604). In Equation 4.5, the second term which is being subtracted is simply the mean value of the first term across the whole time series "r" by virtue of the logarithmic properties expressed in Equations 4.3 and 4.4.

Once we have the Gramian matrices, the covariance matrix between two datasets is simply the Gramian matrix of the first, multiplied by the transpose of the Gramian matrix of the second. Thereby, the block matrix between datasets "1" and "2" is given by Equation 4.6

$$[\Sigma]=\begin{pmatrix}[\Sigma_{11}] & [\Sigma_{12}]\\ [\Sigma_{21}] & [\Sigma_{22}]\end{pmatrix}=\begin{pmatrix}[X_1][X_1]^T & [X_1][X_2]^T\\ [X_2][X_1]^T & [X_2][X_2]^T\end{pmatrix} \qquad 4.6$$

Note that matrices $[\Sigma_{11}]$ and $[\Sigma_{22}]$ of Equation 4.6, are simply the covariance matrices of datasets "1" and "2" which are used in the PCA while the whole block matrix of Equation 4.6 is used in the CCA between the two datasets.

Covariance Matrices with "Trended Volatility"

To get the covariance matrix using trended volatility, we use the standard definitions of variance and covariance between the datasets.

$$\Sigma_{i,j}=\frac{1}{T}\sum_{t=1}^{T}(p_{i,t}-\bar{p}_i)(p_{j,t}-\bar{p}_j)=\frac{1}{T}\sum_{t=1}^{T}\left(p_{i,t}-\frac{1}{T}\sum_{t=1}^{T}(p_{i,t})\right)\left(p_{j,t}-\frac{1}{T}\sum_{t=1}^{T}(p_{j,t})\right) \qquad 4.7$$

When calculating covariance matrix $[\Sigma_{11}]$, both "i" and "j" are from dataset 1. When calculating covariance matrix $[\Sigma_{12}]$, the series "i" is from dataset "1" and the series "j" is from dataset "2". The covariance matrices are then used in the PCA and are appropriately combined to form the block matrices used in the CCA.

4.5 PCA and CCA

We have a total of 10 datasets, 8 of which are (10x1383), and two of which are (22x605). CCA will be carried out between the three tanker routes in $/day (3 combinations), in worldscale (3 combinations), between the two dry bulk routes with 10 rolling quarters and the three tanker routes in $/day (6 combination), and between the two dry bulk routes with 10 and 22 rolling quarters (2 combinations). This gives a total of 10 single dataset covariance matrices for the PCA and 14 block matrices for CCA. The analysis will be carried out using both "de-trended" and "trended" volatility, resulting in a total of 20 covariance matrices for PCA and 28 block matrices for CCA.

The final step is to apply the analysis described in Sections 2 and 3 using the 20 covariance matrices and the 28 block matrices developed thus far. I used and recommend MATLAB, which is reliable, because solutions in other programs such as MAPLE are unstable when solving the polynomials for sets of 22 variables. This is hard to notice until you get correlations exceeding 1. MATLAB yields high precision results which are identical using Method 1 and Method 2 (for both the maximum correlation λ^* and the corresponding portfolio weights $\vec{w}^*$).

5. Results and Discussion

5.1 Principal Component Analysis Results

Principal Components Analysis, as described in Section 3 was carried out on the 10 individual datasets using both de-trended and trended volatility. The first result of PCA is the screen test. This is a visual display of the Eigenvalues which enables us to identify their relative importance and how many we should focus on. As an example, Figure 5.1 shows the screen test for the Panamax with 10 rolling quarters using the de-trended volatility.

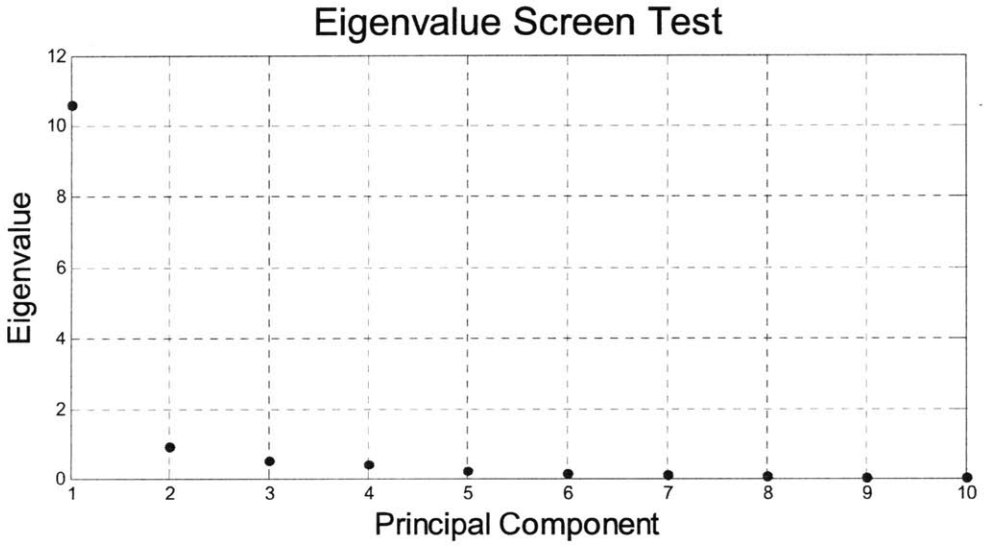

Fig 5.1: Eigenvalue Screen Test for Panamax with De-Trended Volatility

Here we see a sharp decline after the first eigenvalue which means that a single independent statistical factor is very dominant in explaining the variations of this forward curve. Based on this graph, we might decide to focus on the first two or three components since the eigenvalues quickly become insignificant beyond that. In fact, the first

component alone explains approximately 82% of the volatility while the first 3 explain over 93%.

The second result is a plot of the eigenvectors which tells us the weights of the principal components across the various contracts. Figure 5.2 shows the principal component weights of the first three factors for the Panamax with 10 rolling quarters using the de-trended volatility.

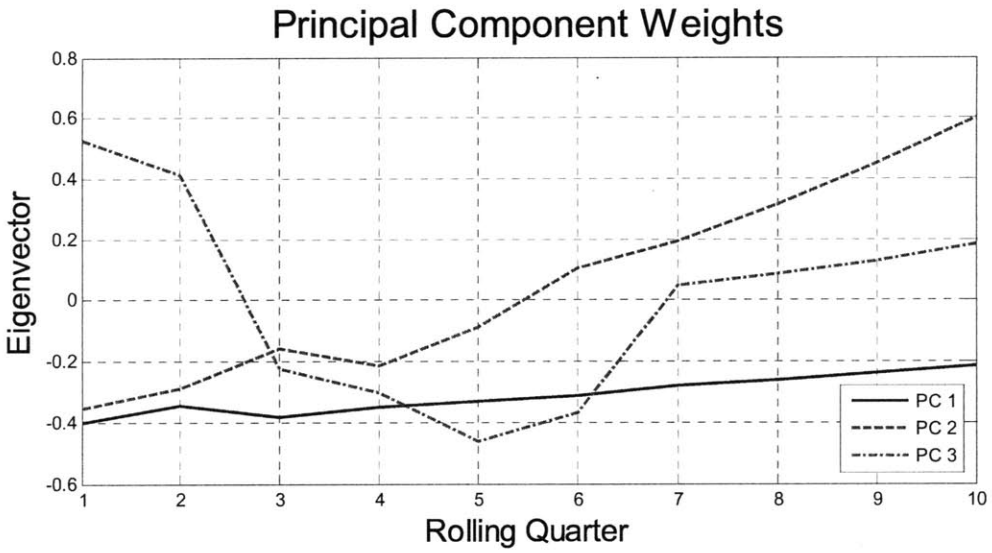

Fig 5.2: Principal Component Weights for Panamax with De-Trended Volatility

The shapes of the Eigenvector curves indicate how changes or shocks from each factor affect the various contracts and consequently the shape of the forward curve. In this example, we see a different effect by each of the first three principal components:

PC 1: Curve Shift

The first principal component has negative weights for all tenors (the whole curve is negative). This corresponds to a shift of the whole forward curve since a positive shock of the first factor will induce a negative shift in all contracts. The shift is not parallel since the shorter maturity contracts are more volatile and will fluctuate more than the longer maturity contracts.

PC2: Curve Tilt

The second principal component has negative weights for the short tenors (rolling quarters 1 to 5) and positive weights for the long tenors (rolling quarters 6 to 10). This corresponds to a tilt of the forward curve since a positive shock of the second factor will shift the prompt contracts down and the distant contracts up.

PC3: Change in Curvature

The third principal component has negative weights for the intermediate contracts (rolling quarters 3 to 6) and positive weights for the prompt and distant contracts. This corresponds to a change in the curvature of the forward curve since a positive shock in the third factor will shift short and distant contracts up while shifting intermediate contracts down.

The PCA graphs for the Panamax using de-trended volatility were used here for illustrative purposes. The full set of graphs for all routes using both de-trended and trended volatility can be found in Appendices A and B respectively.

The independent statistical factors described by the eigenvalues and eigenvectors are individual or combinations of real world parameters such as macroeconomic factors that affect the forward curve. This analysis shows us how much volatility is explained by these independent factors. The next step would be to trace relevant macroeconomic factors that are likely to affect the forward curves, and relate them to the independent statistical factors. We can also compare the eigenvectors in highly correlated markets to identify common statistical factors which affect different sectors.

In Section 5.2 we will see that the Panamax and Cape have highly correlated forward curves. Fig 5.3 shows the principal component weights for the Cape with 10 rolling quarters using de-trended volatility. By comparing Fig 5.2 and 5.3, we see that the first and most important principal component has a very similar shape. It corresponds to a negative curve shift with a decreasing impact as contract tenor increases. Further analysis could identify the corresponding real world factor(s) and confirm if it is indeed the same

for Panamaxes and Capes. If that is the case, one could potentially explain approximately 72% and 82% of the Cape and Panamax forward curve variations just by tracing this factor.

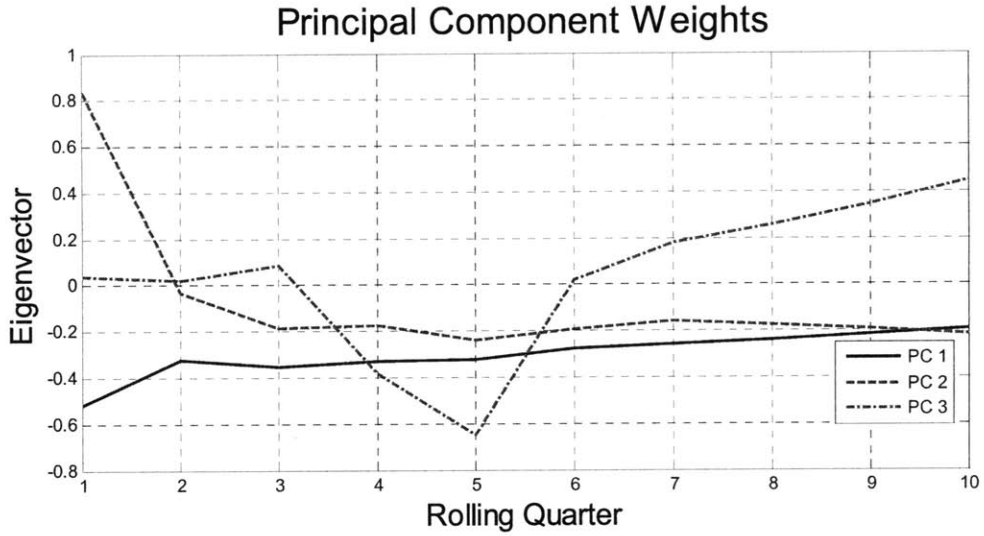

Fig 5.3: Principal Component Weights for Cape with De-Trended Volatility

The cumulative percentage of total volatility explained by the first 5 components was calculated for all routes. The results using de-trended and trended volatility are presented in Tables 5.1 and 5.2 respectively.

PCA Results Using De-Trended Volatility										
	CAPE (22R)	PMX (22R)	CAPE	PMX	TC-2	TD3	TD5	TC2 (WS)	TD3 (WS)	TD5 (WS)
PC1	77.06%	87.65%	71.98%	81.63%	37.39%	46.76%	30.00%	58.04%	67.87%	55.75%
PC2	93.26%	93.29%	86.86%	88.76%	52.59%	60.36%	45.92%	78.17%	82.58%	74.42%
PC3	96.22%	95.63%	92.42%	93.01%	64.68%	70.93%	58.82%	87.46%	90.08%	85.96%
PC4	97.53%	97.19%	95.33%	96.14%	74.29%	79.49%	70.13%	92.31%	94.25%	91.94%
PC5	98.48%	98.39%	97.77%	97.91%	83.45%	86.05%	80.61%	95.30%	96.55%	95.20%

Table 5.1 Cumulative Percentage of De-Trended Volatility Explained by the First 5 Principal Components

PCA Results Using Trended Volatility										
	CAPE (22R)	PMX (22R)	CAPE	PMX	TC-2	TD3	TD5	TC2 (WS)	TD3 (WS)	TD5 (WS)
PC1	99.19%	99.39%	98.99%	99.14%	61.33%	62.25%	48.30%	86.19%	78.31%	75.36%
PC2	99.62%	99.66%	99.46%	99.61%	78.39%	74.52%	68.56%	93.71%	88.09%	85.53%
PC3	99.78%	99.81%	99.76%	99.84%	88.94%	84.13%	82.92%	97.35%	94.04%	93.45%
PC4	99.90%	99.94%	99.88%	99.91%	92.25%	90.10%	88.47%	99.23%	98.24%	98.34%
PC5	99.96%	99.96%	99.94%	99.95%	94.82%	94.22%	93.04%	99.70%	99.29%	99.28%

Table 5.2 Cumulative Percentage of Trended Volatility Explained by the First 5 Principal Components

Tables 5.1 and 5.2 tell us how much of the volatility in the forward curve is explained by the dominant independent statistical factors or alternatively, how many independent statistical factors are needed to adequately explain the variations in the forward curve. Unlike for other indices such as electricity prices, Tables 5.1 and 5.2 indicate that only a few principal components are required for the main shipping forward curves. This means that the task of explaining the variations and predicting the forward curves can potentially be simplified to a great extent.

By comparing Tables 5.1 and 5.2 we see that more volatility is explained by the first few factors when using trended volatility as opposed to de-trended volatility. That may be because trend variations may be captured better by a few components than variations about the trend, and these trend variations may account for a significant portion of the total variation.

We also see that more volatility is explained by the first few factors in dry bulk carriers relative to tankers, in datasets of 22 rolling contracts relative to those with 10 rolling contracts, and in those where the analysis has been carried out with prices in Worldscale (WS) as opposed to time charter equivalent (TCE).

[Sclavounos & Ellefsen 2009] carried out PCA analysis on the TD3 over the period Apr-4-2005 to Feb-6-2009 using monthly rolling futures contracts with tenors ranging from 2 to 5 months. The analysis was carried out using the Worldscale prices and the de-trended measure of volatility. Table 5.3 shows a comparison of our relative results.

Comparison of Results with Previous Findings		
	TD3 (WS)	**TD3 [Sclavounos & Ellefsen 2009]**
PC1	78.31%	86%
PC2	88.09%	95%
PC3	94.04%	98%
PC4	98.24%	100%

Table 5.3 Comparison of TD3 De-Trended Volatility by First 4 Factors with [Sclavounos & Ellefsen 2009]

The results of [Sclavounos & Ellefsen 2009] show a higher percentage of volatility explained by the first factor and consequently all the cumulative results are higher. The difference may be partly explained by the fact that in this route, contracts beyond the first few months are significantly less liquid. Our analysis consists of 10 rolling quarters as opposed to rolling months 2 to 5.

5.2 Canonical Correlation Results

CCA as described in Section 2 was carried out on the 14 dataset pairs using both de-trended and trended volatility (on a total of 28 block matrices). The main results of CCA are the maximum correlation between the dataset pairs and the corresponding portfolio which achieves the maximum correlation. The maximum correlation by each dataset pair using de-trended and trended volatility is shown in Tables 5.4 and 5.5 respectively.

ROUTES	SHIPS	UNITS	RELATION	MAXIMUM CORRELATION
TD5-TC2	Suezmax – Product	$/day	Same	99.85%
TD5-TD3	Suezmax – VLCC	$/day	Same	99.46%
TD3-TC2	VLCC – Product	$/day	Same	99.17%
CAPE-PMX (22R)	Cape – Panamax	$/day	Same	98.16%
CAPE-PMX	Cape – Panamax	$/day	Same	96.02%
TD5-TD3(ws)	Suezmax – VLCC	WS	Same	84.58%
TD3-TC2(ws)	VLCC – Product	WS	Same	76.95%
TD5-TC2(ws)	Suezmax – Product	WS	Same	75.35%
CAPE-TC2	Cape – Product	$/day	Cross	28.22%
CAPE-TD5	Cape – Suezmax	$/day	Cross	27.68%
TD5-PMX	Suezmax – Panamax	$/day	Cross	25.79%
TC2-PMX	Product – Panamax	$/day	Cross	24.91%
TD3-PMX	VLCC – Panamax	$/day	Cross	24.62%
CAPE-TD3	Cape – VLCC	$/day	Cross	22.10%

Table 5.4: Maximum Correlation of Dataset Pairs Using De-Trended Volatility

The first column contains the names of the dataset pairs which are ranked in both tables by maximum correlation. The second column denotes the two ship types of the

dataset pair. The data for bulk carriers is always in $/day so the third column is only used to distinguish between the tanker datasets in which the data is in Worldscale and those where the TCE has first been calculated ($/day). Note that the units must always match between the two datasets of a given pair. In the fourth column, if the datasets of the pair are both from tankers or both from bulk carriers, that is indicated by "same". If one is from tankers and the other from bulk carriers, that is denoted as "cross".

For all dataset pairs except "CAPE-PMX (22R)", the data consists of 10 rolling quarters between Feb-10-2005 and Jul-29-2010. For "CAPE-PMX (22R)", the data consists of 22 Rolling quarters between March-10-2008 and July-29-2010.

ROUTES	SHIPS	UNITS	SECTORS	MAXIMUM CORRELATION
TD5-TC2	Suezmax – Product	$/day	Same	99.96 %
CAPE-PMX (22R)	Cape – Panamax	$/day	Same	99.93 %
TD5-TD3	Suezmax – VLCC	$/day	Same	99.89 %
TD3-TC2	VLCC – Product	$/day	Same	99.87 %
CAPE-PMX	Cape – Panamax	$/day	Same	99.68 %
TD5-TD3 (WS)	Suezmax – VLCC	WS	Same	98.94 %
TD5-TC2 (WS)	Suezmax – Product	WS	Same	97.52 %
TD3-TC2 (WS)	VLCC – Product	WS	Same	96.83 %
CAPE-TD3	CAPE – VLCC	$/day	Cross	92.59 %
TD3-PMX	Panamax – VLCC	$/day	Cross	90.90 %
TD5-PMX	Panamax – Suezmax	$/day	Cross	86.42 %
CAPE-TD5	Cape – Suezmax	$/day	Cross	86.01 %
TC2-PMX	Panamax – Product	$/day	Cross	81.97 %
CAPE-TC2	Cape – Product	$/day	Cross	81.88 %

Table 5.5: Maximum Correlation of Dataset Pairs Using Trended Volatility

Some general conclusions can be derived by examining and comparing Tables 5.4 and 5.5 as summarized in Table 5.6 and discussed below.

MAIN CONCLUSIONS FROM TABLES 5.4 & 5.5	
Conclusion 1	Very high maximum correlations achieved overall
Conclusion 2	Higher correlations with trended as opposed to de-trended volatility
Conclusion 3	Higher correlations within same sector than across sectors
Conclusion 4	Tankers are more correlated than bulk carriers
Conclusion 5	Higher correlation with time charter equivalent than with Worldscale
Conclusion 6	Higher correlations achieved when more rolling quarters are used

Table 5.6: Summary of Main CCA Conclusions on Maximum Correlation of Dataset Pairs

Conclusion 1.

A surprisingly high maximum correlation can be achieved between most datasets, the highest being 99.96%. This is highlighted when considering the corresponding correlations of the physical (spot) markets. [Stopford 2009] calculates the correlation between average monthly earnings of various major shipping market segments over the period 1990 and 2002.

The comparison with our results may not be perfect because in some instances our chosen routes are not 100% representatives of average earnings, because our analysis uses daily as opposed to monthly time increments, and because we are focusing on different time periods. Nevertheless, the comparison provides a good idea of the relationship between the spot market correlations and maximum possible correlations of the forward curves achieved with CCA.

Note that the relevant results to compare to [Stopford 2009] are only those in $/day (not Worldscale), and those calculated using the trended definition of volatility. Table 5.7 provides a list of the ship type pairs for which we and [Stopford 2009] both have results. They have been ranked by "spot correlation" as calculated by [Stopford 2009]. The fourth column shows our corresponding results from Tables 5.5 for

comparison with the third column of spot market correlations. The far right column lists the corresponding results from Table 5.4 for illustrative purposes.

ROUTES	SHIPS	SPOT CORREL.	CANONICAL CORREL. (TRENDED)	CANONICAL CORREL. (DE-TRENDED)
CAPE-PMX (22R)	Cape – Panamax	84%	99.93 %	98.16%
CAPE-PMX	Cape – Panamax	84%	99.68 %	96.02%
TD3-TC2	VLCC – Product	59%	99.87 %	99.17%
CAPE-TD3	CAPE – VLCC	30%	92.59 %	22.10%
CAPE-TC2	Cape – Product	27%	81.88 %	28.22%
TC2-PMX	Panamax – Product	17%	81.97 %	24.91%
TD3-PMX	Panamax – VLCC	7%	90.90 %	24.62%

Table 5.7: CCA Maximum Forward Curve Correlations and Spot Market Correlations by [Stopford 2009]

Across the 6 ship type pairs, the maximum correlation by CCA using 10 rolling quarters, is on average higher than the correlation of the physical (spot) markets, by 54% when using trended volatility and by 12% when using de-trended volatility.

Conclusion 2.

A higher correlation is achieved between the same dataset pairs when using trended volatility than when using de-trended volatility. This is evident by comparing the results of Table 5.4 (de-trended) with the corresponding results of Table 5.5 (trended). The maximum correlation when using trended as opposed to de-trended volatility is higher in all 14 dataset pairs. The range of correlations jumps from 22.1% - 99.85% to 81.88% - 99.96%.

Table 5.8 groups the various dataset pairs according to sector, data units and number of rolling quarters (all are 10 except when noted as "22R"). It then gives the

average maximum correlation within each group when calculated using de-trended and trended volatility.

Group of Database Pairs	Average Max Correlation (De-Trended Volatility)	Average Max Correlation (Trended Volatility)
Tanker-Tanker (TCE)	99.50%	99.91%
Bulk-Bulk (22 R)	98.16%	99.93%
Bulk-Bulk	96.02%	99.68%
Tanker-Tanker (WS)	78.96%	97.76%
Bulk-Tanker	25.56%	86.63%

Table 5.8: Maximum Correlation of Dataset Pairs Using Trended Volatility

Here we see the same result again. However, focusing on the bottom two rows, we also notice that the difference is significantly greater when doing the analysis in Worldscale and particularly when correlating across sectors (tankers with bulk carriers).

We can attempt to explain this by recalling the wave analogy of trended and de-trended volatility. The long wave is captured only by the trended volatility whereas the de-trended volatility only looks at the short waves riding the long wave. The fact that higher correlations are consistently achieved with trended volatility is a strong indication that the trends may be strongly correlated.

It seems that when comparing across sectors (tankers with bulk carriers), a significant part of the correlation is in the trends and is only captured when looking at the long wave. For example, CCA with trended volatility may better capture the effects of global economic factors such as the sub-prime crisis which sends the whole economy (both sectors) on a downward trend. CCA with de-trended volatility, on the other hand, may be impacted more by "daily" sector-specific factors such as an oil price spike or an iron ore port congestion which only impacts one of the two sectors and hence reduces the overall correlation.

Conclusion 3.

Higher maximum correlations are achieved when the ship types in the dataset pair are either both tankers or both bulk carriers, than if there is one from each. That is because intuitively, there is a higher earnings correlation between any two tanker or bulk carrier routes or sizes since they are serving similar markets. When comparing the Cape market (mainly 170,000t batches of iron ore and coal), with that of the TC2 (37,000t batches of clean products such as gasoline), there is relatively little in common and they respond to different shocks. In Table 5.7 we see that also spot market correlations by [Stopford 2009] are higher within the same sectors relative to correlations of tanker-bulk carrier pairs.

Conclusion 4.

Tankers are more correlated than bulk carriers. Note that we must only consider pairs with 10 rolling quarters for consistency in this comparison. The results may be explained by the fact that tankers carry more similar cargos. VLCCs and Suezmaxes for example both transport crude oil while the market for transportation of clean products may also be closely linked. Panamaxes on the other hand transport much more grain and also other cargos besides iron ore and coal which are the predominant Cape cargos.

Conclusion 5.

A higher correlation is achieved between the tanker routes when the analysis is performed using $/day as opposed to Worldscale, in other words after the TCE has been calculated. That is simply because by converting to TCE, the noise due to the annual flat-rate changes is eliminated. The futures prices in $/day are more reflective of reality because our assumption that the applicable flat rate was known in advance at the time of the contract is not a bad one to make.

Conclusion 6.

The last conclusion is that the maximum correlation increases when we add more contracts. Even though a shorter time period is considered, the maximum correlation between the Cape and Panamax is significantly higher with 22 rolling quarters than with 10 rolling quarters. This is true when using both trended and de-trended volatility. The reason is that a larger portfolio of assets (22 as opposed to 10 in each portfolio) provides much more flexibility. One should note that the range of solutions when using fewer rolling quarters is a subset of the range of solutions with more rolling quarters, so the maximum correlation can only increase by adding contracts.

Another interesting result is the minimum correlation attainable within each dataset or the range of possible correlations. While one may want to maximize the correlation for hedging or trading purposes, one may also be interested in minimizing the correlation for diversification. The real positive eigenvalues of the covariance matrix indicate possible correlations that can be achieved between the two datasets. Fig 5.4 shows the possible correlations between the Cape and Panamax forward curves using 22 rolling quarters with de-trended and trended volatility.

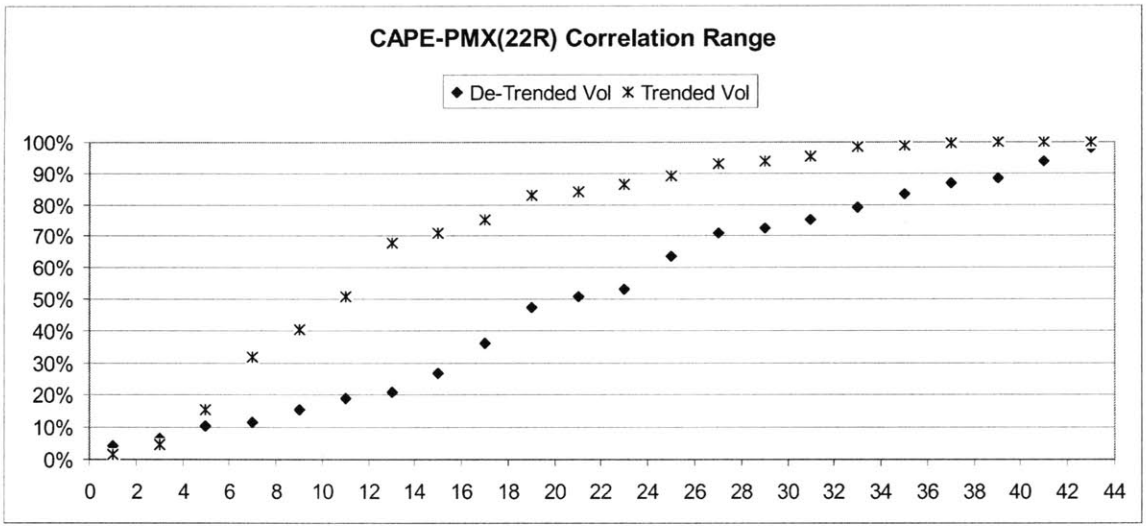

Fig 5.4: Possible Correlations between Cape and Panamax Forward Curves with 22 Rolling Quarters

The analytical results containing all the possible correlations for each dataset pair, using the de-trended and trended volatility can be found in Appendix C and Appendix D respectively.

One can also achieve correlations between any two eigenvalues by combining the portfolios given by the two corresponding eigenvectors. However, the minimum and maximum eigenvalues define the possible range of correlation that can be achieved. In the example presented by 5.4, the possible correlation range is 4.44% to 98.16% using de-trended volatility, and 1.56% to 99.93% using trended volatility. Only the lowest and highest eigenvalues are relevant because any correlation in between can be achieved by combining their corresponding portfolios.

Tables 5.9 and 5.10 show the possible range of correlations between the Cape and Panamax forward markets and how that changes when going from 10 to 22 rolling quarters. Table 5.9 shows the results with de-trended volatility and Table 5.10 has the results with trended volatility.

	CAPE-PMX	CAPE-PMX(R22)
MINIMUM	6.40%	4.44%
MAXIMUM	96.02%	98.16%
RANGE	89.62%	93.72%

Table 5.9: Cape-PMX Correlation Range with 10 and 22 Rolling Quarters using De-Trended Volatility

	CAPE-PMX	CAPE-PMX(22R)
MINIMUM	48.62%	1.56%
MAXIMUM	99.68%	99.93%
RANGE	51.06%	98.37%

Table 5.10: Cape-PMX Correlation Range with 10 and 22 Rolling Quarters using Trended Volatility

In both tables, we see that when going from 10 to 22 rolling contracts, the minimum correlation shifts down and the maximum correlation shifts up, thereby expanding the correlation range. That is again because the range of solutions with 10 rolling quarters is a subset of the range of solutions with 22 rolling quarters.

Figures 5.5 and 5.6 show the minimum and maximum possible correlation for each dataset pair, using de-trended and trended volatility respectively. In both graphs, the dataset pairs are presented from highest to lowest maximum correlation excluding the single dataset pair with 22 rolling quarters which is on the far right.

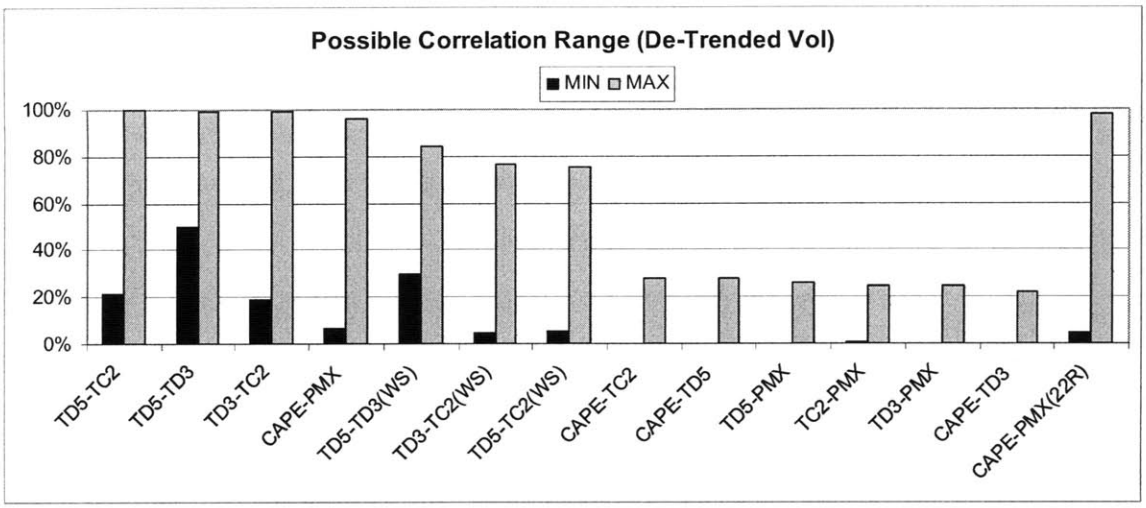

Fig 5.5: Minimum and Maximum Correlation for all Dataset Pairs using De-Trended Volatility

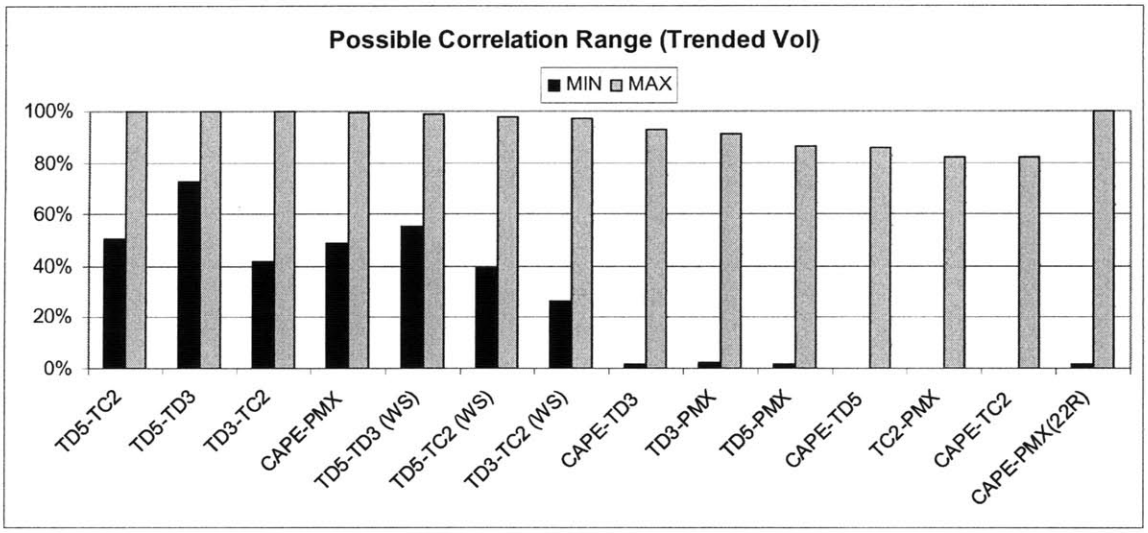

Fig 5.6: Minimum and Maximum Correlation for all Dataset Pairs using Trended Volatility

Earlier we saw that the maximum volatility increases when going from de-trended to trended volatility for the same dataset pair. Here we see that in the vast majority of cases, the minimum possible correlation also shifts up significantly. This indicates that

the inclusion of the trend (long wave) sets a limit to how low the correlation can be. This is a problem similar to that faced in portfolio optimization where diversification is limited by factors affecting the global economy and all sectors in the same way.

Figures 5.7 and 5.8 provide a visual representation of the portfolio that maximizes the correlation between the Cape and Panamax forward curves using 22 rolling quarters. Fig 5.7 uses de-trended volatility while Fig 5.8 uses trended volatility.

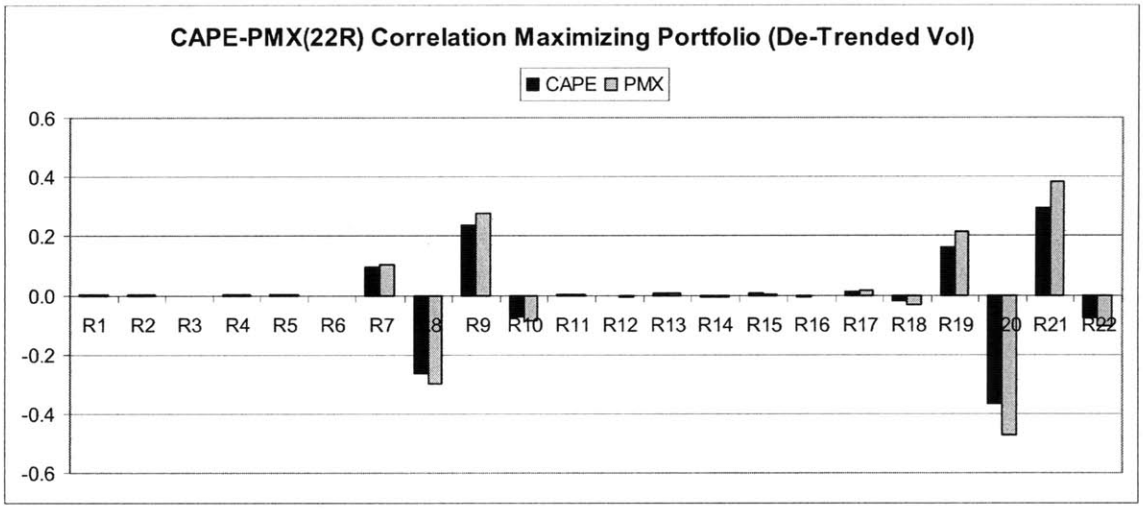

Fig 5.7: Correlation Maximizing Portfolio for CAPE-PMX De-Trended Volatility

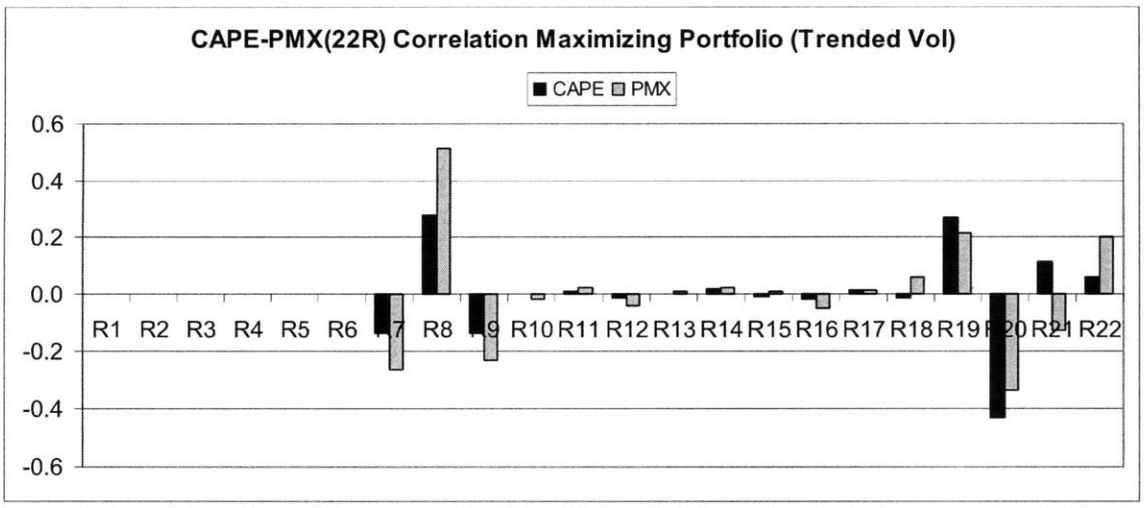

Fig 5.8: Minimum and Maximum Correlation for all Dataset Pairs using Trended Volatility

We see that in the vast majority of cases, to maximize the correlation, we have to go long and short on the same quarters in both datasets. Also, the same quarters are involved when maximizing the correlation between the two dataset using de-trended or trended volatility. Note that the scale on the ordinate axis is irrelevant and that all the signs can also be reversed (going short where long and vice versa) without affecting the correlation. The correlation maximizing portfolios for the remaining dataset pairs, using de-trended and trended volatility, can be found in Appendices E and F respectively.

6. Application Case Studies

6.1 Trading Opportunities from a Hedge-fund Perspective

If we have information additional to that of the market, about correlations between various portfolios, one of the most obvious applications is to use it directly in trading. First we start by identifying the highest correlation pairs. In our analysis we identified pairs with correlations approaching 100%. The next step is to trace the value of the two portfolios over time. We would expect the ratio of the two portfolio's values to remain approximately constant over time, with some departures about the equilibrium. That is because the correlation between the two is high but not perfect.

Alternatively, we create a new portfolio which is a long position of one of the two individual portfolios and a short position on the other. This combined portfolio should have a value that is approximately constant over time with small deviations from its equilibrium. These deviations present trading opportunities which can be exploited based on the assumption that the combined portfolio is mean reverting (i.e. that the correlation between the two datasets is indeed high). We simply buy when the combined portfolio's value is significantly below equilibrium and sell when it is significantly higher.

It is important to trance the portfolios' values carefully over a significant time period and look out for changes in the market because the combined portfolio's equilibrium level or the correlation between the two individual portfolios may change. Note that friction costs i.e. trading commissions will reduce potential profits and may make only significant deviations worthwhile. Also, as more and more parties identify the equilibrium and enter into the same trades, the deviations will become fewer and smaller.

One of the most powerful tools of multivariate statistics, described in [Anderson 2003], is the ability to condition the parameters determined from PCA and CCA on recently observed values. Solving the CCA conditionally on observed values, for example, can give us much better estimates of the correlations between datasets in the near future. Conditioning on recently observed values also allows us to solve for the

portfolio which currently deviates maximally from its equilibrium, thereby presenting the best trading opportunity.

Depending on our trading horizon, we can define the recent period as say, one month whereas the unconditioned parameters are derived from say 5-year data series. The unconditioned parameters are those that we calculated in our PCA / CCA and are denoted with upper case letters while the corresponding lower case letters are assigned to the parameters from the recent period.

Consider a uniformly distributed (across the rolling contracts) portfolio of Suezmax futures X_1, and the recent prices of other futures x_2. The conditional distribution of X_1, given x_2, is normal with a mean value and a covariance matrix given by Equations 6.1 and 6.2 respectively.

$$\left[\bar{X}_1\right]^C = E\left(\left[X_1\right]\middle|\left[x_2\right]\right) = \left[\bar{X}_1\right] + \left[\Sigma_{12}\right]\left[\Sigma_{22}\right]^{-1}\left(\left[x_2\right] - \left[\bar{X}_2\right]\right) \qquad 6.1$$

$$\left[\Sigma_{11}\right]^C = E\left(\left[\left[X_1\right] - \left[\bar{X}_1\right]^C\right]\left[\left[X_1\right] - \left[\bar{X}_1\right]^C\right]^T \middle| \left[x_2\right]\right) = \left[\Sigma_{11}\right] - \left[\Sigma_{12}\right]\left[\Sigma_{22}\right]^{-1}\left[\Sigma_{21}\right] \qquad 6.2$$

In order to carry out conditional PCA and CCA, we simply condition the initial covariance matrix, using Equation 6.2. An interesting observation is that the conditioned covariance matrix of X_1 does not depend at all on x_2 but only on our choice of contracts that we use for the conditioning.

Note that Equation 6.1 results in a deterministic drift which is simply a linear function of the observed values x_2. This, for example, could be the expected drift in a uniformly distributed portfolio of Suezmax futures, conditional on the observed values of other futures relative to their long term mean values.

Say that we are interested in a portfolio of Suezmax futures with weights $\vec{a}$, such that the drift is maximized. The new portfolio, X_φ, has a covariance matrix Ψ based on the conditional expected values of its elements. Following an approach analogous to that of CCA, the maximization of the drift relative to the portfolio variance, results in the

vector equation of Equation 6.3 where $[\sigma_{22}]$ is the observable conditional covariance matrix (using the recent values x_2).

$$\left(\left[\left[\Sigma_{12}\right]\left[\Sigma_{22}\right]^{-1}\right]\sigma_{22}\left[\left[\Sigma_{12}\right]\left[\Sigma_{22}\right]^{-1}\right]^{-1} - \kappa\Psi\right)\vec{a} = 0 \qquad 6.3$$

κ is the largest value which satisfies $\left|\left[\left[\Sigma_{12}\right]\left[\Sigma_{22}\right]^{-1}\right]\sigma_{22}\left[\left[\Sigma_{12}\right]\left[\Sigma_{22}\right]^{-1}\right]^{-1} - \kappa\Psi\right| = 0$.

The solution of Equation 6.3 gives us the portfolio of Suezmax contracts that deviates maximally from its equilibrium, conditional on the observed values of other futures prices. Note that vector x_2 which contains the conditional observed values can take any size, so we are free to include whichever and as many futures as we consider relevant and adequate.

6.2 Cross Hedging Any Physical Exposure in Illiquid Markets

Suppose we have a VLCC on the spot market, and we want to hedge its earnings for the next 10 quarters. Our exposure to the physical market is evenly distributed across the various tenors. If the futures market for VLCC earnings is liquid, we can use that directly to get a "perfect" hedge. If it is illiquid, we may turn to Suezmax futures or another more liquid market, in order to cross hedge. The problem is almost the same as the one solved in Sections 2 and 5.1. The only difference is that now, vector $\vec{a}$ which contains the weights of the VLCC portfolio, is predefined to be a vector full of ones.

Consider another case. Suppose we have a Suezmax Tanker that is on a charter ending a year from now, and then enters into a follow-up charter half a year later. That leaves us with an exposure to the physical market for rolling quarters R5 and R6, which we may want to hedge. Again, if there is no liquidity for those tenors, we may turn to say, the PMX forward curve. The problem is again the same but with vector $\vec{a}$ (now corresponding to Suezmax futures weights) full of zeros except for the 5^{th} and 6^{th} element which are equal to one. In other words, we are looking for the maximum correlation between a unit each of R5 and R6 in the Suezmax forward curve with any combination of PMX futures of any tenor.

There are countless examples of physical exposures that one may wish to hedge using a different forward curve. The problem that needs to be solved in each case is essentially the same. By eliminating the zeros, we reduce the size of the portfolio vector $\vec{a}$ which contains the physical exposures that have to be hedged. Then we are left with a canonical correlation problem, with different size vectors $\vec{a}$ and $\vec{\beta}$. Note that in order for the matrix multiplications to be possible, the vectors must be arranged so that $p_1 \leq p_2$ i.e. the smaller vector corresponding to the physical exposure should be $\vec{a}$, and the full vector of the chosen liquid market should be $\vec{\beta}$. The eigenvalue problem has to be solved subject to the constraint that all the elements in $\vec{a}$ are equal to each other if we have an equal physical exposure to each of the contracts. The resulting $\vec{w}^*$ matrix will

then have to be normalized with respect to the first element being equal to 1 (or any required value).

To solve the problem, we use the fact that portfolios, and hence results, can simply be superimposed. Instead of solving the CCA problem for a reduced size portfolio vector $\vec{a}$ (containing p_1 elements) with the constraint that its elements must be equal to each other, we break it down into p_1 problems with vectors $\vec{a}$ having only 1 element. In other words, we correlate each element of vector $\vec{a}$ with vector $\vec{\beta}$ separately and then combine the results. Each CCA will result in a $\vec{w}^*$ matrix of $1+p_1$ elements. We then normalize all these matrices such that their first element is equal to 1. Then, we exclude the first elements (those equal to 1) so we are left with the optimized $\vec{\beta}$ vectors and we superimpose those to get the portfolio that has maximum correlation with the initial vector $\vec{a}$ that is full of ones.

By breaking down the initial $\vec{a}$ vector into single element vectors, then carrying out CCA with each element, and then superimposing the results, we can find the maximum correlation for any combination of physical exposures. If for example we have double the exposure in one of the quarters, then we normalize the corresponding $\vec{w}^*$ such that its first element is equal to two before superimposing, and so on.

Note that one should use the relevant covariance matrices (using trended or de-trended volatility) depending on whether they wish to hedge the forward curve including its trend or just the volatility about the trend. The second case for example may apply if one is already naturally hedged against trend fluctuations. For example, a global recession may impact ones revenues (the spot market) but also ones costs and interest payments in the same direction which means that they are already naturally hedged to some extent against global recessions. Under that scenario, an attempt to hedge the trend may leave them exposed, so it may be best to only hedge volatility about the trend using the de-trended volatility covariance matrices.

6.3 Temporal vs. Sectoral Separation for CCA

In some cases, there may be liquidity for only a part of a certain forward curve. In tankers, for example, there is usually higher liquidity for the prompt quarters. If there is illiquidity for the contracts corresponding to the physical exposure that we wish to hedge, we may choose to cross-hedge with a different forward curve or we may wish to cross hedge with contracts of different tenors within the same forward curve. To do that, we simply divide our vector $\vec{a}$ into two sub-vectors and perform CCA on those two. This is called temporal separation of the forward curve as opposed to sectoral separation that was discussed previously.

Suppose we want to hedge a specific quarter using contracts for other quarters of the same forward curve. The covariance matrix tells us directly the correlations between that quarter and each of the other quarters. By performing CCA between that quarter and the remaining $p_1 - 1$ rolling quarters of vector $\vec{a}$, we can identify the maximum correlation possible using a portfolio that consists of the whole remaining forward curve. We may also choose to include only a part of the remaining forward curve e.g. all the liquid contracts at the time when we are looking to hedge.

We could also go beyond that and combine temporal and sectoral separation for CCA. For example, if we wish to hedge our physical exposure to R9 of TD3 (VLCC), we can carry out CCA with vector $\vec{a}$ having a single element (TD3-R9) and with vector $\vec{\beta}$ including all liquid contracts of the other forward curves including the TD3 curve (e.g. the more prompt TD3 quarters which may be more liquid). Then, we normalize the resulting vector $\vec{w}^*$ such that its first element is unity. This gives us the portfolio of all the liquid contracts of shipping forward curves that we have chosen to include, that maximizes the correlation with R9 of TD3.

Note that again, we can carry out the analysis for each individual rolling quarter that we wish to hedge and then superimpose the results to get our complete portfolio. If for example our physical exposure is for both R9 and R10 of the TD3, we carry out the same analysis separately for each, and then combine the resulting portfolios.

6.4 Portfolio Optimization and Effective Diversification

Note, that the reverse problem of the one we have been solving can also be very useful. In order to diversify from a particular physical or derivative exposure, we should be solving for the minimum as opposed to the maximum correlation. In section 5.2, we looked at the possible range and the minimum correlations between various datasets. We saw that there is a limit to how low the correlation can be, particularly when including the trends. This limits our ability to diversify.

Say we have only one Panamax on the physical (spot) market for the next 2 years and we want to diversify within the shipping markets. Instead of physically diversifying, which would potentially involve buying or chartering in a different ship, we could use forward curves in a manner that is both more practical and much more effective.

Our physical exposure is evenly distributed across the next 8 rolling quarters. First, using CCA, we identify the combinations of other contracts that minimize the correlation with each of the 8 PMX rolling contracts. Then we create 8 portfolios, each of which diversifies our exposure to a different quarter. Then we combine these 8 portfolios, to achieve the maximum possible diversification within the chosen markets.

Note that a much lower correlation could potentially be achieved, offering better diversification, than simply investing in an additional ship of a different type. This is particularly true if we construct our vector $\vec{\beta}$ with contracts of various forward curves.

6.5 Other Applications

There are potentially countless applications for CCA using shipping forward curves. Some of the main examples such as hedging and trading, as well us the circumstances under which they would be particularly useful have been discussed. Other examples include cross hedging a physical exposure using another market due to lower friction costs including not only liquidity but perhaps lower commissions. Another application is the hedging of certain positions on the paper market when it is difficult to close them due to illiquidity, or the diversification of a portfolio of derivatives as well as physical exposures.

7. RAFL-Valuation of Tankers with Rolling Contracts

7.1 Introduction

The Risk Adjusted Forward Looking ship valuation model (RAFL) is a state of the art valuation model which combines both technical and financial aspects in a fundamental valuation based on risk-adjusted discounting of expected cash flows. A forward view of the main parameters is obtained from derivatives and financial securities that include shipping futures, FFAs, options, interest rate swaps and inflation protected bonds. The inherent risk of cracks is treated as a fictitious credit risk, derived from a reliability model, and is incorporated into the discount rate along with other risk premiums. Other inputs include repair costs and off-hire time, which are calculated with respect to ship age using a database of repairs, while the records of public and private companies are used along with surveys to estimate operating expenses.

The model produces valuations for Capesize bulk carriers that have been found to be in very close alignment with recent transaction prices across all ship ages. It also estimates the volatility of the ship value and uses it to price optionalities that are often included in ship transactions. For detailed information about the RAFL model and for a full application to the segment of Capesize bulk carriers, one should refer to [Hadjiyiannis 2010]. A complete application of the model requires a lot of detailed work including the analysis of a large database of cracks. In this section, we shall make some assumptions and apply a slightly simplified version of the model, using the rolling contracts that we developed, to produce valuations of generic double-hull Suezmax tankers as of the beginning of 2010.

7.2 Brief Overview of RAFL Ship Valuation Model

The RAFL model calculates the ship value by summing the risk adjusted expected monthly cash flows throughout the ship's 27.5-year life, as described by Equation 7.1

$$ShipValue = \sum_{n=1}^{Life-Age_0} \frac{\mathrm{Rev}_n - OpEx_n - \mathrm{Rep}Cost_n - P(fail)_n FailCost}{(1+i_n)^n} \quad 7.1$$

The numerator terms are the revenues, the operating expenses, the repair costs and the expected failure costs, all of which are functions of ship age and time. The discount rate in the denominator is calculated by equations 7.2 to 7.5.

$$i(t) = \left(1 + r'_{WACC}(t)\right) e^{12 S_t(t)} - 1 \quad 7.2$$

$$r'_{WACC}(t) = (1 - w_D) r_e + w_D(t) r_D(t) - I(t) \quad 7.3$$

$$S_t(t) = \frac{1}{t}\left[\frac{1}{18}\int_0^t \lambda(\tau)\,d\tau + \frac{9}{36}\int_{t-5}^t \lambda(\tau)\,d\tau + \frac{25}{36}\int_{t-1}^t \lambda(\tau)\,d\tau\right] \quad 7.4$$

$$r_e(t) = r_f(t) + \bar{\beta}_L MRP + \sum \overline{RP} \quad 7.5$$

The discount rate $i(t)$ is a function of leverage w_D (debt/asset value), the cost of equity r_e, cost of debt r_D, inflation $I(t)$ and the hazard function $\lambda(t)$. The hazard function throughout the ship's life is calculated by the customized ship reliability model developed in [Hadjiyiannis 2010]. Using the relevant parameters calculated by the analysis of a large database of hull cracks and casualty incidents, the hazard function for each repair interval "R" is given by Equation 7.6. The full analysis was applied to Capesize bulk carriers and the resulting hazard function is shown in Fig. 7.1.

$$\lambda_R(t) = c_R - A_R t^{b_R - 1} \qquad 7.6$$

$$c_0 = 0$$

$$c_{R\neq 0} = \frac{1}{T_{R-1}}\left[\frac{\sum_{j=UnInspAreas} D_{Rj}}{\sum_{j=AllAreas} D_{Rj}} + f_{RI}\right]\left\{c_{R-1}T_{R-1}(1-b_{R-1}) - b_{R-1}\ln\left[1-\left(w_1\frac{\sum_{R-1} Failures}{\sum_{R-1} Shipyears} + (1-w_1)(dD_{R-1}+e)\right)\right]\right\}$$

$$b_R = \left[\frac{1}{\ln 2}\right]\ln\left\{\frac{c_R T_R + \ln\left[1-\left(w_1\frac{\sum_{R} Failures}{\sum_{R} Shipyears} + (1-w_1)(dD_R+e)\right)\right]}{c_R\left(\frac{T_R}{2}\right) + \ln\left[1-\left[w_2\frac{\sum_{R}\sum_{t=0}^{t=T/2} Failures}{\sum_{R}\sum_{t=0}^{t=T} Failures} + (1-w_2)\frac{D_{t_R=T_R/2}}{D_R}\right]\left(w_1\frac{\sum_{R} Failures}{\sum_{R} Shipyears} + (1-w_1)(dD_R+e)\right)\right]}\right\}$$

$$A_R = \frac{b_R}{T_R^{b_R}}\left\langle \frac{T_R}{T_{R-1}}\left(\frac{\sum_{j=UnInspAreas} D_{Rj}}{\sum_{j=AllAreas} D_{Rj}} + f_{RI}\right)\left\{c_{R-1}T_{R-1}(1-b_{R-1}) - b_{R-1}\ln\left[1-\left(w_1\frac{\sum_{R-1} Failures}{\sum_{R-1} Shipyears} + (1-w_1)(dD_{R-1}+e)\right)\right]\right\} + \ln\left[1-\left(w_1\frac{\sum_{R} Failures}{\sum_{R} Shipyears} + (1-w_1)(dD_R+e)\right)\right]\right\rangle$$

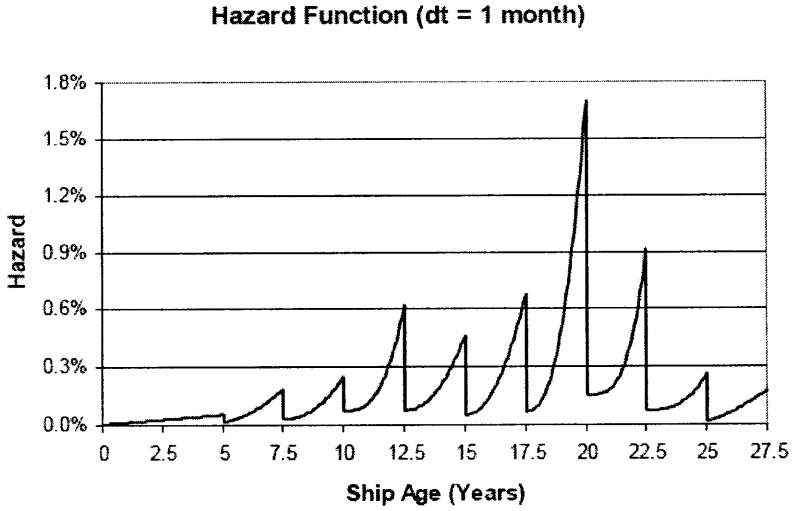

Fig 7.1 Hazard Function Throughout a Cape's Life [Hadjiyiannis 2010]

7.3 Applying the RAFL Model to Suezmax Tankers

7.3.1 Overview

The calculation of the numerator and denominator parameters as a function of time involves the analysis of forward looking parameters at the time of the valuation, including the risk free rate, inflation etc. Since we are carrying out the valuations for the beginning of 2010, which is the same as for the valuations of Capes in [Hadjiyiannis 2010], all we need to do is make the key relevant adjustments to those valuations as opposed to carrying out the complete analysis from scratch.

Starting from the numerator, the revenues initially given by the futures of Capes, will now be replaced by the rolling contracts for the TD5 which were developed earlier. That is because the TD5 is indeed very indicative of average earnings for Suezmax Tankers (it is used by the Baltic to quote average daily earnings).

The operating expenses and repair costs are a function of ship age and time. The base values and the variation with respect to age will be replaced by figures representative of typical Suezmax tankers. However, the function with respect to time, which depends on macroeconomic parameters such as inflation, will be kept the same.

The monthly probability of failure throughout the ship's life is approximated by the hazard function which will be scaled accordingly following a literature review presented in Section 7.3.2. It should be noted that the initial calculation of the hazard function for Capes involved the collection and analysis of a lot of data including ~30,000 cracks from 240 ships. The cost of failures, however, is significantly higher for the Suezmax, both because the repairs are more difficult to carry out and because of the risk of pollution, so these figures have to be adjusted accordingly.

Regarding the discount rate, the hazard function will simply be scaled as explained previously. The cost of debt and the leverage as a function of age and time will be kept the same as for Capes. The cost of equity will be adjusted by changing the relevant betas and risk premiums while leaving the risk free rate as a function of time unchanged (this was derived from the term structure of interest rates).

7.3.2 Tanker vs. Bulk Carrier Reliability

The purpose here is to compare the structural reliability of a typical double hull Suezmax tanker to that of a typical single hull Capesize bulk carrier. An important thing to consider is the impact of fatigue and corrosion as the ship ages since that will be different for the two ship types.

On a high level, we would expect the tanker to be stronger due to the absence of hatches. The double hull also gives it a greater moment of inertia about the neutral axis, which means that a given bending moment corresponds to a lower maximum bending stress at the outermost fibers. High loading rates of up to 16,000tons per hour, occasional impact by 30ton grabs during discharge, and alternating voyages between abrasive iron ore and corrosive coal cargos, result in severe fatigue and hull degradation for the bulk carrier with respect to age. Lastly, due to the potential environmental impact of oil pollution, one would expect that tankers are built to better specifications and are required to adhere to higher maintenance standards.

Various methods have been developed to model corrosion and fatigue in ageing vessels as well as their impact on hull strength and reliability. One of the most systematic and complete approaches is developed in [Paik et al 2003]. They examine the time dependent ultimate longitudinal strength reliability of a 170,000dwt bulk carrier, a 105,000dwt double hull tanker and a 254,000dwt single hull tanker type FPSO unit under vertical bending moments, accounting for corrosion, fatigue cracking and denting damage. Their method is based on a calculation of strength "reduction factors" for each structural member due to fatigue, corrosion and denting. The reduction factors are then used to relate the current ultimate strength to the original (intact) ultimate strength of each member. The fatigue crack, general / pitting corrosion and local denting damage reduction factors are calculated by Equations 7.7 to 7.9 respectively.

$$R_{xr} = \frac{CurrentStrength}{OriginalStrength} = \frac{\sigma_u (A_o - A_c)}{\sigma_u A_o} = \frac{A_o - A_c}{A_o} \qquad 7.7$$

$$R_{xr} = \left(\frac{A_o - A_r}{A_o} \right)^{0.73} \qquad 7.8$$

$$R_{xd} = C_3 \left[C_1 \ln\left(\frac{d}{t} \right) + C_2 \right] \qquad 7.9$$

A_o is the original plate area, A_c is the plate area no longer contributing to longitudinal strength due to the presence of the crack, A_r is the area involved by pit corrosion at the smallest cross section, d is the dent depth, t is the plate thickness and C_1, C_2 and C_3 are empirically determined regression coefficients.

To calculate the extent of corrosion, they assume a model of the form $t_r = C_1 (T - T_c - T_t)^{C_2}$, where t_r is the corrosion depth, T is time (life of the component), T_c is the coating life, T_t is the transition time between coating failure and corrosion initiation, and C_1, C_2 are coefficients determined by statistical analysis [Paik and Thayamballi 2002].

Fatigue cracking is modeled using the Paris-Erdogan Law, $\frac{\partial a}{\partial N} = A(\Delta K)^n = A\left(Y \Delta\sigma \sqrt{\pi a}\right)^n$, where α is the crack length, N is the number of stress cycles, A and n are material properties, and K is the stress intensity defined by the applied stress σ and the geometric factor Y. This is a more rigorous approach than the cumulative damage models conventionally used in the industry which are usually based on S-N curves (a plot of the number of cycles to failure against stress level), combined with Miner's rule ($D = \sum_j D_j \leq 1$, where D_j is the fatigue damage of each load). Recent examples of those include the Joint Tanker Project (JTP) and Joint bulker project (JBP) analysis procedures described by [Lotsberg 2006].

Limitations of the approach of [Paik et al 2003] include the fact that the Paris-Erdogan law, in its original form, is known to produce over-conservative results in complicated structures such as ships [Hadjiyiannis 2010], while as discussed by [Ok et al 2007], the effects of different pitting locations and pitting lengths, which were not

considered in this study, may contribute significantly to strength reduction. [Amlashi and Moan 2005] explore the effects of pitting corrosion in more detail. The great benefit of the approach of [Paik et al 2003] is the easy combination of the various effects. The total reduction factor for each component is simply the product of the individual reduction factors (R's).

Using this model, they go on to calculate the time varying reliability index and probability of failure under various scenarios for the three ship types. They also incorporate the effect of repairs which are scheduled based on the IACS requirement that the longitudinal strength should remain above 90% of its original value. Some key parameters of the bulk carrier and double hull tanker are summarized in Table 7.1.

PARAMETER	SYMBOL	BULK CARRIER (170,000DWT)	D.HULL TANKER (105,000DWT)
Cross Sectional Area	A_X (m^2)	5.652	5.318
Height of Neutral Axis	h_{NA} (m)	11.188	9.188
Neutral Axis to Depth	h_{NA}/D	42%	43%
Moment of Inertia	I (m^4)	694.3	359.5
Deck Section Modulus	Z_D (m^3)	44.354	29.679
Bottom Section Modulus	Z_B (m^3)	62.058	39.126

Table 7.1 Key Parameters of Double Hull Tanker and Bulk Carrier Considered by [Paik et al 2003]

The reliability index and probability of failure stays flat for the first 5 years before corrosion, fatigue and damages begin to have an effect. Then there is a gradual increase with sudden spikes during repairs. For both the bulk carrier and the double hull tanker, the probability of failure is initially about 0.01 and then fluctuates between 0.02 and 0.05 throughout the ship's life. Using a similar approach, [Wang et. Al 2003] calculates the reliability index of an oil tanker under various corrosion levels as shown in Fig. 7.2

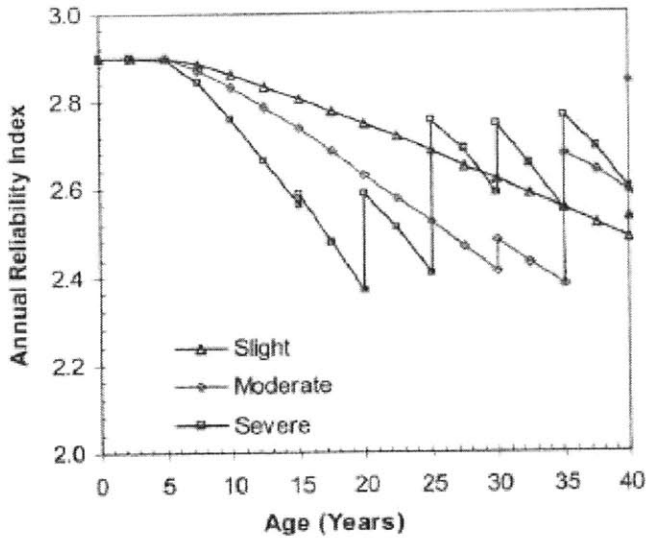

Fig. 7.2 Annual Reliability Index of Hull Girder Strength of an Oil Tanker for different Corrosion Levels [Wang et al 2003]

[Husein and Guedes Soares 2009] carry out a reliability analysis for a Suezmax Tanker and Handymax bulk carrier under various loading conditions. They use a stochastic model for both the still water and wave induced bending moments and evaluate the corresponding stresses after also calculating the effective position of the neutral axis in the non-linear elasto-plastic domain. The reliability analysis is performed using the computer program COMREL [Gollwitzer et al 1988], and the limit state equation corresponds to hull girder failure under vertical bending moment [Guedes Soares et al 1996, IACS 2006]. The reliability index for the tanker in the fully loaded sagging condition was 2.95 while for the bulk carrier it is summarized in Table 7.2.

RELIABILITY INDEX FOR HANDYMAX BULK CARRIER		
Loading Condition	Sagging	Hogging
Alternate Loading	1.429	2.562
Homogeneous	2.867	3.885
Ballast	1.182	2.32

Table 7.2 Reliability Index for the Handymax Bulk Carrier Under Various Loading Conditions [Husein and Guedes Soares 2009]

While the reliability index is acceptable for the tanker in the fully loaded condition (the only one considered) and for the bulk carrier in homogeneous loading and in all hogging states, it is very low for the bulk carrier in the sagging condition during ballast and alternate loading. This could be related to the hatch openings and stress concentrations discussed earlier. [Husein and Guedes Soares 2009] suggest increasing the thickness of the deck plating as a design modification to solve the problem.

[Bai 2006] applied reliability assessment to a double hull tanker to get the time dependent reliability index and probability of failure considering age related degradations including corrosion and fatigue. The results are shown in Fig. 7.3. We see the probability of failure reaching 7% immediately before the repairs.

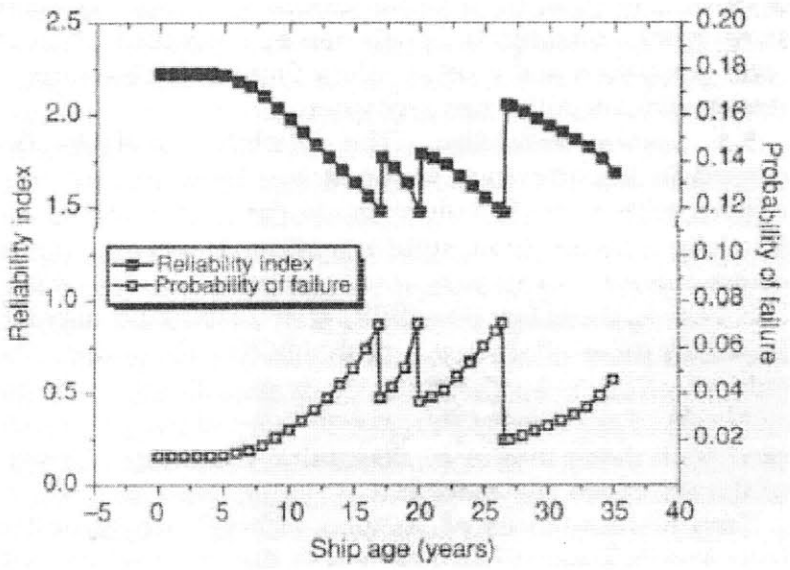

Fig 7.3. Time Dependent Reliability Index of a Double Hull Tanker Considering the Repair Scheme, Corrosion and Fatigue Cracks [Bai 2006]

[Debek & Konieczny 2006] carry out safety analysis on a Panamax bulk carrier using Comrel combined with the Adaptive Mote Carlo Method. The ultimate strength calculations were performed with the ALPS/HULL program. They calculate the probability of failure under each loading condition and in total using the 20-year Gumbel distribution and predicting values for the 1-year distribution.

	BALLAST	HOMOGEN	ALTERNATE	TOTAL
Fraction of Ship Life (15% at harbor)	35%	25%	25%	100%
Hull Failure Probability - 20 Years	0.0487%	14%	4.25%	18.3%
B - 20 years	3.3	1.08	1.72	0.91
Hull Failure Prob. - 1 Year (predicted)	0.00462%	1.26%	0.398%	1.61%
B - 20 years (predicted)	3.92	2.24	2.66	2.14

Table 7.3 Reliability Results for Ultimate Hull Strength Calculated with Comrel for 20-years and predicted for 1-year [Debek & Konieczny 2006]

They also generate results for the 1-year safety index that can be directly compared with those of [Guedes Soares et al 1996] for Single and double hull tankers.

	D.HULL TANKER	S.HULL TANKER	PANAMAX BULK CARRIER
Sagging	2.74	3.39	2.24 (Homogeneous Loading)
Hogging	2.97	3.46	2.66 (Alternate Loading)

Table 7.4. Comparison of Safety Index (1-Year Gumbel β) Values for Single/Double Hull Tankers [Guedes Soares et al 1996] and for a Panamax Bulk Carrier [Debek & Konieczny 2006]

Note that $\beta=3.7$ (based on a 1-year Gumbel distribution) is normally considered the appropriate target safety index value for a new ship. That is higher than all the above values. Again we see that the tanker is a more reliable structure than the bulk carrier, even though none of them achieve the $\beta=3.7$ level.

Now that we have seen predictions and calculations of hull reliability and probability of failure it is interesting to see if there is agreement with casualty data. [IACS 2001] presents casualty statistics compiled over the 20-year period 1978-1998. The annual probability of hatch cover failure (for ILLC 66 Initial design) is predicted by structural reliability analysis at 0.0935% and estimated from casualty data at 0.029%-0.14%. This result shows some consistency. Table 7.4 provides a summary of the main results for bulk carriers.

	TOTAL LOSSES	SERIOUS CASUALTIES	FATALITIES	FATALITIES/ SHIP-YEAR
General Water Ingress	72	115	850	0.0115
Shell Failure	62	98	572	0.0078
Deck Fittings Failure	3	7	44	0.000598
Hatch Cover Failure	9	11	246	0.00334

Table 7.5. Risk Contributions in Bulk Carriers 1978-1998 [IACS 2001]

0.017 fatalities per ship year occurred over the 20 years on average in bulk carriers over 20,000dwt. Approximately 73 percent of those were due to hull damage (46% shell failure, 19% hatch cover failure and 8% other). Fig 7.4 compares the risk of fatality to the crew across various ship types based on the database of casualties.

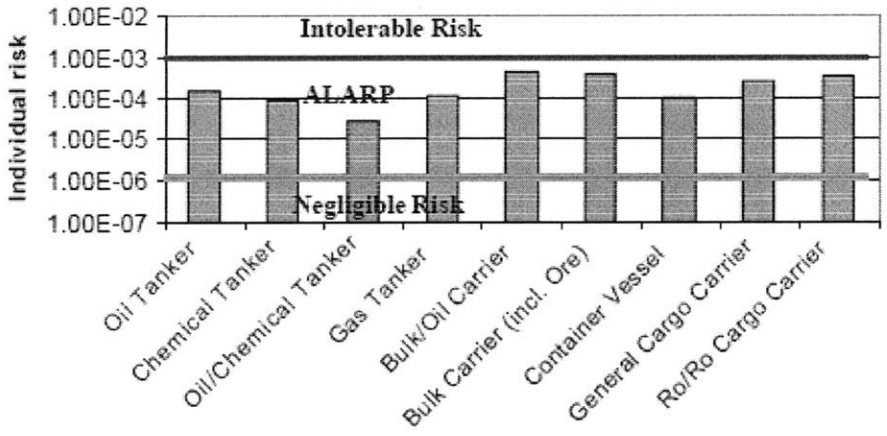

Fig 7.4. Risk of fatality to crew [IACS 2001]

Comparing the Oil Tanker with the Bulk Carrier (incl. Ore), we see that tankers are in general safer as is also predicted by the structural analysis of the publications discussed earlier. One thing to keep in mind is that double hull tankers have not been around for very long and this is even more important when examining pre-2000 data as in [IACS 2001]. The double hull was designed to increase safety but also has some drawbacks and according to the results of [Guedes Soares et al 1996] presented in Table 7.3, we can't draw definite conclusions. We will also have to wait in order to accumulate sufficient casualty data to draw reliable statistical conclusions.

7.3.3 The Hazard Function and Expected Failure Costs

Based on Section 7.3.3 and on discussions with experienced industry people, we can make an assumption about the hazard function and expected failure costs of a Suezmax tanker relative to those of a Capesize bulk carrier. Note that the RAFL model assumes three types of failures that occur with different probabilities. These are small emergency repairs, large emergency repairs and total loss.

We shall estimate that the hazard function i.e. the likelihood of failure is about one third for the Suezmax tanker while the failure costs about three times as high compared to the Cape. As discussed in Setcion 7.3.3, the hazard function is significantly lower because tankers are inherently stronger, they suffer less damage during cargo operations, and they have stricter regulations both in design and maintenance due to the possibility of oil pollution.

Failure costs, on the other hand, are significantly higher because repairs are more difficult and expensive due to the lack of hatch openings and the limitations on cutting and welding around areas with flammable gasses, while expected sinking costs are much higher due to the possibility of oil pollution. Note that the expected loss of hire and loss of ship value in the event of failure is incorporated via the hazard function into the discount rate in the denominator.

Since the scaling multiplier of the probability of failure cancels out with that of the cost of failure, the whole numerator term of expected failure costs is left unchanged. However, the hazard function also appears in the discount rate of the denominator where the scaling factor will have an effect.

7.3.4 The Discount Rate

The RAFL model valuation includes an estimation of the cost of equity for various market participants and then a weighted average calculation based on the percentage of the fleet owned by each group of participants. The build-up method is applied to each group starting from CAPM returns and adding various risk premiums such as size premium, liquidity premium, control premium, patient capital premium and non-diversification premium (using the total beta as opposed to market beta for private companies whose owners are heavily invested in them).

To simplify the analysis, we shall carry out the valuation from the perspective of a typical public shipping company that operates tankers. For our list of comparables, we select listed companies predominantly involved in the operation of tankers and particularly Suezmaxes. The list is presented in Table 7.6.

TICKER NAME	MARKET BETA	DEBT/ ASSETS	REV (M)	CASH/ REV	EXCESS CASH (M)	ASSET BETA	OP. ASSET BETA
TNP	0.79	58.93	444.93	**66.57%**	135.54	0.44	0.47
GMR	0.85	70.48	350.52	15.02%	0	0.39	0.39
FRO	1.23	74.02	1,133.29	7.29%	0	0.47	0.47
OSG	1.45	43.88	1,093.62	**43.41%**	107.29	0.90	0.93
TK	0.93	54.71	2,172.05	19.45%	0	0.53	0.53
VLCCF	1.02	32.13	67.34	11.82%	0	0.76	0.76
TOP	1.63	61.16	107.98	0.00%	0	0.76	0.76
CPLP	0.85	69.59	123.48	2.87%	0	0.40	0.40
MEAN			686.65	20.80%			**0.59**

Table 7.6 List of Comparable Tanker / Suezmax Public Companies

[Data from Googlefinance 2010]

The Asset beta is calculated using Equation 7.10 with the typical debt beta of 0.2. We then adjust for excess cash (defined as excess over the value which yields the average Cash/Revenues) using Equation 7.11, to get the operating asset beta.

$$\beta_A = \frac{D}{A}\beta_D + \left(1 - \frac{D}{A}\right)\beta_E \qquad 7.10$$

$$\beta_{OA} \approx \frac{A}{A - ExcCash}\beta_A \qquad 7.11$$

Since the valuation is from the perspective of a non-family owned public company with well diversified investors and high liquidity, we do not concern ourselves with patient capital, the total beta, control premiums and illiquidity premiums. The only CAPM adjustment is the size premium, using the famous Duff & Phelps relationships. In particular, we will use the Duff & Phelps relation between size premium over CAPM, and the log of the revenues, shown in Equation 7.12 [Pratt & Grabowsky 2008].

$$SP = 8.817 - 1.55\log(REV) \qquad 7.12$$

Since this is the only CAPM adjustment for the cost of equity, the sum of mean risk premiums is given by Equation 7.13 with the average annual revenues from our list of comparables ($686.65M).

$$\sum \overline{RP} = 8.817 - 1.55\log(686.65) = 4.42\% \qquad 7.13$$

Next, we have to re-lever the beta with the ship's leverage being a function of time, and assume a market risk premium for which we will use the typical value of 5.2%. After substituting back into Equation 7.5, our cost of equity takes the form:

$$r_E(t) = r_f(t) + \left(\frac{\beta_{OA} - w_D(t)\beta_D}{w_E(t)}\right)MRP + \sum \overline{RP} = r_f(t) + \left(\frac{0.59 - 0.2w_D(t)}{1 - w_D(t)}\right)5.2\% + 4.42\% \qquad 7.14$$

We then substitute Equation 7.14 into Equation 7.3 to get the inflation adjusted weighted average cost of capital as shown in Equation 7.15.

$$r'_{WACC}(t) = (1 - w_D(t))\left[r_f(t) + \left(\frac{0.59 - 0.2w_D(t)}{1 - w_D(t)} \right) 5.2\% + 4.42\% \right] + w_D(t) r_D(t) - I(t) \quad 7.15$$

The risk free rate $r_f(t)$ is obtained from the term structure of T-Bills as of the beginning of 2010, the cost of debt $r_D(t)$ has a constant 2.5% spread over $r_f(t)$, and inflation $I(t)$ is obtained from the term structures of TIPS and T-BILLS. We maintain the same assumptions regarding leverage $w_D(t)$ as for Capes. The debt linearly decreases from 70% to zero at the age of 17 for a new ship and at the age of 18.5 years for a 5-year old ship. For 10 or 15-year old vessels, the debt decreases from 60% to zero at 20 years. Older vessels are financed solely by equity.

Next, we incorporate the crack risk by solving Equation 7.4 using the scaled hazard function, and then we substitute into Equation 7.2 for the time varying discount rate. Table 7.7 summarizes the range in cost of equity and discount rate for the various ships throughout their life. Figure 7.5 shows the discount rate and discount factor throughout the new ship's life as an example.

SHIP AGE	NEW	5 YEAR	10 YEAR	15 YEAR	20 YEAR
Max Cost of Equity	12.6%	12.60	12.10	12.10	12.10
Min Cost of Equity	11.83%	11.83	10.78	10.13	7.87
Max Discount Rate	9.65%	9.55	9.42	9.18	9.15
Min Discount Rate	4.47%	4.47	4.86	4.87	6.42

Table 7.7 Range of Cost of Equity and Discount Rate for RAFL Valuations of Suezmax Tankers

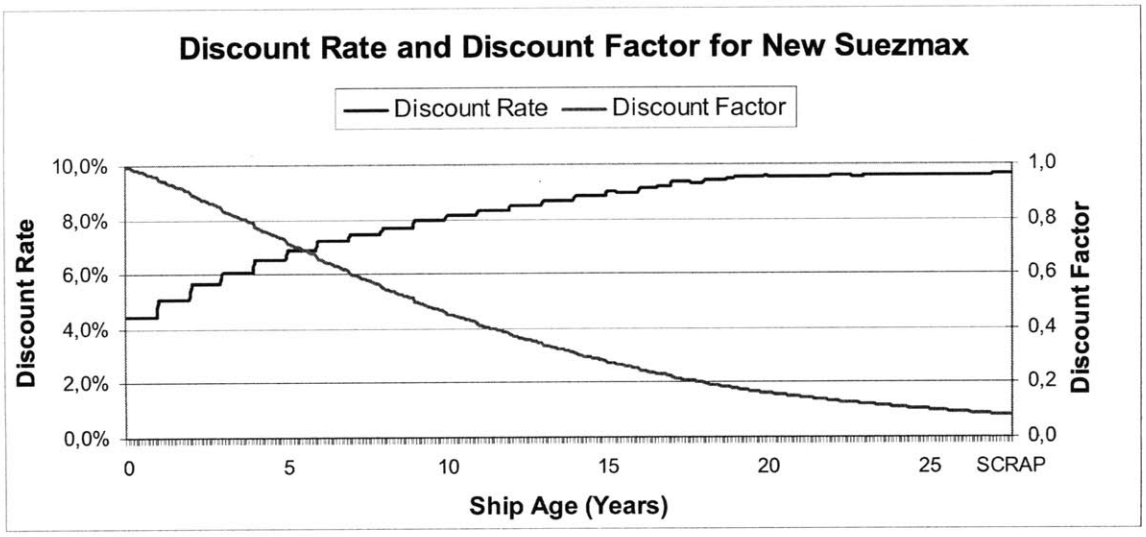

Fig 7.5 Discount Rate and Discount Factor Throughout the life of a New Suezmax

Excluding the 20-year old ship, the cost of equity range is between 10.13% and 12.6% while the discount rate range is between 4.47% and 9.65%. These values are considerably lower than for the valuation of Capes, predominantly because of the relatively low adjusted beta values of Tanker operating companies (0.59 compared to 1.34 for Capes). For the 20-year old Suezmax, the low cost of equity during the first years is mainly due to the low leverage (an all equity acquisition is assumed), combined with the low short term interest rates in January 2010 (0.38% for the first year).

7.3.5 Rolling Contracts and Projected Revenues

For the revenue projections, we start with the baseline revenues for a modern Suezmax, based on the rolling quarters of the earlier analysis. The value is held constant beyond the 10 rolling quarters. This introduces some inaccuracy relative to the Cape valuation because the liquid futures for Capes span out to 5 years as opposed to only 2.5, giving more reliable revenue projections. As for Capes, in order to get more stable values and eliminate uncertainty due to daily fluctuations, we take the average prices of the rolling contracts between November 2009 and February 2010 (centered about the beginning of the year). The results are summarized in Table 7.8

Period (Rolling Quarter)	Base Rate (Modern Suezmax)
R1	$26.192
R2	$22.777
R3	$23.181
R4	$25.351
R5	$28.670
R6	$28.965
R7	$28.985
R8	$29.027
R9	$29.069
R10	$29.111
Continuation	$29.111

Table 7.8 Base Rate for Modern Suezmax Tanker as of the Beginning of 2010

The forward curve is in backwardation for the first two quarters and then in contango thereafter. The results are not much different if we select a different period centered about the beginning of the year (e.g. 1 month before and after). Note also that

the curve is almost flat from R5 onwards, so the continuation value beyond R10 is not a bad assumption.

The adjustment for ship age has to be slightly different than that for Capes. Experience suggests that tankers up to 10 years old are considered modern and have approximately the same earnings. However, the decline with age for older ships is more pronounced than in Capes due to the risk of pollution and reputational consequences.

Therefore, we assume that a Suezmax has the same earnings until the age of 10, and 70% of the earnings of a new ship when at the age of 20 (as opposed to 80% for Capes). A regression of modern and 15 year old Suezmax earnings between January 2008 and July 2010, using data from [Clarksons 2010], suggests that a 15-year old Suezmax earns 87.5% as much as the modern Suezmax under 1-year time charters and 87.6% under 3-year time charters.

Based on the above, earnings are kept equal to the base values of Table 7.8 until the age of 10 years; they linearly decrease to 87.5% by the age of 15 years (2.5% less per year), 70% by the age of 20 years (3.5% less per year) and then continue decreasing at the same rate until the end of the ship's life at 27.5 years when it is earning 45.5% as much as a new ship. Note also that, as for Capes, a 5% commission on revenues is deducted to give net earnings.

Sensitivity analysis in [Hadjiyiannis 2010] suggested that the residual value is not a very important parameter, particularly for newer ships. Here it is assumed to be the same as for Capes ($5.5M when the ship is 27.5 years old) because the Suezmax has a typical lightship of 18,000t as opposed to 22,000t for Capes, but the scrap price for tankers in $/ton is usually slightly higher to make up for the difference. The scrap value of a Suezmax as reported by [Clarksons 2010], averaged at 4.96m between January 1976 and July 2010 with an upward trend, so our long term assumption is in the ballpark.

7.3.6 Operating & Repair Costs

Operating and repair costs vary with both age and time. Regular inflation has been accounted for in the discount rate so repair costs in the numerator are only a function of age. However, real inflation (over US inflation) of operating costs has to be accounted for in the other numerator term. The same real inflation of operating expenses is assumed as for Capes. That is 0.721%, linearly declining to zero over 30 years.

The variation of dry-dock and operating costs with respect to age is also assumed to take the same form as for Capes for which a detailed analysis had been carried out, since there are many similarities including class rules and repair scheduling. The base rates, however, have to be adjusted. This means that there will be a scaling of the Cape costs to match those of the Suezmax. For this purpose, we will consult the results of [Moore Stephens 2010], which are based on the analysis of large data samples.

According to [Moore Stephens 2010], average Cape and Suezmax dry-dock costs for the year 2009 were $1,909,589 and $1,757,652 respectively, while the average repair time was 29 and 28 days respectively. The difference in repair time is very small so the off-hire time due to repairs is left the same as for Capes. Note that the expected off-hire time due to failures is different for the two ship types and that is treated separately through the hazard function. Based on the average repair costs, Cape dry-dock costs are scaled by a factor of 0.92 to get the corresponding values for the Suezmax.

Based on [Moore Stephens 2010], Suezmax operating costs are composed of approximately 50% crew costs, 12% stores, 13% regular repairs and maintenance (non dry-dock), 10% insurance and 15% administration costs. Table 7.9 summarizes the average Cape and Suezmax daily operating costs for the years 2007, 2008 and 2009.

YEAR	SUEZMAX AVERAGE OP. COSTS ($/DAY)	CAPE AVERAGE OP. COSTS ($/DAY)	SUEZMAX / CAPE AVERAGE OP. COSTS
2009	9,309	7,512	1.239
2008	8,014	6,459	1.241
2007	7,316	6,082	1.203

Table 7.9 Cape and Suezmax Mean Operating Costs for Past 3 Years – Data from [Moore Stephens 2010]

Note that operating costs increased between 2008 and 2009 by 16.3% for Capes and by 16.2% for Suezmaxes which is almost identical. Based on the results of Table 7.9, the Suezmax base operating costs as a function of ship age are obtained by scaling the corresponding values for Capes by the average ratio of 1.23.

7.3.7 Value Volatility and Pricing of Optionalities

Following the analysis in [Hadjiyiannis 2010] which is based on portfolio theory, the annualized percentage volatility of the ship value boils down to the following simple approximation:

$$\sigma_{ShipVal} \approx \frac{1}{ShipVal}\sqrt{\sum_{i=1}^{10}\sum_{j=1}^{10} PV(\mathrm{Re}v_i)PV(\mathrm{Re}v_j)Cov(\mathrm{Re}v_i,\mathrm{Re}v_j)} \qquad 7.16$$

The indices "i" and "j" denote the periods of the rolling contracts. Since the price of the 10th rolling quarter is also assigned to the continuation value, the present value of the revenues for i=10 and j=10 include those from the beginning of the 10th rolling quarter up until the end of the ship's life (excluding the scrap value which is assigned zero volatility along with all costs).

The covariance between two assets is calculated as the percent variance of the two assets multiplied by the correlation between them. In [Hadjiyiannis 2010], the calculation is performed using Black-Implied volatilities from option prices. Here, we can use the covariance matrix developed earlier for the TD5 rolling contracts.

Having calculated the annualized percentage volatility of the ship's value, the Black-Scholes formula allows us to calculate the values of at-the-money call and put options with 1 week, 2 week, 2 month and 6 month tenors. This is for the pricing of optionalities such as purchase "subject to board of directors' (BOD) approval". The value of zero-dividend calls and puts is given by Equation 7.17 (Black-Scholes) and Equation 7.18 (put-call parity) respectively.

$$C = N\left(\frac{\ln\left(\frac{S}{PV(K)}\right)}{\sigma\sqrt{T}} + \frac{\sigma\sqrt{T}}{2}\right)S - N\left(\frac{\ln\left(\frac{S}{PV(K)}\right)}{\sigma\sqrt{T}} - \frac{\sigma\sqrt{T}}{2}\right)PV(K) \qquad 7.17$$

$$P = C - S + PV(K) \qquad 7.18$$

"PV" and "N" denote "present value" and "normal distribution" respectively. "S" is the price of the underlying and "K" is the strike price, both of which are set equal to the current ship value since we are only concerned with at-the-money options. Sensitivity of the option values "F" with respect to the various parameters is given by the Greeks which are defined in Equations 7.19 to 7.23.

$$\delta = \frac{\partial F}{\partial ShipVal} \qquad (7.19)$$

$$\Gamma = \frac{\partial^2 F}{\partial^2 ShipVal} \qquad (7.20)$$

$$\theta = \frac{\partial F}{\partial \tau} \qquad (7.21)$$

$$\delta = \frac{\partial F}{\partial r_f} \qquad (7.22)$$

$$\Lambda = \frac{\partial F}{\partial \sigma} \qquad (7.23)$$

Note that the option valuations have to be carried out using the risk free rate corresponding to their tenors. The term structure of T-Bills, which are used as a proxy to the risk free rate, was upward sloping at the beginning of 2010 with 1-week, 2-month and 1-year rates at 0.11%, 0.15% and 0.38% respectively.

7.3.8 Results

The RAFL valuation model was used with the adjustments and assumptions discussed in Sections 7.3.3 to 7.3.7. The resulting Suezmax values as of the beginning of 2010 are summarized along with their annualized volatilities in Table 7.10.

SHIP AGE	RAFL VALUATION	RAFL VOLATILITY
New	$73.43M	27.34%
5-Year	$61.04M	28.96%
10-Year	$43.56M	31.25%
15-Year	$26.20M	36.17%
20-Year	$12.39M	44.91%

Table 7.10 RAFL Suezmax Valuations for Beginning of 2010

Table 7.11 presents a summary of the reported Suezmax sale and purchase (S&P) transactions during the months of December 2009 and January 2010. Only the first entry was reported in December while the rest were in January.

SHIP NAME	DWT	BLT	PRICE	NOTES
Viking Crux	145,200	1991	$7.97M	Auction, SS-Due / Out of Class
Romea Champion	154,970	1992	$16.5M	For Conversion
Tropic Brilliance	154,970	1992	$16.5M	For Conversion
African Ruby	150,173	1994	$15M	
Tango	150,096	2008	$68M	
Waltz	150,096	2008	$68M	
South Sea	150,001	2005	$61M	
Navigator	149,996	2006	$63M	
Brillante Virtuoso	149,601	1992	$12.5M	

Table 7.11 Suezmax Transactions in Dec. 2009 and Jan 2010 [Cotzias 2009, Cotzias 2010]

Figure 7.6 shows a plot of the RAFL valuations as of Dec'09/Jan'10 along with the S&P transaction prices of Dec'09 and Jan'10. The assumed long term scrap value is shown in black at the age of 27.5 years.

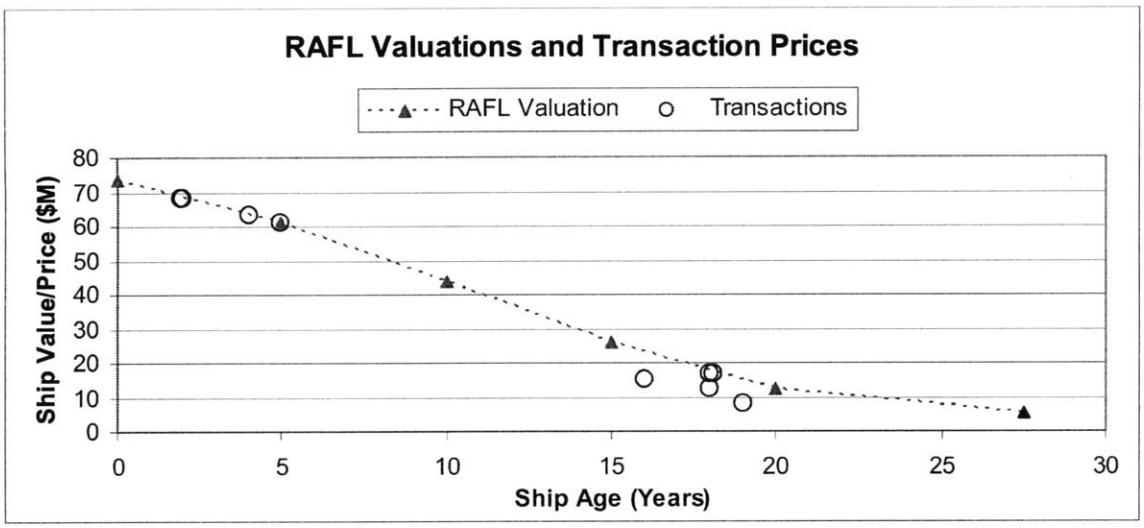

Fig 7.6 RAFL Suezmax Valuations and Actual Suezmax Transactions for Dec 2009 - Jan 2010

The RAFL valuations are remarkably similar to transaction prices, particularly for relatively modern ships. The RAFL model, however, produces valuations that are higher than some of the older vessel transaction prices. That may be for design and regulatory factors concerning older vessels that have not been factored into the model. The model makes no design or regulation distinction with respect to ship's age i.e. it predicts the value of a modern vessel as it ages. Currently older ships, however, may be single hull, meaning that they are about to be phased out, or they may be of the early double hull designs which are in some cases only have an extended phase out date.

For the reasons discussed above, a 27.5 year lifetime may not be a good assumption for the older vessels. Furthermore, their earnings may equal a smaller fraction of those of a new ship than the fraction assumed. Some of these ships are sold for conversion to other ship types so their price is governed by other factors. For example, the oldest vessel in the S&P transactions (the only one reported in December), which lies significantly below the RAFL valuation, was sold at an auction being out of class, with its special survey due. The cost to make this ship operational, either as a tanker or as a

converted ship, would have to be added to the transaction price, to make the comparison with the RAFL valuation more relevant.

Figure 7.7 shows the annualized ship value volatility calculated by the RAFL model as a function of the ship's age and Figure 7.8 shows the calculated Call option values. Since we are only dealing with zero-dividend, at-the-money options, call and put options are almost identical in value. The complete set of tabulated values along with the Greeks can be found in Appendix G.

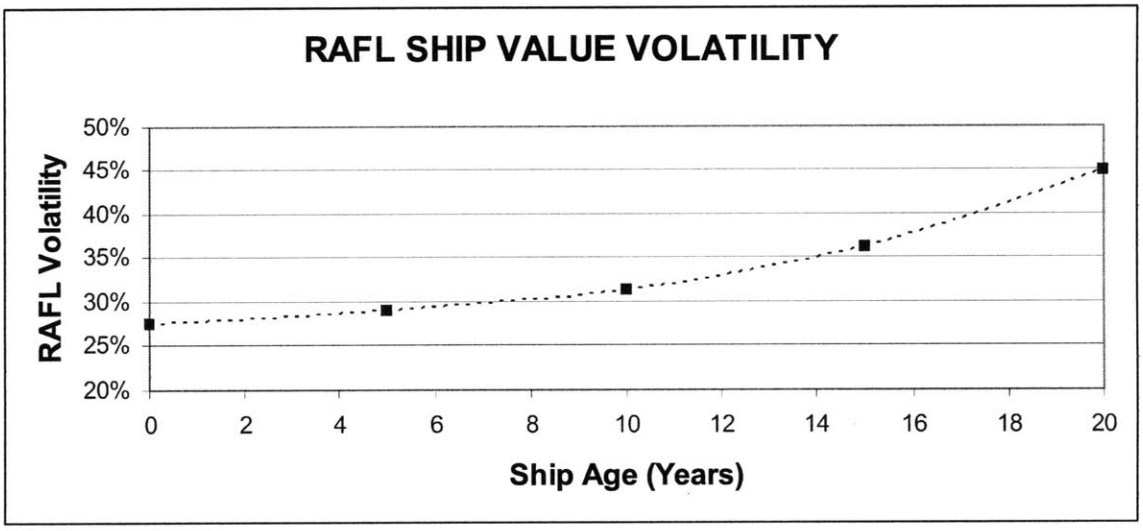

Fig 7.7 RAFL Suezmax Volatilities for Dec 2009 - Jan 2010 Valuations

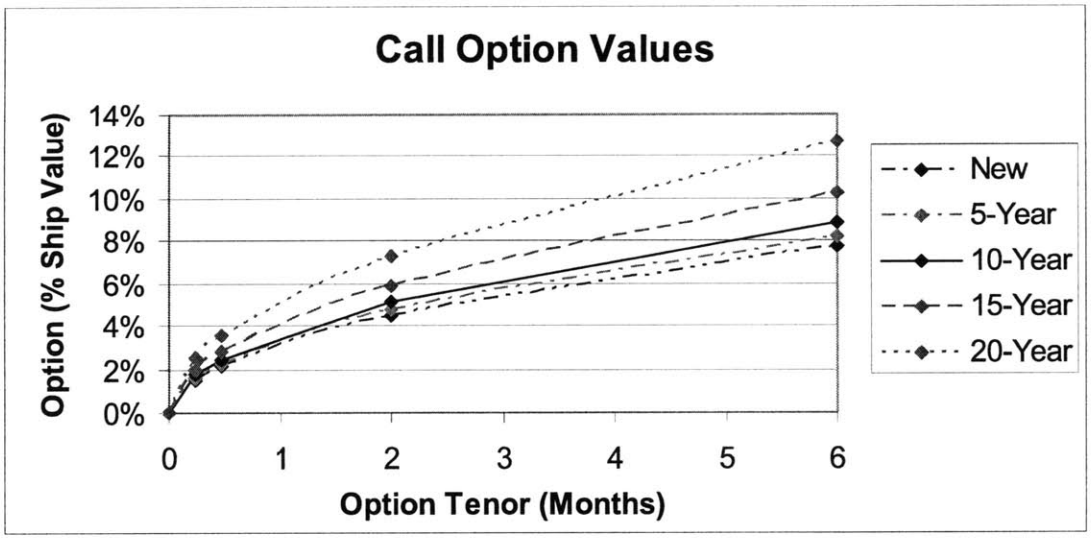

Fig 7.8 RAFL Suezmax Call Option Values for Dec 2009 - Jan 2010 Valuations

The ship value volatilities are significantly lower than the corresponding volatilities of Cape values but they follow the same trend with respect to ship age. This result is consistent with the lower adjusted beta value of 0.59 for the tanker companies relative to 1.34 for Capes.

The option prices for Suezmax tankers also follow the same pattern as for Capes but with lower values due to the lower volatility. As shown by Fig 7.8, the newer the ship and the shorter the option tenor, the lower the option value as a percentage of the ship value. Here again, option values are still very significant, running in the hundreds of thousands or millions of dollars, and therefore have to be considered seriously during transactions that involve optionalities such as the "subject to BOD approval".

8. Conclusions

Price series of the main liquid shipping forward curves have been analyzed in detail. The analysis began with the creation of price series for continuously rolling contracts in order to remove the effect of approaching maturity on the volatility dictated by the Samuelson hypothesis.

PCA was then carried out on these forward curves to demonstrate that a significant amount of their variation can be analyzed by a few principal components. The effect of the independent statistical factors was discussed, and it was shown that the task of explaining and predicting the various shipping forward curves can potentially be simplified substantially.

CCA was carried out, demonstrating that shipping curves are highly correlated when using both "trended" and "de-trended" volatility. The circumstances and the markets in which correlation is higher were identified and discussed. The results of this analysis can be used for a variety of purposes including trading from a hedge fund perspective, cross hedging any physical exposure in illiquid markets, portfolio optimization etc. These have been discussed in detail using several case studies.

Conditioning, which is one of the most powerful tools of multivariate statistics, is also examined in order to expand the information content of the unconditional PCA/CCA analysis for obtaining deterministic drifts and for demonstrating how the best trading opportunities can be unveiled conditional on recently observed data.

The RAFL ship valuation model was adjusted for its application to tankers and used with the rolling contract prices of Suezmax tankers. The resulting valuations were very close to transaction prices of the corresponding period for relatively modern vessels. Small deviations in older ships have been explained with regards to phase out regulations and other factors. The ship value volatility is smaller than for Capes but increases similarly with ship age. The option values for typical tenors are very significant, running in the hundreds of thousands or millions of dollars, and they increase as a percentage of the ship value with age. These results have to be considered seriously when optionalities are involved in shipping transactions.

9. Appendices

Appendix A - PCA Screen-Tests and Eigenvectors (De-Trended Vol.)

CAPE (22R)

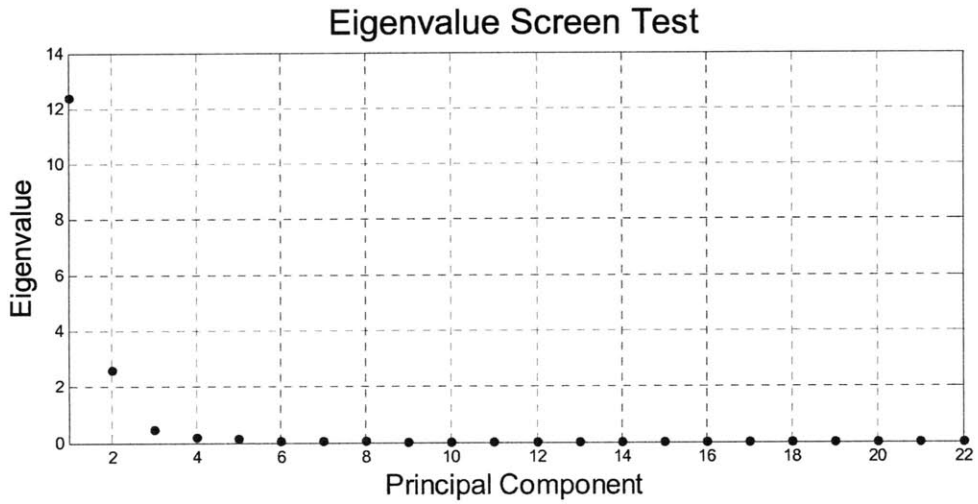

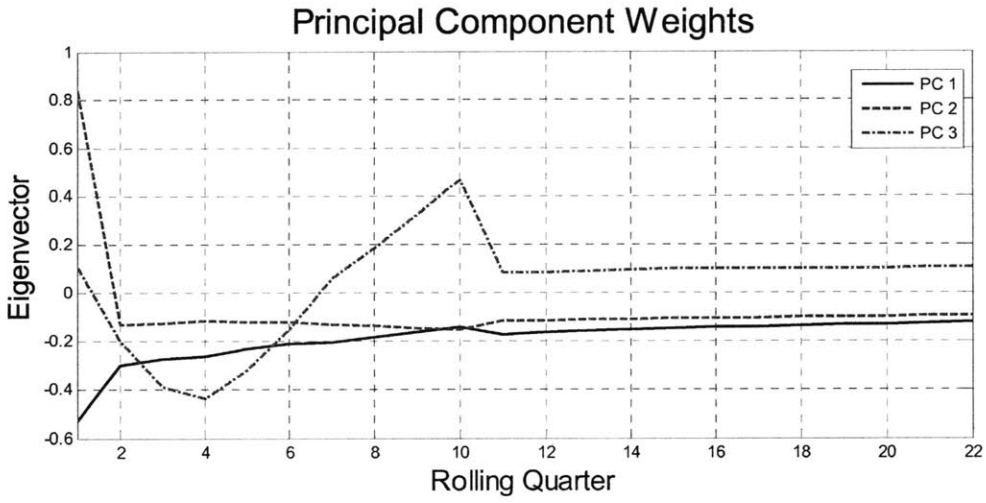

PMX (22R)

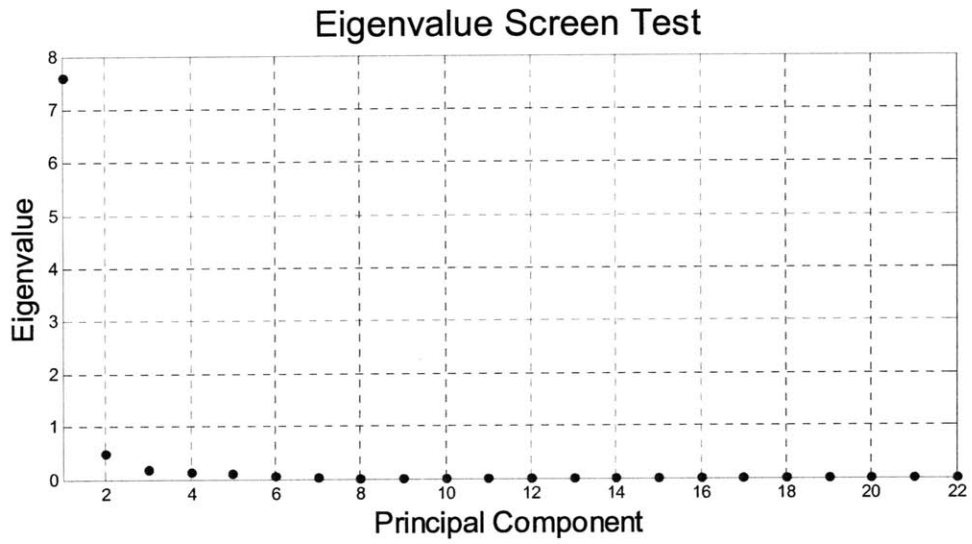
Eigenvalue Screen Test
Eigenvalue
Principal Component
0
1
2
3
4
5
6
7
8
2
4
6
8
10
12
14
16
18
20
22

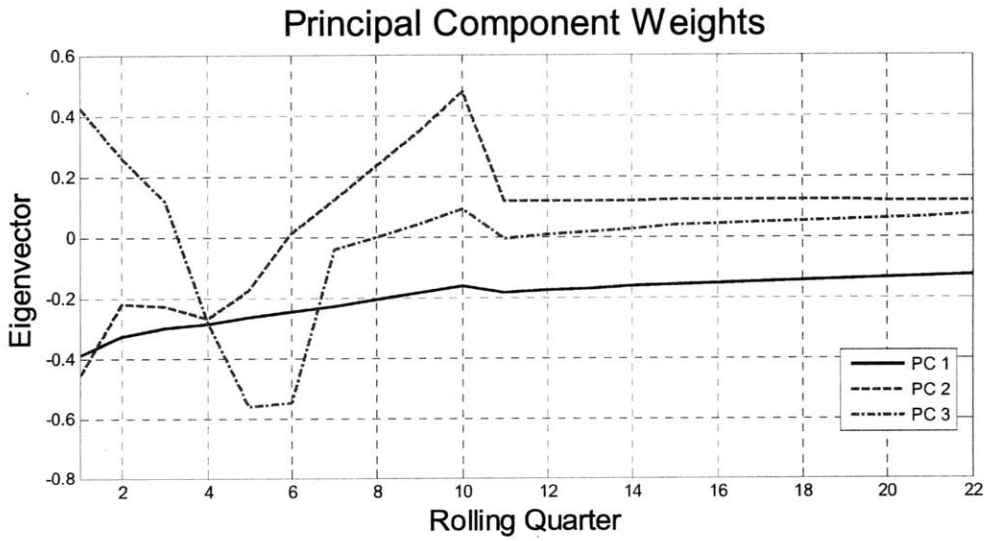
Principal Component Weights
Eigenvector
Rolling Quarter
PC 1
PC 2
PC 3
0.6
0.4
0.2
0
-0.2
-0.4
-0.6
-0.8
2
4
6
8
10
12
14
16
18
20
22

CAPE

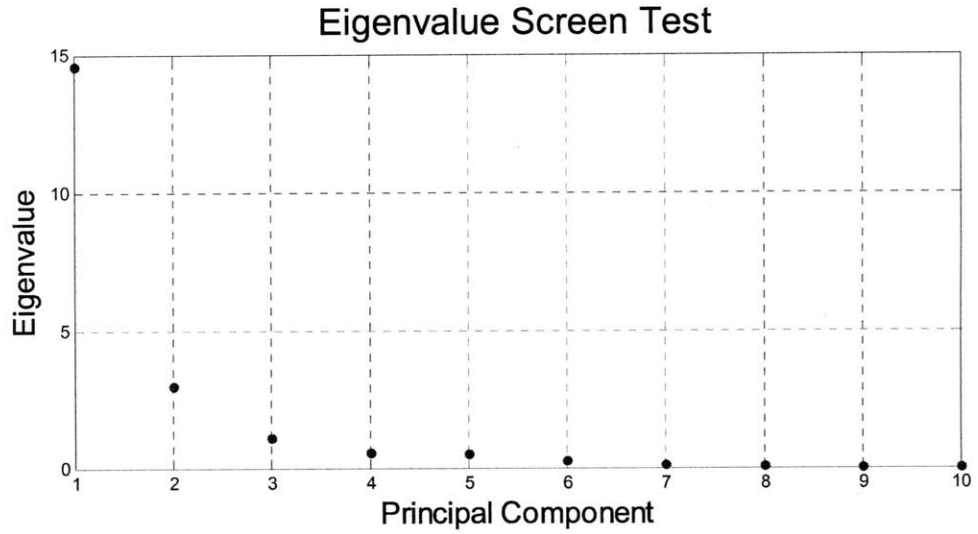
Eigenvalue Screen Test
Eigenvalue
Principal Component
15
10
5
0
1
2
3
4
5
6
7
8
9
10

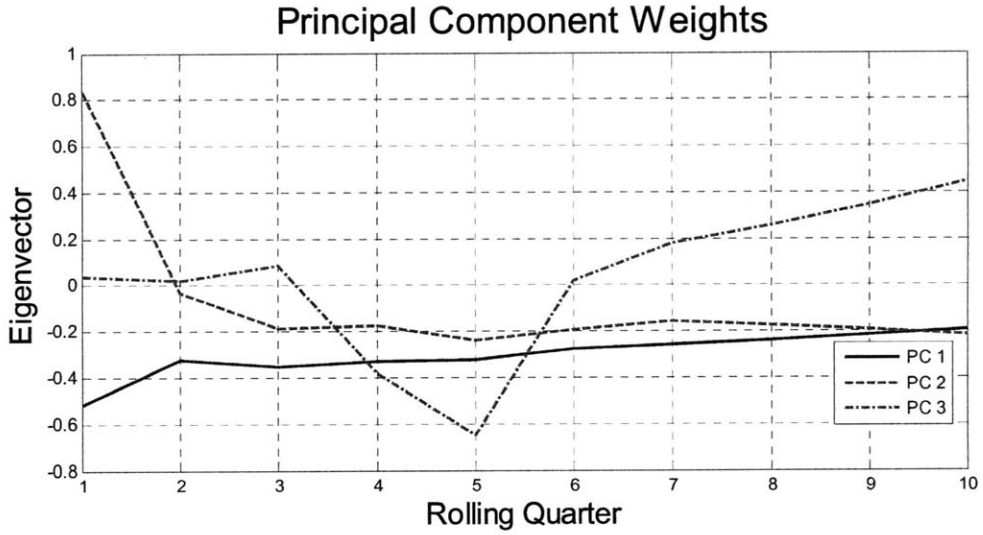
Principal Component Weights
Eigenvector
Rolling Quarter
PC 1
PC 2
PC 3
1
0.8
0.6
0.4
0.2
0
-0.2
-0.4
-0.6
-0.8
1
2
3
4
5
6
7
8
9
10

PMX

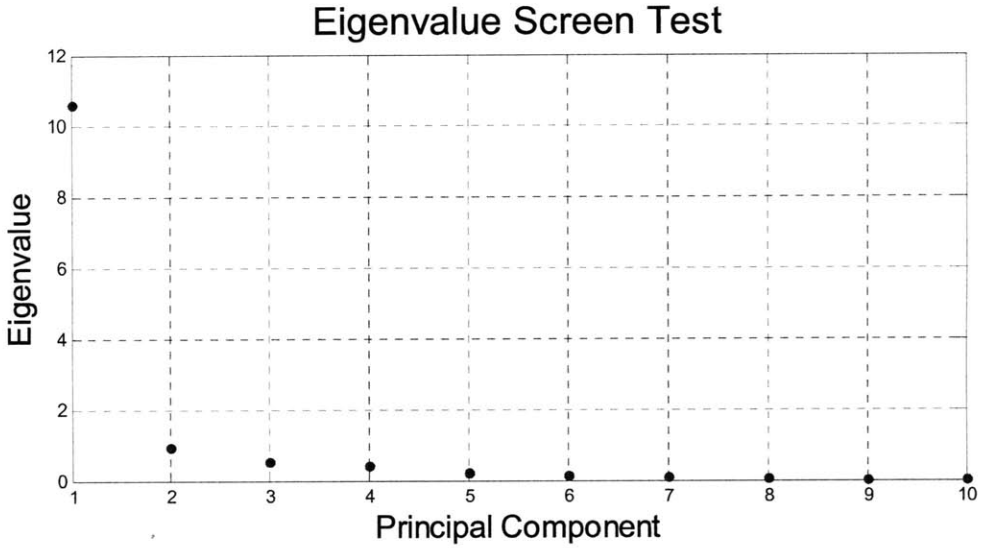
Eigenvalue Screen Test
Eigenvalue
Principal Component
0
2
4
6
8
10
12
1
2
3
4
5
6
7
8
9
10

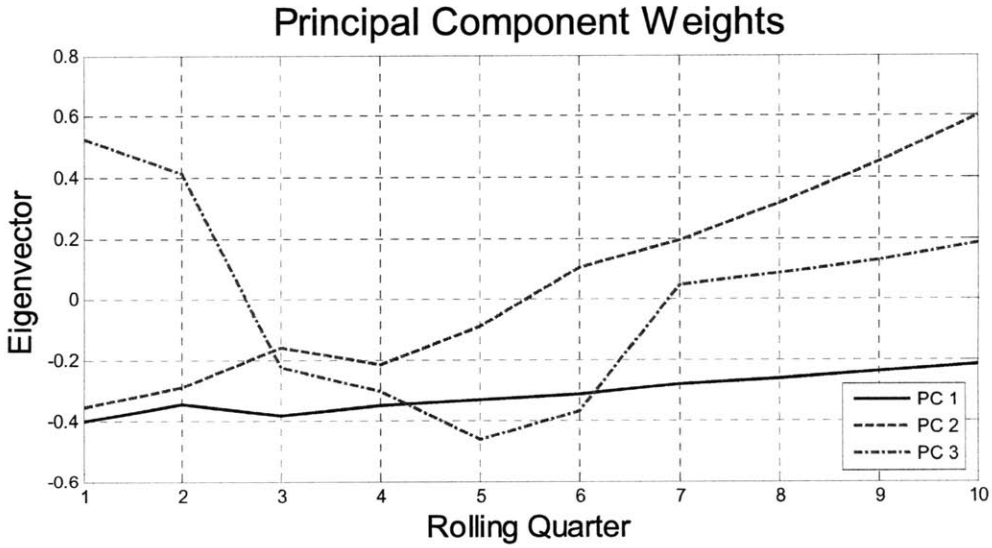
Principal Component Weights
Eigenvector
Rolling Quarter
PC 1
PC 2
PC 3
0.8
0.6
0.4
0.2
0
-0.2
-0.4
-0.6
1
2
3
4
5
6
7
8
9
10

TC2

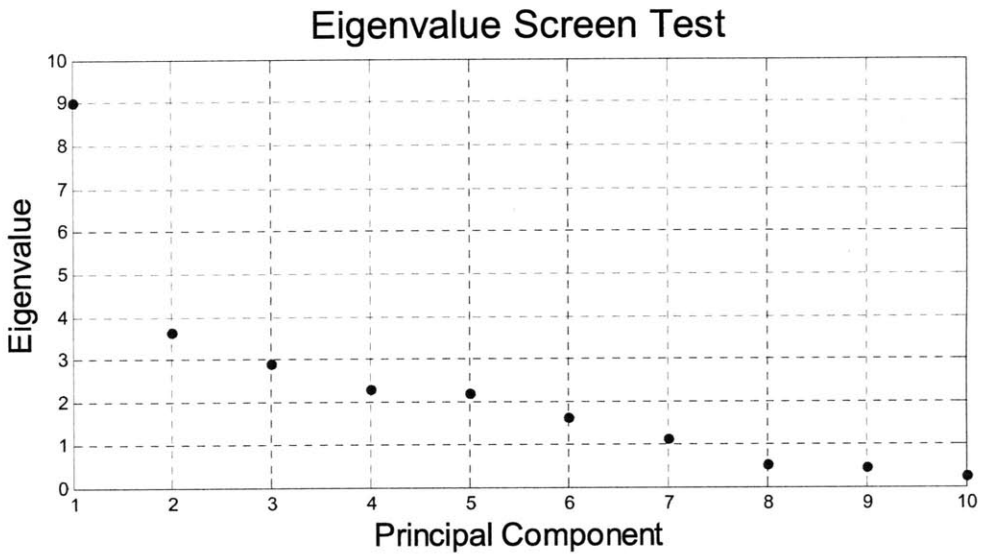
Eigenvalue Screen Test
Eigenvalue
Principal Component
0
1
2
3
4
5
6
7
8
9
10

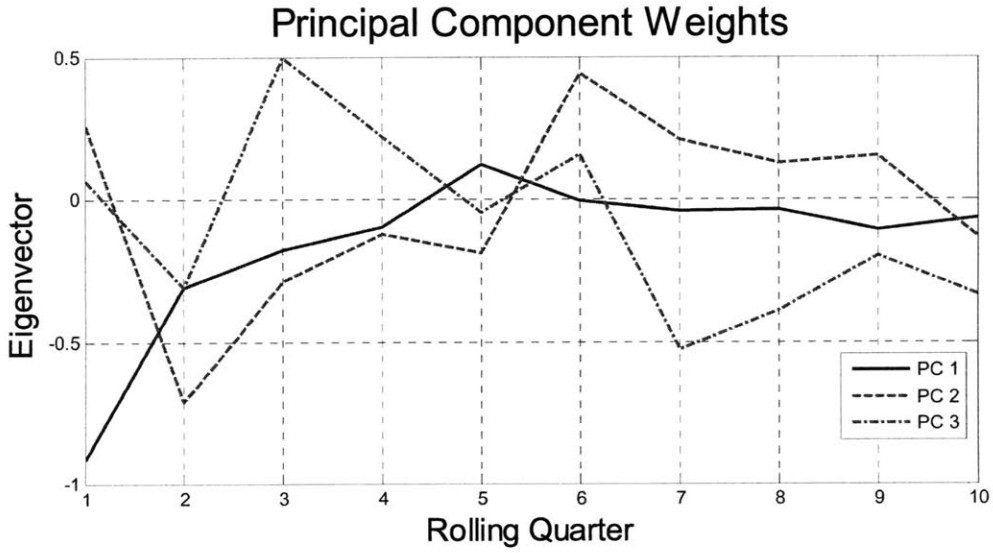
Principal Component Weights
Eigenvector
Rolling Quarter
PC 1
PC 2
PC 3
0.5
0
-0.5
-1
1
2
3
4
5
6
7
8
9
10

TD3

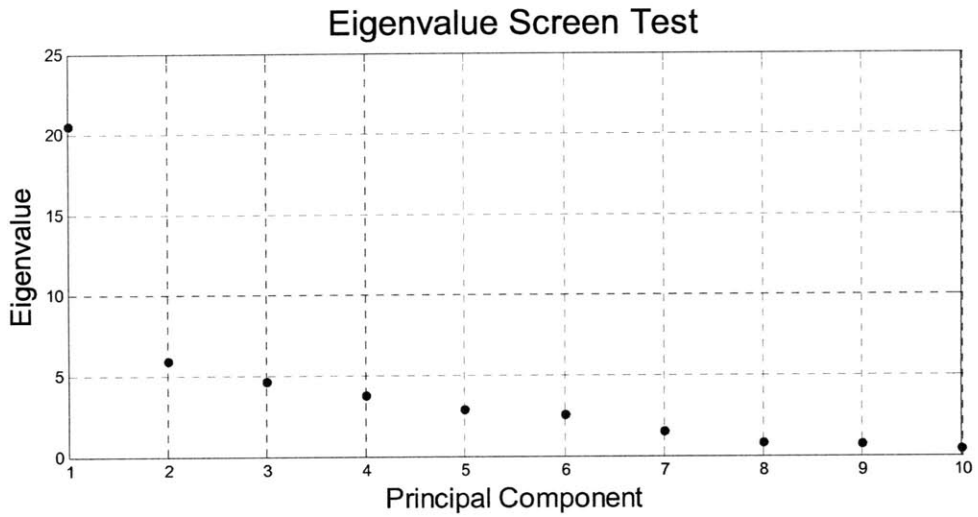
Eigenvalue Screen Test
Eigenvalue
Principal Component
0
5
10
15
20
25
1
2
3
4
5
6
7
8
9
10

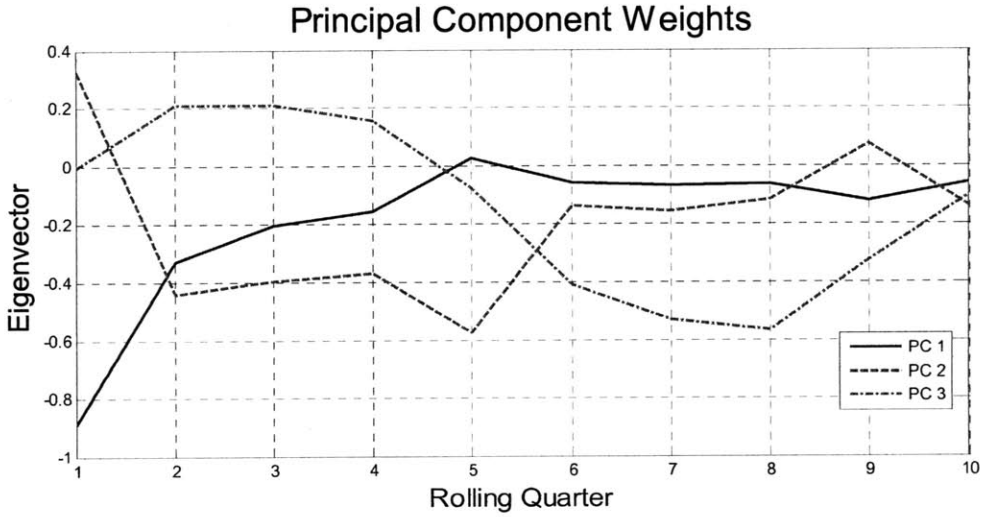
Principal Component Weights
Eigenvector
Rolling Quarter
PC 1
PC 2
PC 3
0.4
0.2
0
-0.2
-0.4
-0.6
-0.8
-1
1
2
3
4
5
6
7
8
9
10

TD5

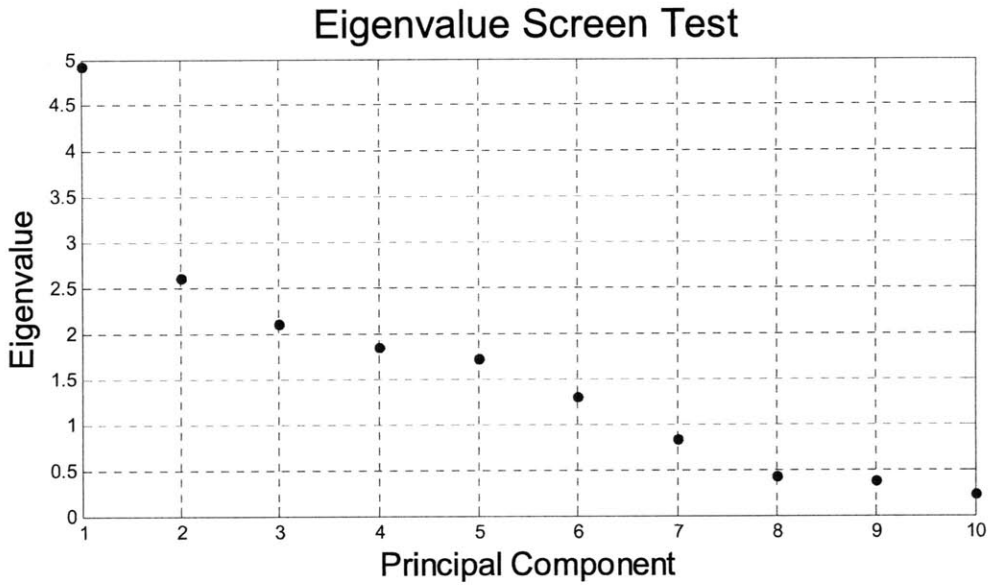
Eigenvalue Screen Test
Eigenvalue
Principal Component
5
4.5
4
3.5
3
2.5
2
1.5
1
0.5
0
1
2
3
4
5
6
7
8
9
10

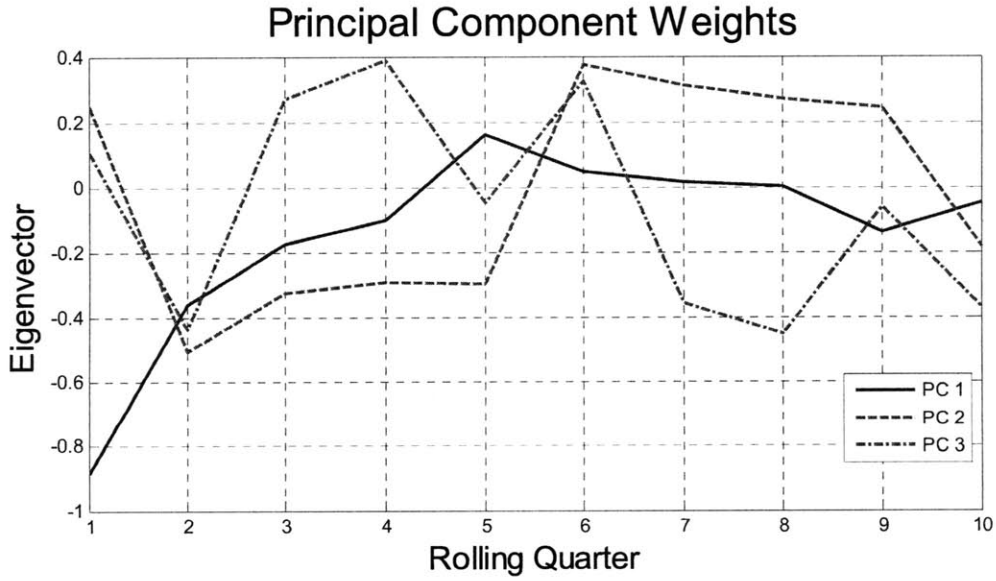
Principal Component Weights
Eigenvector
Rolling Quarter
0.4
0.2
0
-0.2
-0.4
-0.6
-0.8
-1
1
2
3
4
5
6
7
8
9
10
PC 1
PC 2
PC 3

TC2 (WS)

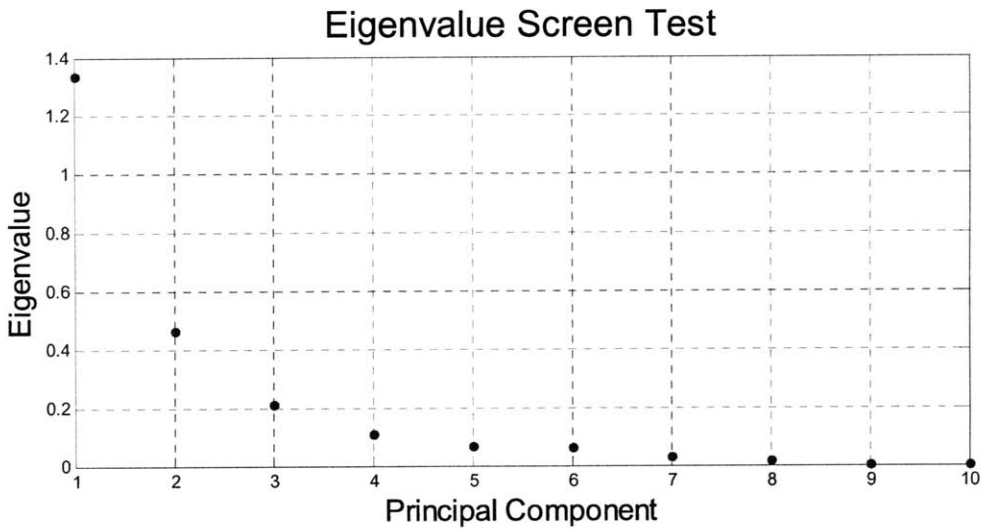
Eigenvalue Screen Test
Eigenvalue
Principal Component
1.4
1.2
1
0.8
0.6
0.4
0.2
0
1
2
3
4
5
6
7
8
9
10

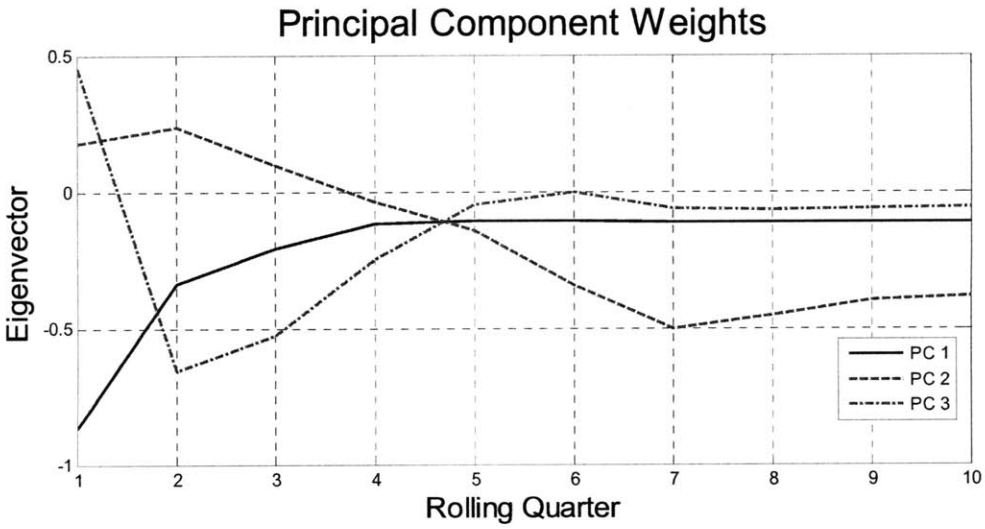
Principal Component Weights
Eigenvector
Rolling Quarter
0.5
0
-0.5
-1
1
2
3
4
5
6
7
8
9
10
PC 1
PC 2
PC 3

TD3 (WS)

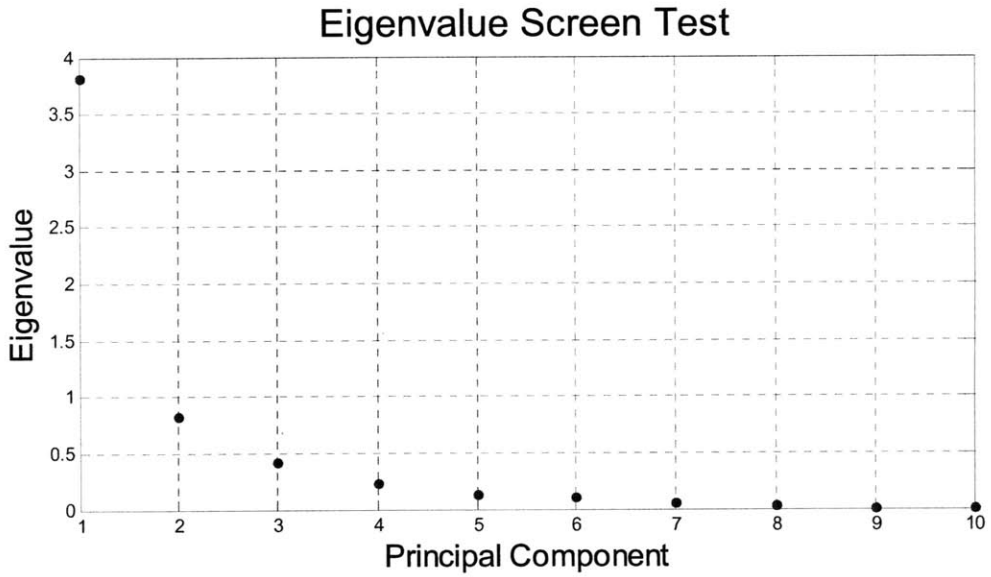
Eigenvalue Screen Test
Eigenvalue
Principal Component
0
0.5
1
1.5
2
2.5
3
3.5
4
1
2
3
4
5
6
7
8
9
10

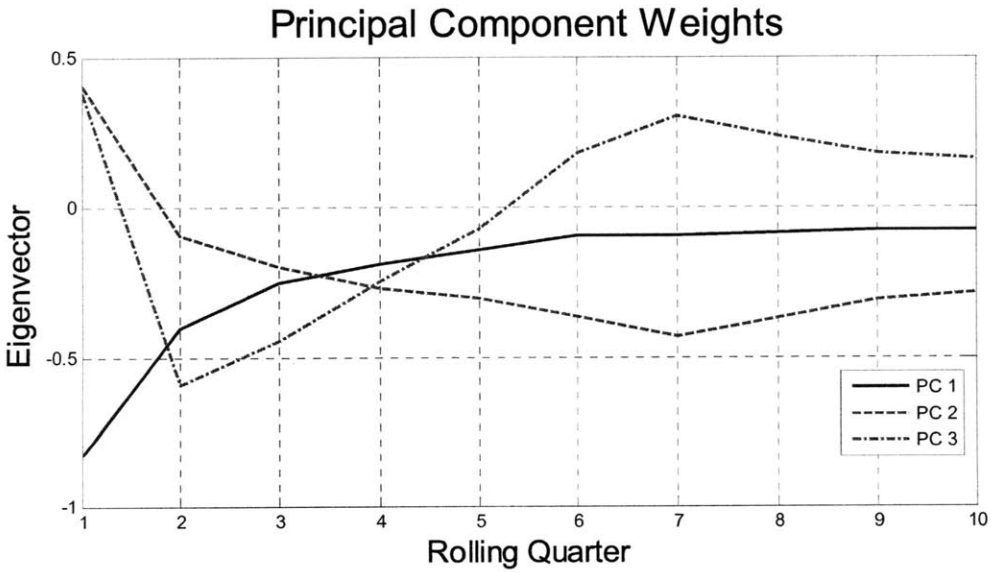
Principal Component Weights
Eigenvector
Rolling Quarter
PC 1
PC 2
PC 3
0.5
0
-0.5
-1
1
2
3
4
5
6
7
8
9
10

TD5 (WS)

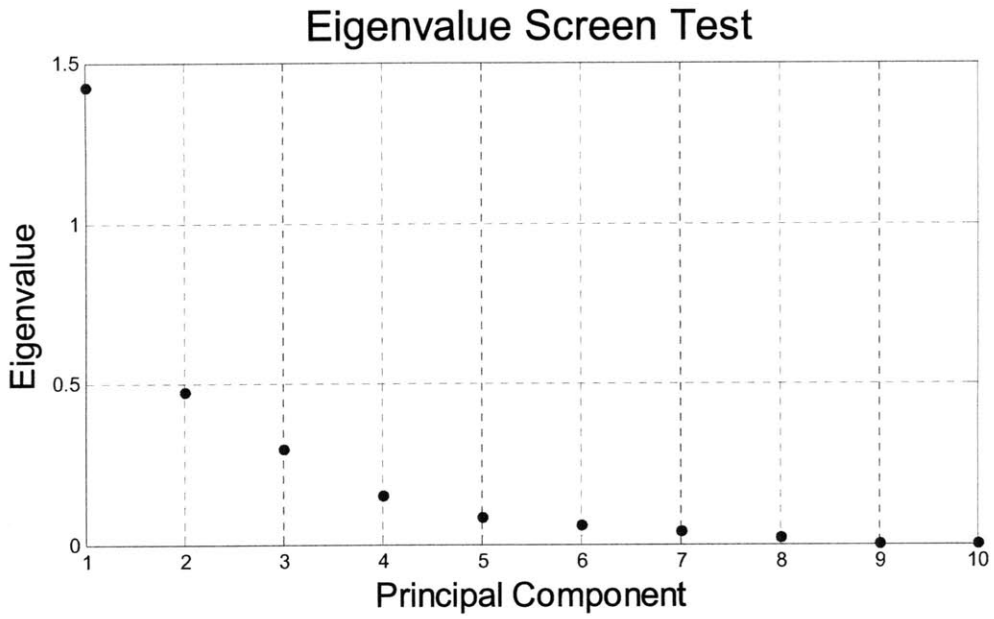
Eigenvalue Screen Test
Eigenvalue
Principal Component
1.5
1
0.5
0
1
2
3
4
5
6
7
8
9
10

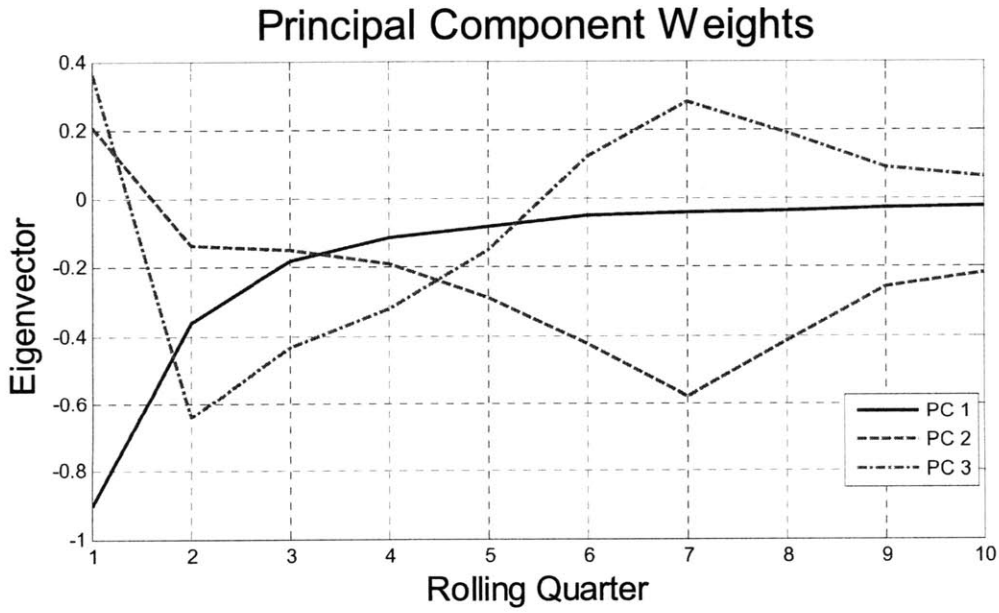
Principal Component Weights
Eigenvector
Rolling Quarter
0.4
0.2
0
-0.2
-0.4
-0.6
-0.8
-1
1
2
3
4
5
6
7
8
9
10
PC 1
PC 2
PC 3

Appendix B - PCA Screen-Tests and Eigenvectors (Trended Vol.)

CAPE (22R)

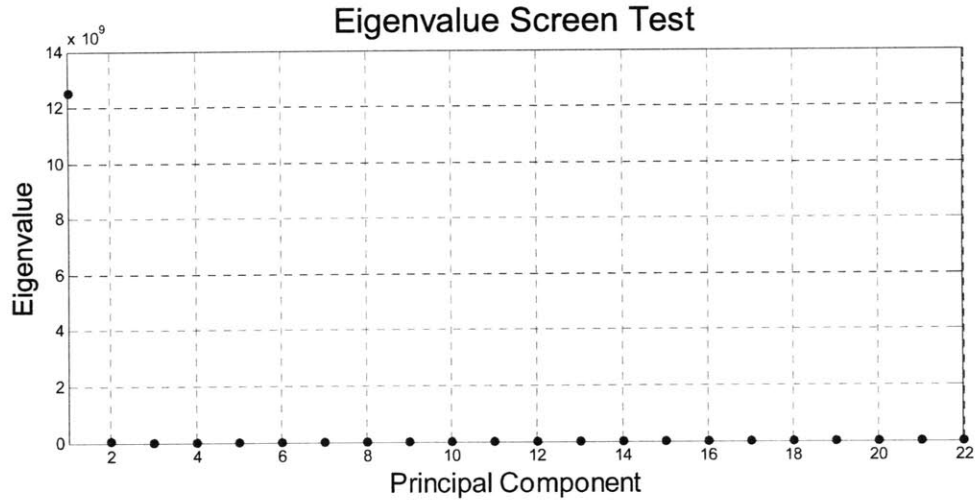

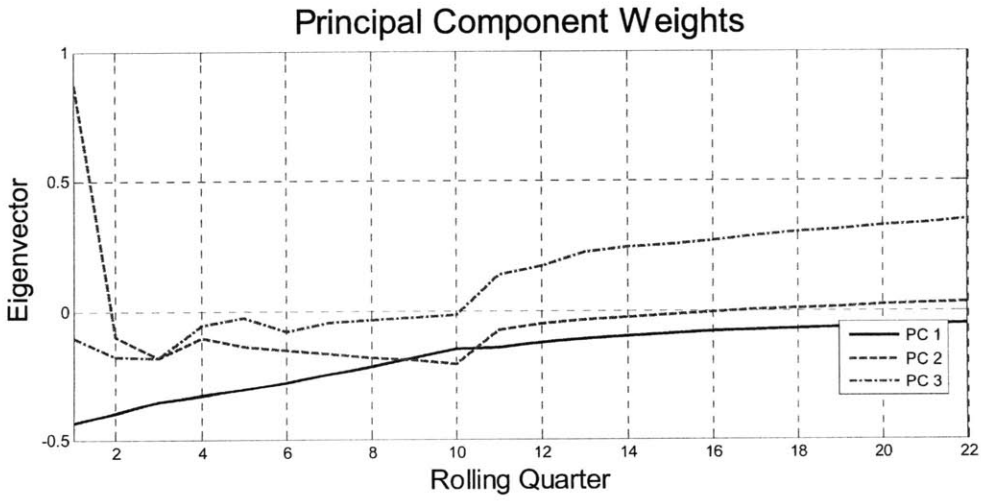

PMX (22R)

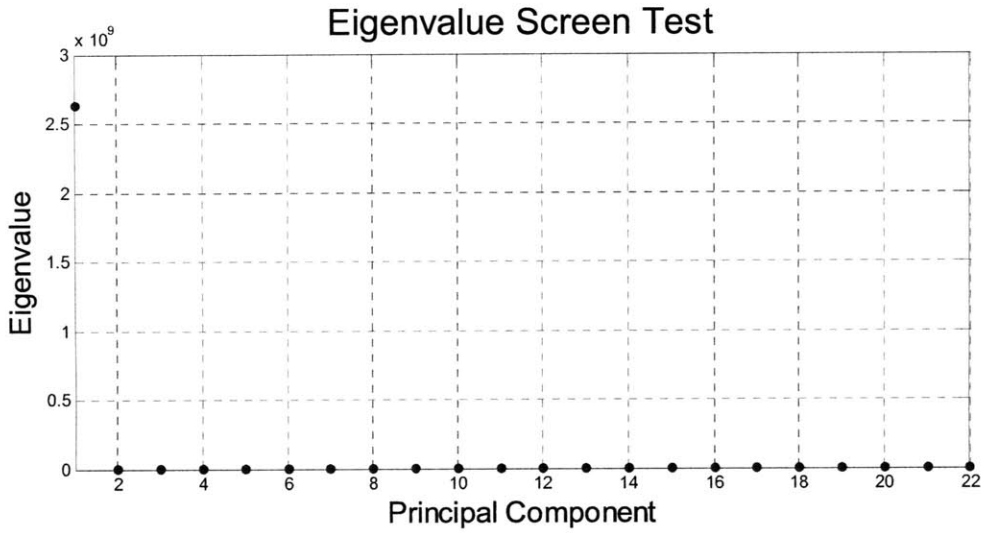
Eigenvalue Screen Test
x 10^9
Eigenvalue
Principal Component

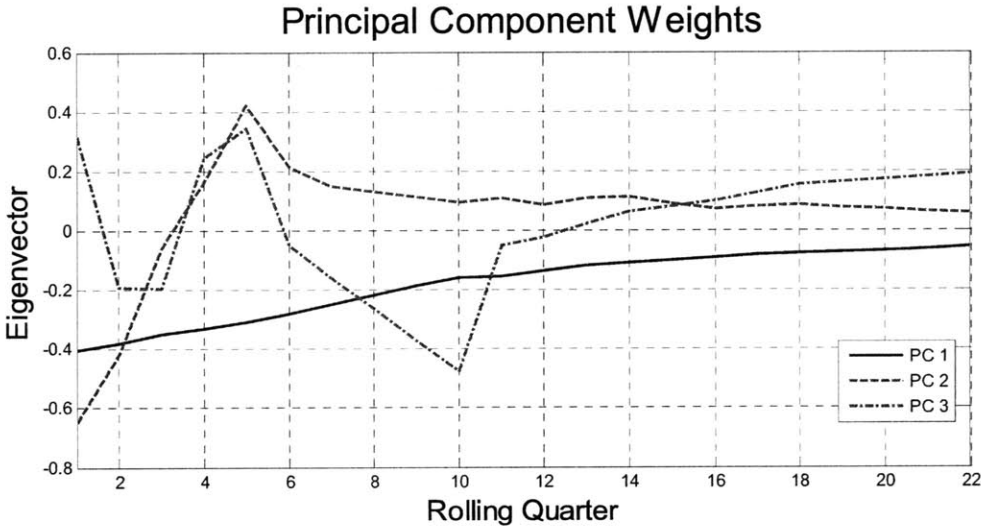
Principal Component Weights
Eigenvector
Rolling Quarter
PC 1
PC 2
PC 3

CAPE

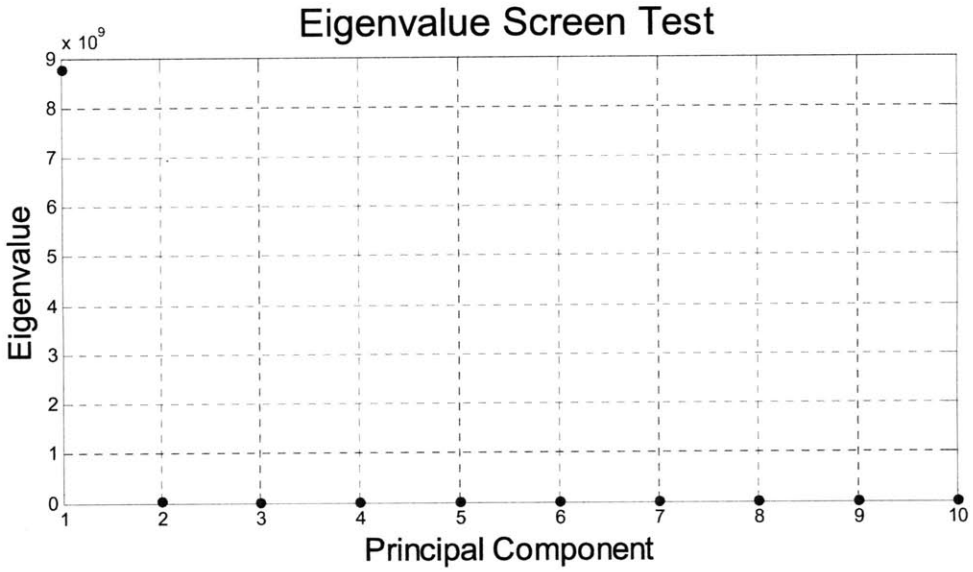
Eigenvalue Screen Test
x 10^9
Eigenvalue
Principal Component

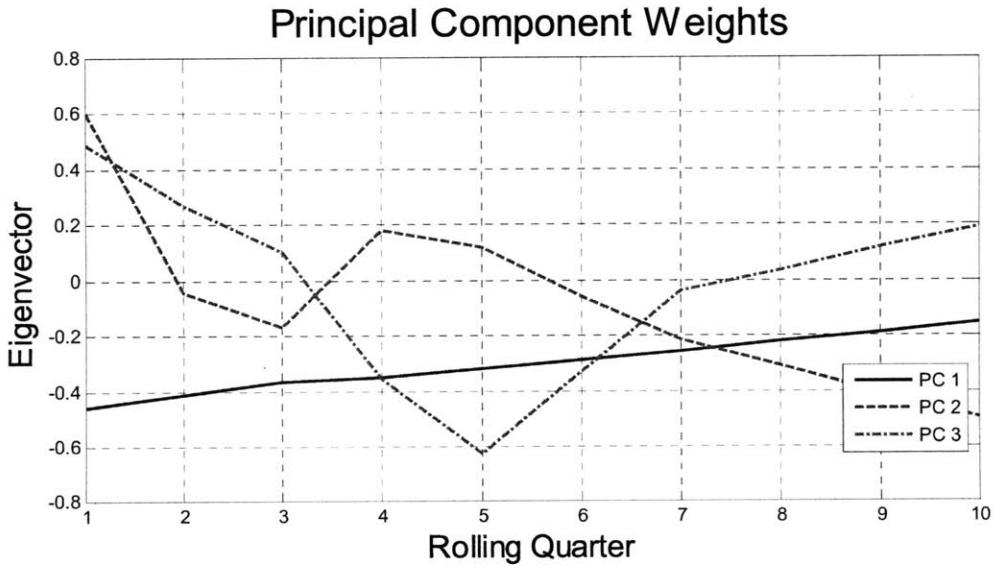
Principal Component Weights
Eigenvector
Rolling Quarter
PC 1
PC 2
PC 3

PMX

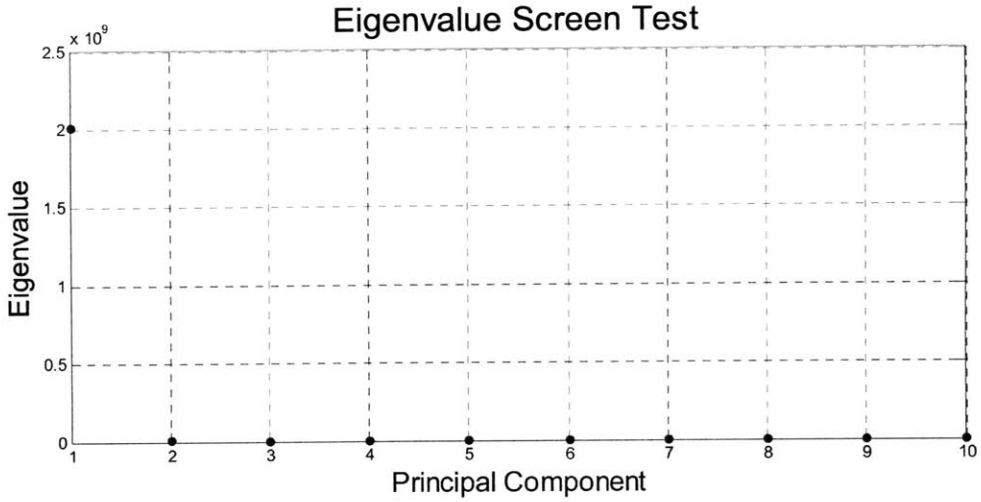
Eigenvalue Screen Test
x 10^9
2.5
2
1.5
1
0.5
0
Eigenvalue
1
2
3
4
5
6
7
8
9
10
Principal Component

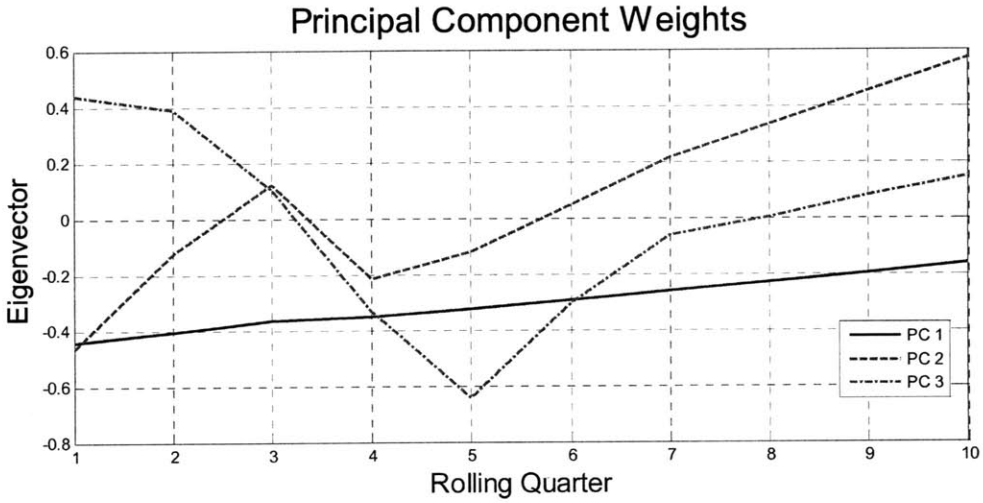
Principal Component Weights
0.6
0.4
0.2
0
-0.2
-0.4
-0.6
-0.8
Eigenvector
1
2
3
4
5
6
7
8
9
10
Rolling Quarter
PC 1
PC 2
PC 3

TC2

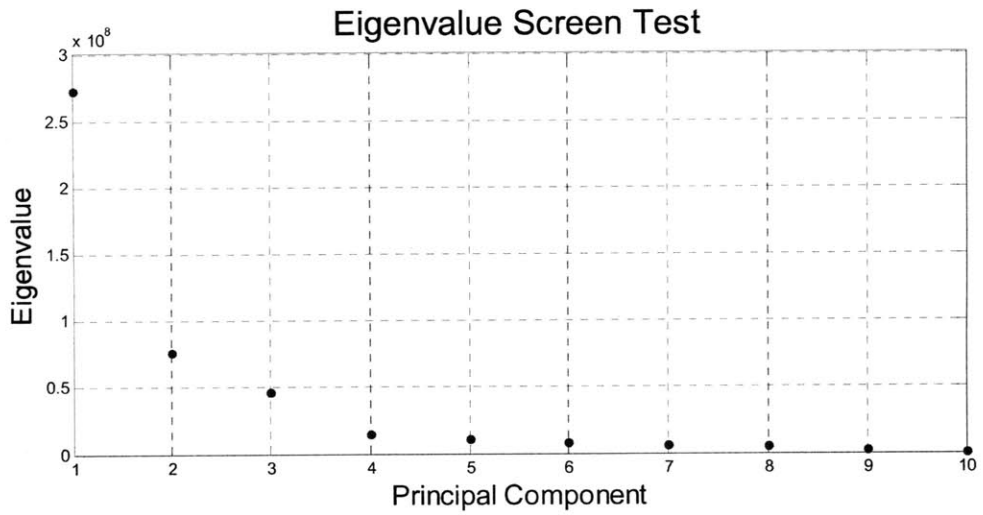
Eigenvalue Screen Test
x 10^8
Eigenvalue
Principal Component

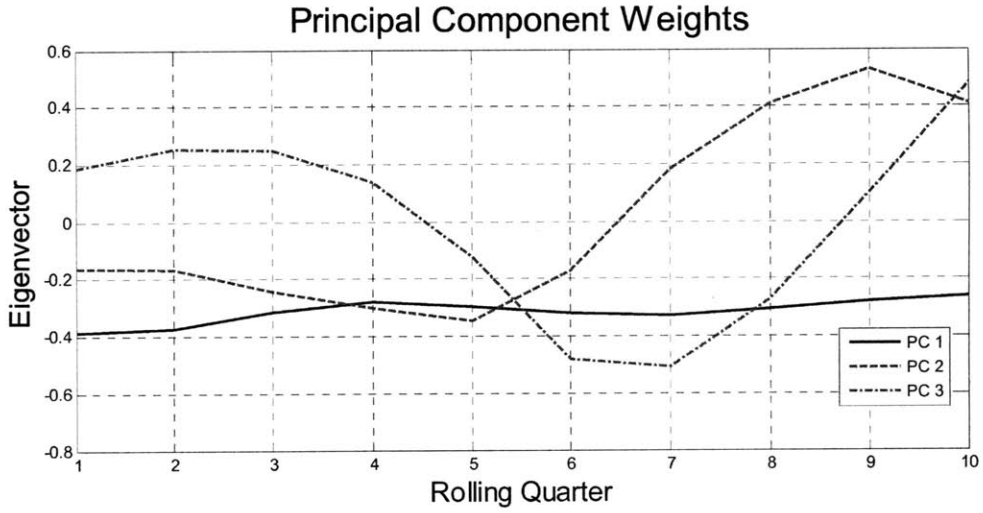
Principal Component Weights
Eigenvector
Rolling Quarter
PC 1
PC 2
PC 3

TD3

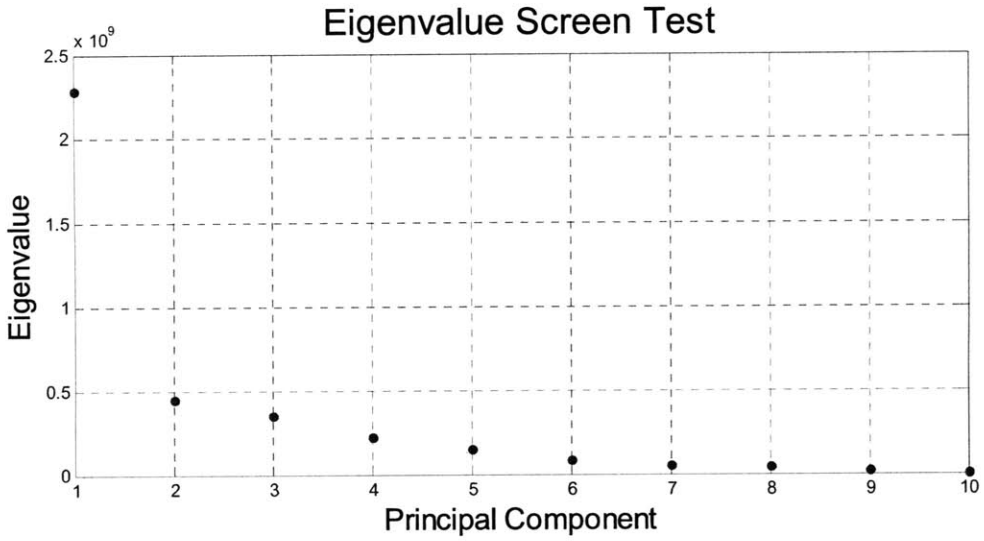
Eigenvalue Screen Test
x 10^9
2.5
2
1.5
1
0.5
0
Eigenvalue
1
2
3
4
5
6
7
8
9
10
Principal Component

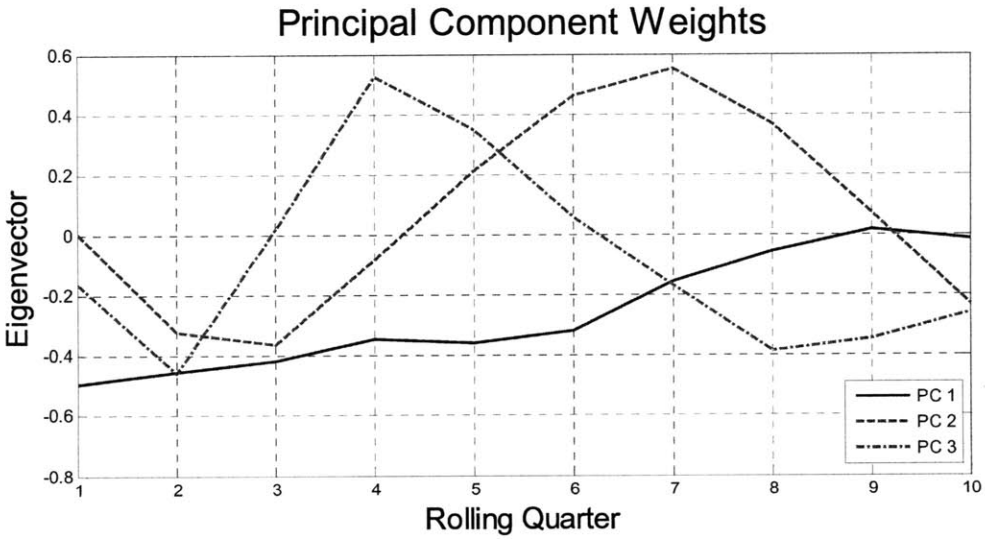
Principal Component Weights
0.6
0.4
0.2
0
-0.2
-0.4
-0.6
-0.8
Eigenvector
1
2
3
4
5
6
7
8
9
10
Rolling Quarter
PC 1
PC 2
PC 3

TD5

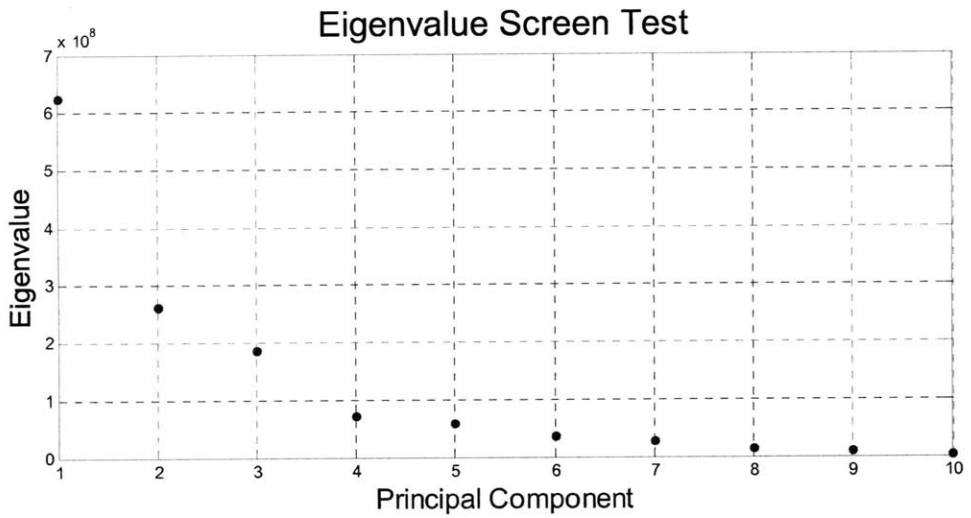
Eigenvalue Screen Test
x 10^8
Eigenvalue
Principal Component
0
1
2
3
4
5
6
7
1
2
3
4
5
6
7
8
9
10

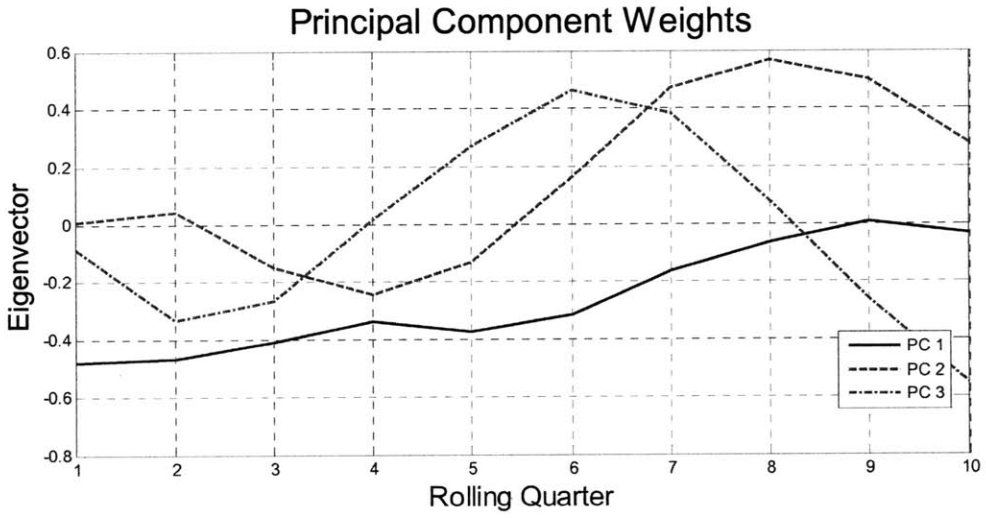
Principal Component Weights
Eigenvector
Rolling Quarter
PC 1
PC 2
PC 3
0.6
0.4
0.2
0
-0.2
-0.4
-0.6
-0.8
1
2
3
4
5
6
7
8
9
10

TC2 (WS)

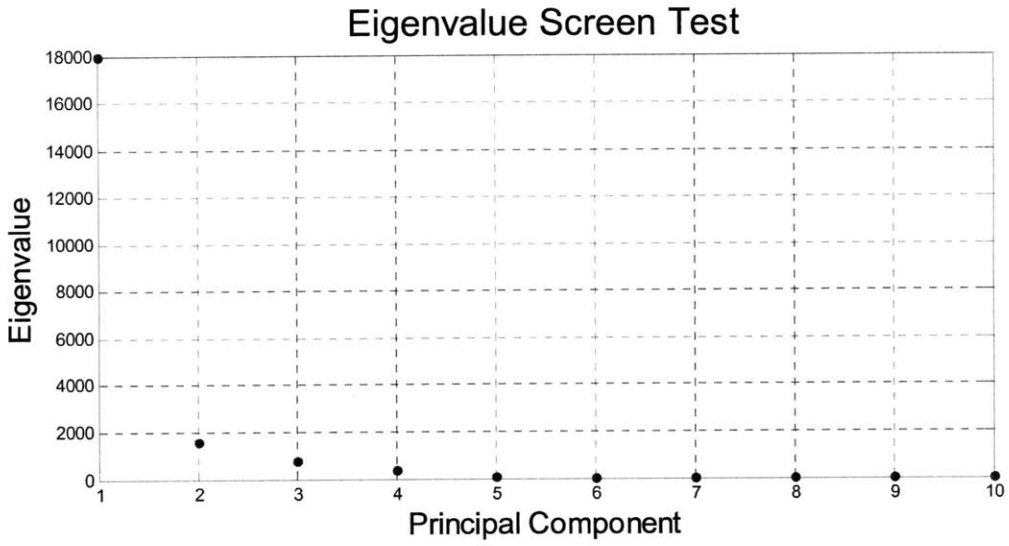
Eigenvalue Screen Test
Eigenvalue
Principal Component
18000
16000
14000
12000
10000
8000
6000
4000
2000
0
1
2
3
4
5
6
7
8
9
10

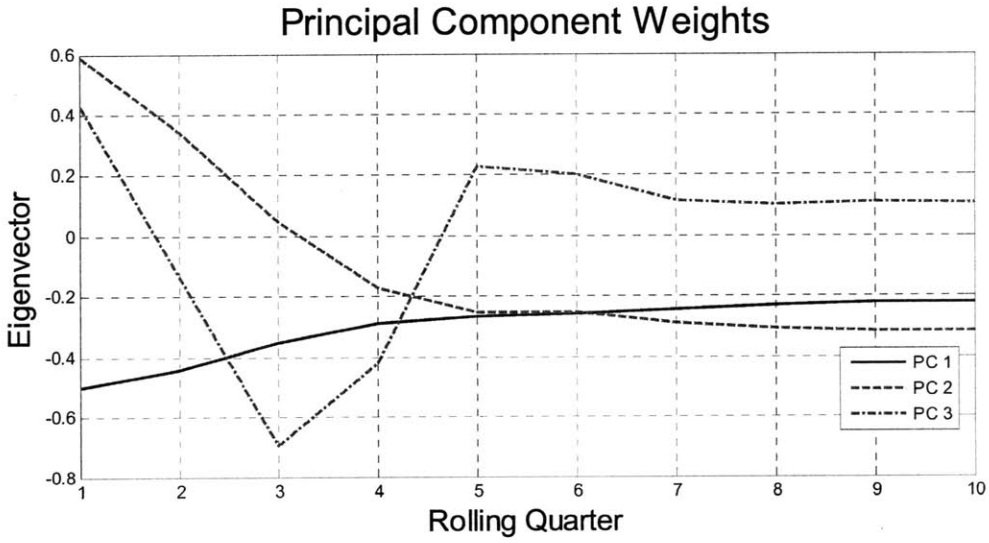
Principal Component Weights
Eigenvector
Rolling Quarter
0.6
0.4
0.2
0
-0.2
-0.4
-0.6
-0.8
1
2
3
4
5
6
7
8
9
10
PC 1
PC 2
PC 3

TD3 (WS)

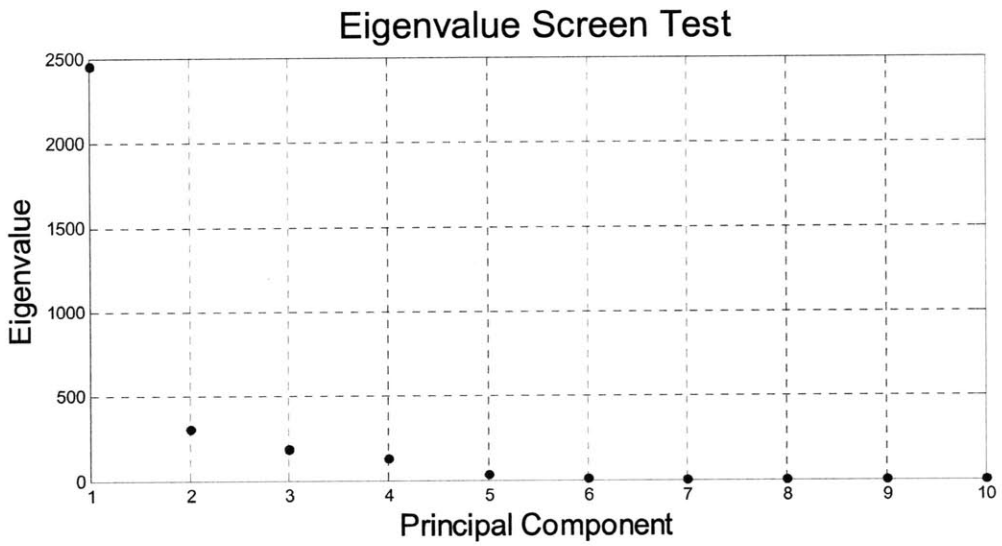
Eigenvalue Screen Test
Eigenvalue
2500
2000
1500
1000
500
0
1
2
3
4
5
6
7
8
9
10
Principal Component

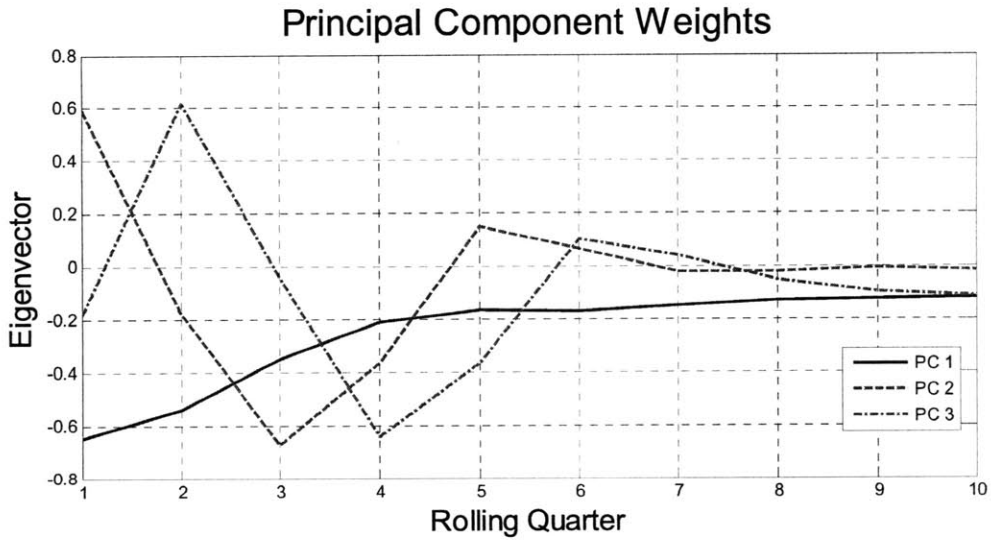
Principal Component Weights
Eigenvector
0.8
0.6
0.4
0.2
0
-0.2
-0.4
-0.6
-0.8
1
2
3
4
5
6
7
8
9
10
Rolling Quarter
PC 1
PC 2
PC 3

TD5 (WS)

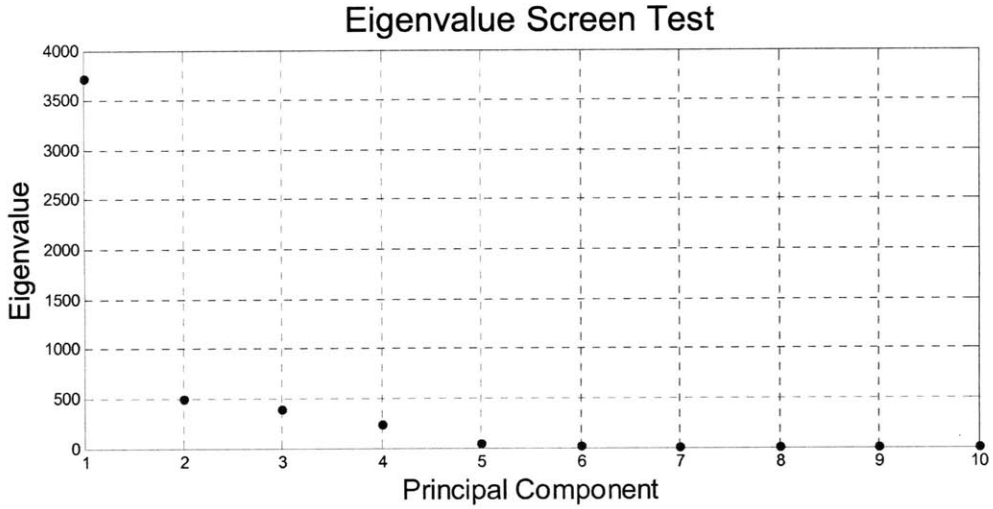
Eigenvalue Screen Test
Eigenvalue
4000
3500
3000
2500
2000
1500
1000
500
0
1
2
3
4
5
6
7
8
9
10
Principal Component

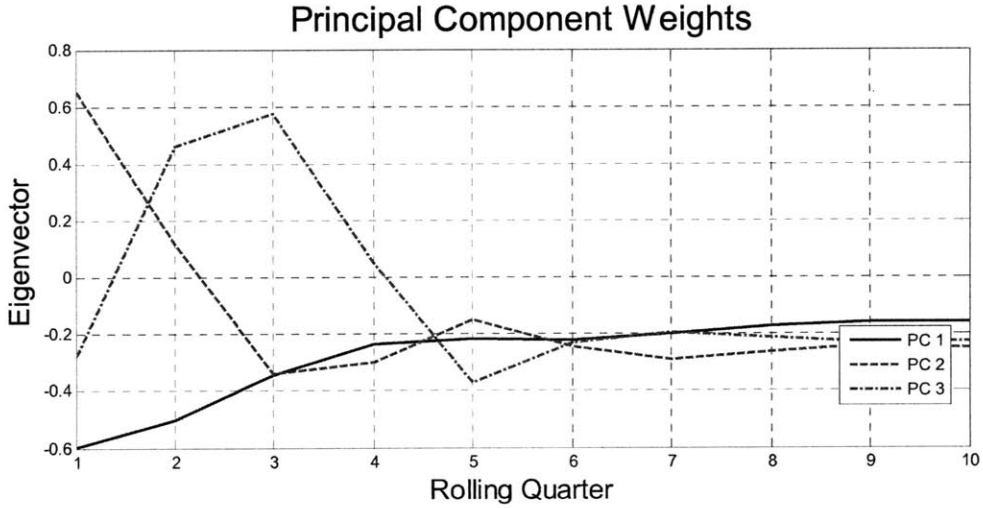
Principal Component Weights
Eigenvector
0.8
0.6
0.4
0.2
0
-0.2
-0.4
-0.6
1
2
3
4
5
6
7
8
9
10
Rolling Quarter
PC 1
PC 2
PC 3

Appendix C - CCA Eigenvalues / Possible Correlation Range (De-Trended Vol.)

TD5-TC2	TD5-TD3	TD3-TC2	CAPE-PMX	TD5-TD3(ws)	TD3-TC2(ws)	TD5-TC2(ws)	CAPE-TC2	CAPE-TD5	TD5-PMX	TC2-PMX	TD3-PMX	CAPE-TD3
0.21254	0.49691	0.18695	0.06399	0.30116	0.04279	0.05268	0.00015	0.00279	0.00087	0.00541	0.00102	0.00286
-0.21254	-0.49691	-0.18695	-0.06399	-0.30116	-0.04279	-0.05268	-0.00015	-0.00279	-0.00087	-0.00541	-0.00102	-0.00286
0.38924	0.56908	0.35862	0.45918	0.32258	0.08401	0.09492	0.01464	0.01232	0.02230	0.01061	0.01843	0.00822
-0.38924	-0.56908	-0.35862	-0.45918	-0.32258	-0.08401	-0.09492	-0.01464	-0.01232	-0.02230	-0.01061	-0.01843	-0.00822
0.51528	0.65628	0.48708	0.55240	0.35871	0.13373	0.12661	0.02525	0.02078	0.03255	0.01858	0.02176	0.03469
-0.51528	-0.65628	-0.48708	-0.55240	-0.35871	-0.13373	-0.12661	-0.02525	-0.02078	-0.03255	-0.01858	-0.02176	-0.03469
0.70247	0.75245	0.63680	0.57107	0.41625	0.15688	0.15321	0.04428	0.04299	0.04366	0.03046	0.03618	0.04525
-0.70247	-0.75245	-0.63680	-0.57107	-0.41625	-0.15688	-0.15321	-0.04428	-0.04299	-0.04366	-0.03046	-0.03618	-0.04525
0.79773	0.82409	0.73720	0.59723	0.43435	0.21981	0.22332	0.05736	0.06062	0.05794	0.06748	0.05322	0.06408
-0.79773	-0.82409	-0.73720	-0.59723	-0.43435	-0.21981	-0.22332	-0.05736	-0.06062	-0.05794	-0.06748	-0.05322	-0.06408
0.88533	0.87120	0.82620	0.63952	0.49557	0.30924	0.28400	0.07803	0.07460	0.05935	0.08048	0.07799	0.07816
-0.88533	-0.87120	-0.82620	-0.63952	-0.49557	-0.30924	-0.28400	-0.07803	-0.07460	-0.05935	-0.08048	-0.07799	-0.07816
0.90360	0.88692	0.86213	0.68968	0.53108	0.33019	0.37662	0.10475	0.09565	0.10175	0.10288	0.10832	0.08858
-0.90360	-0.88692	-0.86213	-0.68968	-0.53108	-0.33019	-0.37662	-0.10475	-0.09565	-0.10175	-0.10288	-0.10832	-0.08858
0.94216	0.94768	0.92596	0.78470	0.64765	0.37660	0.43561	0.11351	0.11039	0.11590	0.11573	0.14418	0.13992
-0.94216	-0.94768	-0.92596	-0.78470	-0.64765	-0.37660	-0.43561	-0.11351	-0.11039	-0.11590	-0.11573	-0.14418	-0.13992
0.99642	0.98257	0.97996	0.91274	0.70012	0.52243	0.59554	0.20925	0.23677	0.22635	0.23711	0.24329	0.20044
-0.99642	-0.98257	-0.97996	-0.91274	-0.70012	-0.52243	-0.59554	-0.20925	-0.23677	-0.22635	-0.23711	-0.24329	-0.20044
0.99849	0.99465	0.99173	0.96020	0.84580	0.76946	0.75353	0.28224	0.27683	0.25795	0.24909	0.24624	0.22100
-0.99849	-0.99465	-0.99173	-0.96020	-0.84580	-0.76946	-0.75353	-0.28224	-0.27683	-0.25795	-0.24909	-0.24624	-0.22100

Appendix D - CCA Eigenvalues / Possible Correlation Range (Trended Vol.)

TD5-TC2	TD5-TD3	TD3-TC2	CAPE-PMX	TD5-TD3(ws)	TD5-TC2(ws)	TD3-TC2(ws)	CAPE-TD3	TD3-PMX	TD5-PMX	CAPE-TD5	TC2-PMX	CAPE-TC2
0.50553	0.72862	0.41464	0.48618	0.55352	0.39199	0.26551	0.01641	0.02403	0.01688	0.00174	0.00098	0.00015
-0.50553	-0.72862	-0.41464	-0.48618	-0.55352	-0.39199	-0.26551	-0.01641	-0.02403	-0.01688	-0.00174	-0.00098	-0.00015
0.84684	0.86714	0.67527	0.59803	0.66490	0.60343	0.54828	0.10869	0.06992	0.06590	0.06808	0.03050	0.07661
-0.84684	-0.86714	-0.67527	-0.59803	-0.66490	-0.60343	-0.54828	-0.10869	-0.06992	-0.06590	-0.06808	-0.03050	-0.07661
0.92262	0.88388	0.75322	0.74909	0.78475	0.69900	0.58136	0.16391	0.12824	0.10023	0.14852	0.06888	0.13280
-0.92262	-0.88388	-0.75322	-0.74909	-0.78475	-0.69900	-0.58136	-0.16391	-0.12824	-0.10023	-0.14852	-0.06888	-0.13280
0.94623	0.95140	0.91359	0.85880	0.79844	0.80667	0.77530	0.22516	0.25693	0.23103	0.21438	0.25936	0.25331
-0.94623	-0.95140	-0.91359	-0.85880	-0.79844	-0.80667	-0.77530	-0.22516	-0.25693	-0.23103	-0.21438	-0.25936	-0.25331
0.95809	0.98429	0.92670	0.86774	0.90370	0.84058	0.79303	0.29983	0.28737	0.30169	0.33798	0.32017	0.37927
-0.95809	-0.98429	-0.92670	-0.86774	-0.90370	-0.84058	-0.79303	-0.29983	-0.28737	-0.30169	-0.33798	-0.32017	-0.37927
0.96668	0.98557	0.94392	0.89021	0.93307	0.88256	0.82306	0.38649	0.35840	0.36634	0.37188	0.39352	0.40131
-0.96668	-0.98557	-0.94392	-0.89021	-0.93307	-0.88256	-0.82306	-0.38649	-0.35840	-0.36634	-0.37188	-0.39352	-0.40131
0.99491	0.99521	0.99103	0.91056	0.94770	0.91975	0.87813	0.53333	0.48436	0.37496	0.57400	0.44800	0.58398
-0.99491	-0.99521	-0.99103	-0.91056	-0.94770	-0.91975	-0.87813	-0.53333	-0.48436	-0.37496	-0.57400	-0.44800	-0.58398
0.99576	0.99606	0.99615	0.99384	0.97745	0.94927	0.92766	0.67297	0.62982	0.64760	0.66830	0.61088	0.64675
-0.99576	-0.99606	-0.99615	-0.99384	-0.97745	-0.94927	-0.92766	-0.67297	-0.62982	-0.64760	-0.66830	-0.61088	-0.64675
0.99917	0.99830	0.99832	0.99560	0.98515	0.97379	0.94011	0.75933	0.68518	0.68762	0.72336	0.69164	0.66274
-0.99917	-0.99830	-0.99832	-0.99560	-0.98515	-0.97379	-0.94011	-0.75933	-0.68518	-0.68762	-0.72336	-0.69164	-0.66274
0.99964	0.99889	0.99874	0.99679	0.98937	0.97525	0.96832	0.92589	0.90895	0.86424	0.86009	0.81974	0.81879
-0.99964	-0.99889	-0.99874	-0.99679	-0.98937	-0.97525	-0.96832	-0.92589	-0.90895	-0.86424	-0.86009	-0.81974	-0.81879

Appendix E – CCA Correlation Maximizing Portfolios (De-Trended Vol.)

	TD5-TC2	TD5-TD3	TD3-TC2	CAPE-PMX	TD5-TD3(ws)	TD3-TC2(ws)	TD5-TC2(ws)	CAPE-TC2	CAPE-TD5	TD5-PMX	TC2-PMX	TD3-PMX	CAPE-TD3
R1	-0.0002	0.0002	-0.0014	0.0000	0.0001	-0.0006	0.0011	0.0023	-0.0176	0.0031	-0.0038	-0.0067	0.0057
R2	-0.0002	-0.0108	0.0020	-0.0003	-0.0019	0.0007	0.0054	-0.0181	0.0128	-0.0181	0.0154	0.0245	-0.1072
R3	-0.0040	0.0068	0.0021	0.0003	0.0014	-0.0019	-0.0055	-0.0094	-0.0081	0.0076	-0.0098	-0.0169	-0.0617
R4	0.0121	-0.0054	-0.0169	-0.0001	-0.0062	-0.0037	0.0031	0.0623	0.0728	0.0249	0.0048	-0.0075	0.3016
R5	-0.0061	0.0048	0.0313	0.0000	0.0029	-0.0040	0.0067	-0.0588	-0.1058	-0.0034	-0.0115	-0.0191	-0.2058
R6	-0.0290	-0.0460	-0.0265	0.0000	-0.0461	-0.0253	0.0291	0.1435	0.3859	-0.0466	0.0345	0.0738	0.1405
R7	0.1588	0.0620	0.0146	0.1806	0.0552	0.0015	0.0071	-0.3990	-0.0260	0.0065	-0.0070	-0.0159	0.3779
R8	-0.3692	0.1047	0.1197	-0.4765	0.2934	0.2897	-0.3139	0.6375	-0.7869	0.0232	0.0018	-0.0109	-0.7754
R9	0.5073	-0.6286	-0.4474	0.4147	-0.5036	-0.4515	0.3291	-0.5915	0.3908	-0.0068	-0.0090	-0.0060	0.0684
R10	-0.2856	0.4922	0.3549	-0.1185	0.2000	0.1926	-0.0456	0.2198	0.0613	-0.0118	0.0050	0.0026	0.2436
R1	-0.0001	-0.0021	-0.0030	0.0000	-0.0001	0.0011	-0.0003	-0.0066	-0.0091	0.0131	0.0027	-0.0103	-0.0058
R2	-0.0023	-0.0008	-0.0049	-0.0004	-0.0003	-0.0015	0.0049	0.0038	-0.0151	0.0044	-0.0082	-0.0222	0.0070
R3	0.0049	0.0052	0.0018	0.0005	-0.0001	-0.0019	-0.0010	-0.0187	-0.0459	0.0282	-0.0195	-0.0605	-0.0629
R4	0.0057	-0.0131	0.0002	-0.0002	-0.0105	-0.0060	0.0078	0.0716	0.2113	-0.0867	0.0791	0.2253	0.0646
R5	-0.0022	0.0287	0.0011	0.0001	0.0002	-0.0070	0.0135	-0.0212	-0.0713	0.0324	-0.0464	-0.1110	-0.0424
R6	-0.0345	-0.0453	-0.0079	0.0000	-0.0509	-0.0206	0.0322	0.0285	0.0151	0.0446	0.0092	-0.0145	0.1005
R7	0.1557	0.0538	0.0132	0.1965	0.0438	-0.0045	0.0079	-0.0040	0.0018	-0.1325	-0.1979	-0.0206	-0.0312
R8	-0.3635	0.0707	0.1763	-0.5271	0.3632	0.4322	-0.5208	-0.0186	-0.0462	-0.3107	0.6061	0.4113	-0.0105
R9	0.5110	-0.4432	-0.6377	0.4680	-0.6290	-0.6522	0.6870	-0.0165	-0.0542	0.8280	-0.7073	-0.7730	-0.0379
R10	-0.2825	0.3715	0.4684	-0.1372	0.2879	0.2485	-0.2135	0.0215	0.0121	-0.4299	0.2869	0.3976	0.0314

Appendix F – CCA Correlation Maximizing Portfolios (Trended Vol.)

	TD5-TC2	TD5-TD3	TD3-TC2	CAPE-PMX	TD5-TD3(ws)	TD5-TC2(ws)	TD3-TC2(ws)	CAPE-TD3	TD3-PMX	TD5-PMX	CAPE-TD5	TC2-PMX	CAPE-TC2
R1	-0.0025	-0.0018	0.0063	0.0000	-0.0571	0.0335	0.0022	-0.0029	-0.0011	0.0018	-0.0079	0.0010	-0.0028
R2	0.0080	-0.0411	-0.0193	0.0002	0.0437	-0.0234	-0.0076	0.0085	0.0003	-0.0006	0.0148	0.0030	0.0110
R3	-0.0092	0.0715	0.0083	-0.0005	0.2129	-0.1864	0.0192	0.0302	0.0008	-0.0006	0.0288	0.0025	0.0090
R4	-0.0017	-0.0105	0.0112	0.0006	0.2932	-0.0361	0.0130	-0.0135	0.0011	-0.0036	0.0028	-0.0049	0.0078
R5	0.0016	0.0446	-0.0071	-0.0002	-0.1833	-0.0127	-0.0140	0.0065	0.0007	-0.0046	-0.0009	-0.0045	-0.0047
R6	-0.0053	0.0952	0.0224	-0.0001	-0.1393	-0.0237	-0.0182	0.0036	0.0027	-0.0059	0.0007	-0.0075	-0.0011
R7	0.0388	-0.0680	0.0439	0.1658	0.0297	-0.1384	-0.1021	-0.5457	0.0005	-0.0013	-0.2980	-0.0026	0.0793
R8	-0.1162	-0.0490	-0.0936	-0.1050	-0.0426	0.2895	0.3869	0.5630	0.0011	-0.0014	0.6974	-0.0021	0.2538
R9	0.3715	-0.5870	-0.2217	-0.2871	-0.1192	-0.6997	-0.6446	0.4086	0.0022	-0.0031	-0.6259	-0.0002	-0.8358
R10	-0.2709	0.5656	0.2453	0.2264	0.0395	0.4259	0.3602	-0.4658	0.0022	-0.0007	0.1779	0.0011	0.4796
R1	0.0003	0.0042	-0.0049	0.0000	-0.0632	-0.0038	0.0029	-0.0015	-0.0077	0.0219	-0.0027	0.0132	-0.0038
R2	0.0132	-0.0268	-0.0636	0.0005	0.0701	0.0145	-0.0055	-0.0003	0.0058	-0.0230	0.0011	-0.0250	-0.0009
R3	-0.0193	0.0534	0.0003	-0.0011	0.2111	-0.1268	0.0115	0.0010	0.0183	-0.0316	-0.0038	-0.0174	-0.0121
R4	-0.0108	-0.0206	0.0839	0.0011	0.3534	-0.0317	0.0038	0.0034	-0.0143	0.0095	0.0097	0.0007	0.0118
R5	-0.0139	0.0427	-0.0153	-0.0003	-0.2250	0.0678	-0.0064	0.0032	0.0061	-0.0033	0.0109	-0.0012	0.0103
R6	0.0034	0.0431	0.0699	-0.0002	-0.1841	-0.0356	-0.0194	0.0046	0.0056	0.0003	0.0077	0.0060	0.0063
R7	0.0744	-0.0377	0.1156	0.3590	0.2315	-0.2482	-0.0483	0.0021	-0.4614	0.4552	0.0017	-0.0428	0.0002
R8	-0.2201	-0.0452	-0.2419	-0.2213	-0.1968	0.3118	0.2139	0.0021	0.3954	-0.8302	0.0025	-0.3253	0.0029
R9	0.6843	-0.3960	-0.5925	-0.6348	-0.5439	-0.0738	-0.4180	0.0039	0.5870	0.2969	0.0033	0.8374	0.0011
R10	-0.5003	0.3775	0.6630	0.4971	0.3756	0.0088	0.2647	0.0044	-0.5342	0.1153	0.0002	-0.4357	-0.0029

Appendix G – RAFL Suezmax Option Valuations with Greeks

New Ship

Tenor	1 week	2 week	2 months	6 months
Call	**$1.111.434**	**$1.572.148**	**$3.276.987**	**$5.719.366**
Put	**$1.109.881**	**$1.569.042**	**$3.258.639**	**$5.580.116**
Call delta:	0,50778538	0,511009487	0,523146058	0,542402257
Put delta:	-0,4922146	-0,488990513	-0,476853942	-0,457597743
Gamma:	1,4326E-07	1,01282E-07	4,85908E-08	2,79423E-08
Call rho:	695664,538	1382714,74	5856152,776	17054246,71
Put rho:	-716394,82	-1441344,244	-6378895,769	-19590448
Call theta:	-28913251	-20452273,36	-9845868,667	-5761100,366
Put theta:	-28832503	-20371527,48	-9735794,503	-5482864,926
Vega:	4061544,04	5742796,898	11939005,52	20596725,89

5-Year Old:

Tenor	1 week	2 week	2 months	6 months
Call	**$978.677**	**$1.384.329**	**$2.885.062**	**$5.032.042**
Put	**$977.386**	**$1.381.747**	**$2.869.810**	**$4.916.283**
Call delta:	0,508221307	0,511625855	0,524414057	0,544457485
Put delta:	-0,491778693	-0,488374145	-0,475585943	-0,455542515
Gamma:	1,62683E-07	1,1501E-07	5,5169E-08	3,17133E-08
Call rho:	577767,0173	1147925,076	4854321,472	14101214,55
Put rho:	-596082,0742	-1199723,458	-5316710,347	-16361627,88
Call theta:	-25458315,8	-18007389,51	-8665863,266	-5063433,666
Put theta:	-25391190,09	-17940265,22	-8574358,289	-4832135,727
Vega:	3376299,466	4773794,588	9923045,744	17112442,47

10-Year Old:

Tenor	1 week	2 week	2 months	6 months
Call	**$753.491**	**$1.065.772**	**$2.220.720**	**$3.870.052**
Put	**$752.570**	**$1.063.930**	**$2.209.836**	**$3.787.449**
Call delta:	0,508838762	0,512498868	0,526212119	0,547394673
Put delta:	-0,491161238	-0,487501132	-0,473787881	-0,452605327
Gamma:	2,11283E-07	1,49363E-07	7,16319E-08	4,11534E-08
Call rho:	411738,1411	817597,2464	3449983,134	9986615,666
Put rho:	-425893,284	-857630,1756	-3807828,742	-11750960,57
Call theta:	-19599169,09	-13862036,03	-6667817,913	-3888734,14
Put theta:	-19551269,74	-13814137,69	-6602522,089	-3723685,308
Vega:	2409169,064	3406243,329	7078824,664	12200603,68

15-Year Old:

Tenor	1 week	2 week	2 months	6 months
Call	**$524.470**	**$741.789**	**$1.545.039**	**$2.688.287**
Put	**$523.916**	**$740.681**	**$1.538.493**	**$2.638.605**
Call delta:	0,510172588	0,514384644	0,530101834	0,553814529
Put delta:	-0,489827412	-0,485615356	-0,469898166	-0,446185471
Gamma:	3,03487E-07	2,14528E-07	1,02829E-07	5,89955E-08
Call rho:	246945,8444	489777,445	2057121,25	5910355,852
Put rho:	-256856,9495	-517806,834	-2308170,919	-7163952,62
Call theta:	-13640221,41	-9645979,002	-4635382,044	-2693685,577
Put theta:	-13611411,81	-9617170,014	-4596109,14	-2594415,11
Vega:	1448906,219	2048396,652	4254699,622	7323063,115

20-Year Old:

Tenor	1 week	2 week	2 months	6 months
Call	**$307.864**	**$435.387**	**$906.263**	**$1.573.125**
Put	**$307.602**	**$434.863**	**$903.168**	**$1.549.631**
Call delta:	0,512555042	0,51775257	0,537058572	0,565426682
Put delta:	-0,487444958	-0,48224743	-0,462941428	-0,434573318
Gamma:	5,16842E-07	3,6528E-07	1,74891E-07	1,00044E-07
Call rho:	116196,8899	229965,691	957902,6392	2716004,931
Put rho:	-122050,2444	-246518,5	-1106433,57	-3466804,224
Call theta:	-8005082,815	-5659524,12	-2715162,115	-1568869,083
Put theta:	-7991458,825	-5645900,41	-2696590,053	-1521924,317
Vega:	685067,6707	968352,184	2009072,001	3447798,562

10. References

Anderson, T.W. (2003) ***An Introduction to Multivariate Statistical Analysis – 3rd Edition***, Wiley Series in Probability and Statistics, Wiley-Interscience, John Wiley and sons, Inc., 2003

Amlashi, H.K.K., Moan, T., (2005) ***On the strength assessment of pitted stiffened plates under biaxial compression loading***, Proceedings of the 24th International Conference on Offshore Mechanics and Arctic Engineering, Halkidiki, Greece

Basilevsky, A.T. (1994) ***Statistical Factor Analysis and Related Methods: Theory and Applications***, Wiley Series in Probability and Mathematical Statistics, Probability and Mathematical Statistics Section, Wiley-Interscience, June-7-1994

Clarksons (2010) Data provided by *Clarksons* Shipbrokers – Private Correspondence, Clarksons Ltd., 2010

Cotzias (2010) ***S&P Monthly report January 2010***, N. Cotzias Shipping Group, Shipbrokers since 1893
http://www.cotzias.gr/index1.html

Cotzias (2009) ***S&P Monthly report December 2009***, N. Cotzias Shipping Group, Shipbrokers since 1893
http://www.cotzias.gr/index1.html

Debek, P. and Konieczny, L. (2006) ***A Complete Reliability Evaluation of a Bulk Carrier Hull Structure, Ship Structure Division***, CTO S.A. Poland, 3rd International ASRANet Colloquium 10-12th July 2006, Glasgow, UK

Gollwitzer, S., Abdo, T. & Rackwitz, R. (1988) ***FORM – Program Manual***, Munich

Googlefinance (2010) Google Finance
www.google.com/finance
Accessed July 2010

Guedes Soares, C., Dogliani, M., Ostergaard, C., Parmentier, G. & Pedersen, P.T. (1996) ***Reliability Based Ship Structural Design***, Transactions of the Society of Naval Architectures and Marine Engineers (SNAME), Vol. 104: 357-389

Hadjiyiannis, N.A. (2010) ***Structural and Economic Analysis of Capesize Bulk Carriers***, PhD Thesis, Department of Mechanical Engineering, Massachusetts Institute of Technology, May 19th 2010

Houssein A.W., Guedes Soares, C (2009) ***Reliability Analysis of the Ultimate Limit State Variables for a Tanker and a Bulk Carrier***, Analysis and Design of marine Strectures by Carlos Guedes Soares and P.K. Das, 2009 ISBN 978-0-415-54394-9 , pp. 513

IACS (2006) ***Common Structural Rules for Double Hull Oil Tankers***, International Association of Classification Societies, London

IACS (2001) ***Bulk carrier Safety – Formal Safety Assessment – Fore-End Water Tight Integrity***, Maritime Safety Committee 74th session, Agenda Item 5, MSC 74/5, Feb 2001

James, W. and Stein, C. (1961) ***Estimation with Quadratic Loss***, Proceedings of the fourth Berkeley Symposium on Mathematical Statistics and Probability, Volume I, pp. 361-379, University of California, Berkeley

Lotsberg, I. (2006) ***Assessment of Fatigue Capacity in the New Bulk Carrier and Tanker Rules***, Det Norske Veritas (DNV), Marine Structures 19 (2006) pp. 83-96

Moore Stephens (2010) Moore Stephens – Chartered Accountants – Private Correspondence

Ok, D., Pu, Y., Incecik, A. (2007) ***Artificial Neuron Networks and their Application to Assessment of Ultimate Strength of Plates with Pitting Corrosion***, School of Marine Science and Technology, University of Newcastle upon Tyne, Ocean Engineering Vol. 34, Issues 17-18, Dec 2007, pp. 2222-2230

Paik, J.K., Wang, G., Thayamballi, A.K., Lee, J.M., Park, Y.I. (2003) ***Time-Dependent Risk Assessment of Ageing Ships Accounting for General / Pit Corrosion, Fatigue Cracking and Local Denting Damage***. Proceedings of SNAME, Annual Meeting of the World Maritime Technology Conference, San Francisco

Paik, J.K. and Thayamballi, A.K. (2002) ***Ultimate Strength of Ageing Ships***, Proceedings of the Institute of Mechanical Engineers, Vol. 216 Part M, Journal of Engineering for the Marine Environment

Pratt, S.P., Grabowsky R.J. (2008) ***Cost of Capital: Applications and Examples – 3rd Edition***, Wiley Finance, John Wiley and Sons, Inc.

Samuelson, P.A. (1965) ***Proof that Properly Anticipated Prices Fluctuate Randomly***, Industrial Management Review, 6, 41-49

Sclavounos, P.D. and Ellefsen, P.E. (2009) ***Multi-Factor Model of Correlated Commodity Forward Curves for Crude Oil and Shipping Markets***, Department of Mechanical Engineering, Massachusetts Institute of Technology, March 2009

Stein, C. (1956) ***Inadmissibility of the Usual Estimator of the Mean of a Multivariate Normal Distribution***, Proceedings of the third Berkeley Symposium on Mathematical and Statistical Probability, Volume I, pp. 197-206, University of California, Berkeley

Stopford, M. (2009) ***Maritime Economics – 3rd Edition***, by Martin Stopford, First published by Allen and Unwin 1988, Published by Routledge, 2009

Wang, G, Spenser, J., Sun, H.H. (2003) ***Assessment of Corrosion Risks to Ageing Ships Using an Experience Database***, Proceedings of the 22nd International Conference on Offshore Mechanics and Arctic Engineering (OMEA'03), Cancun, Mexico 8-13 June 2003